

Oscillations: swings and vibrations from a mathematical viewpoint

Henk Broer, Marcello Seri and Floris Takens

March 22, 2023

Contents

Preface	9
Preamble: oscillations and mathematics	11
1. It oscillates by itself	19
1.1. The pendulum, the spring and some other examples	19
1.1.1. The pendulum	19
1.1.2. The spring	21
1.1.3. The U-pipe	24
1.1.4. The L-C circuit	25
1.1.5. On modeling	26
1.2. The pendulum as a spring: linearization	27
1.3. The phase plane and the line element field	29
1.3.1. The phase plane	29
1.3.2. Line element fields	38
1.4. Energy	40
1.4.1. Kinetic and potential energy	40
1.4.2. Conservation of energy	42
1.4.3. Energy conservation and the phase portrait . .	43
1.5. Period of oscillation	46
1.5.1. A general expression for the period of oscillation	49
1.5.2. Spring and pendulum	50
1.6. Exercises	52
1.6.1. The vertical spring	52
1.6.2. The horizontal pendulum	52
1.6.3. Symmetries of the line elements field	53

1.6.4. Ellipses and time rescalings on the spring	53
1.6.5. Amplitudes and energies	54
1.6.6. Phase portraits	54
1.6.7. The cycloid	55
1.6.8. Huygens's isochronous and tautochronous curve	56
1.6.9. Period and surface	57
1.6.10. Elliptic integrals	58
1.6.11. The potential energy of the pendulum	59
2. It oscillates in resonance	61
2.1. Friction	61
2.1.1. A friction directly proportional to the velocity .	61
2.1.2. The R-L-C circuit	63
2.2. Loss of energy due to friction	65
2.2.1. When the undamped motion oscillates	66
2.2.2. The general case	68
2.3. The damped harmonic oscillator with periodic forcing, resonance	72
2.3.1. "The" solution in the harmonic case	74
2.3.2. Resonance in harmonic oscillators with periodic forcing	76
2.4. Resonance in non-harmonic oscillators with periodic forcing	79
2.4.1. Parametric resonance	79
2.4.2. Josephson junction	81
2.5. The stabilization of oscillations	81
2.5.1. First attempt	83
2.5.2. Second attempt	84
2.5.3. Third attempt	84
2.6. Exercises	86
2.6.1. Negative damping	86
2.6.2. Tossing a fair coin	86
2.6.3. A "controlled" oscillator	86
2.6.4. A damped oscillator with forcing	87
2.6.5. The Van der Pol-Liénard differential equation .	88

3. Oscillations in daily life	91
3.1. Two further examples of oscillators	94
3.1.1. A plank bridge	94
3.1.2. Rolling of a ship	95
3.2. Coupling finitely many oscillations	96
3.2.1. Lissajous figures	97
3.2.2. Beats	100
3.2.3. More than two degrees of freedom	109
3.3. Vibrations of continuous media	110
3.3.1. Discretizing the continuum	110
3.3.2. Strings, beams, etc.	123
3.3.3. Other vibrational phenomena	127
3.4. Relaxation oscillations	130
3.5. Exercises on Hooke's n -body problem	134
Appendices	135
A. Johann Bernoulli's brachistochrone	137
A.1. Geometric optics	138
A.1.1. Fermat implies Snell	139
A.1.2. A conservation law	141
A.2. The brachistochrone as a light ray	144
A.3. Scholium	146
B. Small oscillations and the Foucault problem	149
B.1. Beats revisited	149
B.2. The Foucault pendulum	153
B.2.1. The spherical pendulum	154
B.2.2. Small oscillations	156
B.2.3. Spherical precession	156
B.3. Scholium	158
B.4. Another exercise of Bottema	160
C. Chaos in periodically forced oscillators	161
C.1. The Hénon attractor	162
C.1.1. Iterating a map	162

Contents

C.1.2. The Benedicks-Carleson Ansatz	166
C.2. The stroboscopic map	168
C.2.1. Determinism again	168
C.2.2. The stroboscopic phase portrait	169
C.2.3. Hénon-like strange attractors	171
C.3. Scholium	172
C.3.1. Return map and Poincaré map	173
C.3.2. Towards an understanding of chaos	173
C.3.3. Without friction	174
D. More on resonance	177
D.1. Huygens's clocks	179
D.2. Arnold resonance tongues and fractal geometry	179
D.3. A theoretical digression into circle maps	181
D.3.1. Denjoy and Kolmogorov	183
D.3.2. The Arnold family of circle maps	185
D.3.3. A second digression, on topology and on measure theory	187
D.3.4. Back to Huygens's clocks	188
D.4. Parametric resonance: Mathieu's equation and the like	189
D.5. Scholium	194
D.5.1. Quasiperiodic Hill versus Schrödinger	194
D.5.2. Celestial resonance	199
D.5.3. A final exercise on Kepler's third law	205
E. Solutions of selected exercises	209
E.1. Exercises from Chapter 1.6	209
E.1.1. Exercise 1.6.1	209
E.1.2. Exercise 1.6.2	210
E.1.3. Exercise 1.6.3	211
E.1.4. Exercise 1.6.4	212
E.1.5. Exercise 1.6.5	213
E.1.6. Exercise 1.6.6	214
E.1.7. Exercise 1.6.7	215
E.1.8. Exercise 1.6.8	217

E.1.9. Exercise 1.6.9	217
E.1.10. Exercise 1.6.10	218
E.1.11. Exercise 1.6.11	219
E.2. Exercises from Chapter 2.6	220
E.2.1. Exercise 2.6.1	220
E.2.2. Exercise 2.6.2	221
E.2.3. Exercise 2.6.3	223
E.2.4. Exercise 2.6.4	224
E.2.5. Exercise 2.6.5	225
E.3. Exercise from Chapter 3	227
E.4. Exercise from Appendix B	229
E.5. Exercise from Appendix D	230

Preface

This book started in the 1980's as a syllabus for teacher courses in mathematics, that were widely visited. At the time differential equations were included in the school curriculum and a mathematical treatment of *oscillations* was well in reach of the audiences. Later on the syllabus was also used by master and graduate students, in particular a few times for didactical projects at secondary schools. In the book Christiaan Huygens's work on the pendulum clock and on resonance phenomena plays a fundamental role.

In the present version we revise the material with fresh eyes and include appendices on chaos and resonance, subjects that have developed greatly since the 1980's. Among other things we include a few celestial resonances. Also, we could not help ourselves from adding an appendix on Johann Bernoulli's brachistochrone which happens to be the cycloid, also the curve that Huygens made extensive use of. Moreover, there is the Groningen connection, where Bernoulli worked from 1695 till 1705 lived and worked. Another appendix deals with small oscillations, among other things applied to the Foucault experiment to show the rotation of the earth; here also spherical precession will be discussed, a phenomenon that complicates the Foucault experiment and briefly mention the role that Heike Kamerlingh Onnes played here.

Since Floris Takens had a profound influence on the original contents, but also since he played a major role in the later developments, we found it appropriate to add his name posthumously as

Contents

a co-author. We thank Jan Epema and the late Max Kuipers for their help in preparing the original syllabus. ...

Henk Broer and Marcello Seri
Groningen, Spring 2023

Preamble: oscillations and mathematics

At the time of the ancient Greeks, geometry, arithmetic and algebra were already playing a leading role in mathematics and astronomy [116, 133]. We have to wait until the 16th and 17th century for infinitesimal considerations to seriously enter the picture, in the end leading to the differential and integral calculus we know today. The development of these *new methods* went hand in hand with gaining astonishing new insights in mechanics and optics. Nowadays we speak of classical mechanics and geometric optics. These developments mark the beginning of the *scientific revolution*.

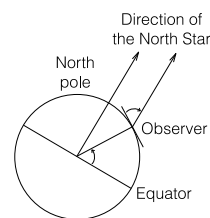
Classical mechanics studies phenomena of motion, for example all kinds of vibrations and oscillations. Other examples are provided by the rotating and oscillatory motion of the planets and moons of our solar system, the study of which is central in celestial mechanics. Both examples are governed by the same principles.

Proper celestial observations started alongside the introduction of telescopes, with the effect of bridging optics and mechanics. Although these subjects seem far apart, we must realize that precise celestial observations also need good clocks and such clocks require oscillating devices to function, like a regularly moving pendulum or a vibrating balance spring.

Navigation on the open sea

Travel across deserts and seas has been a prime motivation for these developments. Indeed, from early on, some knowledge of celestial phenomena and the corresponding time tables has been indispensable for determining the travelers position on earth and the direction to travel in. And when ships no longer stayed close to the coast, navigation became an increasingly difficult problem. Indeed, how to determine one's position on the open sea? Nowadays with the Global Positioning System (GPS) this seems a piece of cake, but at those times it surely was a big issue.

Determining the latitude on the Northern hemisphere is relatively easy. The North Star, or Polaris, is an almost fixed point in the sky very close to the northern celestial pole. With help of a sextant one can, at least in principle, determine the angle between the North Star and the horizon. This angle is exactly the northern latitude of your position, see the figure on the side.



The determination of the longitude, however, is a quite different matter [125]. For this, one needs a clock that keeps track of, say, the Greenwich time. Sailors on board, then, can determine 12 noon local time by shooting the sun. If the time difference is T hours, then the longitude equals

$$T \times \frac{360}{24} = 15 T \text{ degrees.}$$

So the real problem is to have a good clock on board that is synchronous with Greenwich. The development of such a clock touches on one of the themes of this book, also compare with [30].

Huygens and some other names

A few of the names that were important for the era at hand are Galileo Galilei (1564-1642), Johannes Kepler (1571-1630), Christiaan Huygens (1629-1695), Isaac Newton (1643-1727), Gottfried Wilhelm Leibniz (1646-1716) and Johann Bernoulli (1667-1748).

Next to geometry, arithmetic and algebra as inherited from the ancient Greeks, a *new method* was developed where infinitesimal considerations began to play a serious role. This eventually led to the differential and integral calculus as this is known to us now and where the main players in the era under consideration were Newton, Leibniz and also Bernoulli. Among other things this led to a full mathematical understanding of Kepler's work on the solar system.

Galileo laid the mathematical foundation of this development, by developing the telescope and by deducing the first kinetic theory of celestial bodies based on a principle of relativity and heliocentrism. This took place half a century before calculus was born.

The torch was carried further by Huygens in his groundbreaking *Horologium Oscillatorium* [82, 1] on the pendulum clock, which forms a major inspiration for the present book. He used intricate infinitesimal considerations with amazing results, but only at the end of his life, on the instigation of Leibniz, he developed plans to learn 'real' calculus.

Huygens life time fell in the Dutch Golden Age that roughly runs from 1588 to 1672. For general background see Israel [83]. This was a period of great wealth for the Republic of the United Netherlands. The *Vereenigde Oost-Indische Compagnie* (VOC) caused trade to expand quickly, which attracted immigrants and stimulated the growth of the main cities and ports. In this age the Dutch trade, industry,

Contents

science and art as well as the military were among the most acclaimed in the world.

Christiaan Huygens was born as the son of Constantijn Huygens (1596-1687), a well-known poet, composer and diplomat in which capacity he was secretary to the Princes of Orange Frederik Hendrik and Willem II. Christiaan as a young man already was outstanding in his ability to solve problems in mathematics and mechanics. In 1644 he took up studies in mathematics and law, at first at Leiden University, and later in Breda. Under the influence of the Princes of Orange Maurits and especially the more enlightened Frederik Hendrik, these cities had an excellent capacity for teaching and, thanks to the intellectual freedom, also for science. Many scientists and philosophers from abroad fled, looking for shelter in the Netherlands, which contributed to a stimulating and high intellectual atmosphere.

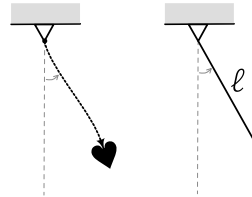
Christiaan Huygens was both a scientist and an engineer, compare with [2, 3, 21, 54, 126, 132, 140]. His more theoretical work ranges from mechanics and optics to astronomy; we already mentioned his *Horologium Oscillatorium*. In particular he also wrote about Saturn's rings. Concerning his practical work, he invented and improved various instruments like lenses, microscopes, telescopes and clocks. Huygens had a great international reputation: From 1663 on he was a Fellow of the Royal Society in London and between 1666 and 1683 he was Directeur de Récherche at the Académie des Sciences in Paris.

A few problems of Huygens

Galileo had already observed that the period of oscillation of a pendulum is independent of its mass and that, for small deflections, this period is approximately independent of the amplitude. These discoveries inspired a closer investigation of the pendulum motion.

So Huygens, both for their practical applications and for a deeper understanding of these phenomena, posed the following problems.

1. What is generally understood by a pendulum is a mathematical ideal of a 'real' pendulum. For instance, in the mathematical pendulum we assume that all mass is concentrated in one point. What should be the length ℓ of an ideal pendulum to ensure that it moves exactly as the 'real' one?
2. What is the exact period of oscillation of a pendulum as a function of its length and especially of the amplitude of oscillation?



It was already known that this period is not constant, but increases with the amplitude.

3. The motion of a pendulum mass can be thought of as that of a bead that slides without friction along a circular wire under the influence of constant gravity. Is there a wire profile along which the period of oscillation is exactly independent of the amplitude?

The curve Huygens was looking for is now known as the *isochronous curve*.

The first and third of these problems were rather nasty in Huygens's time and formed exactly the kind of problems that motivated the further development of the calculus. Since then they have become rather simple exercises, compare with Section 1.6. Indeed, from our approach it directly follows that the isochronous curve, which is ac-

tually called cycloid, is also the *tautochronous* curve along which the down time of the bead is the same from whatever height it drops. Due to Johann Bernoulli we know that the curve is also *brachistochrone*: along this curve it takes the shortest time for the bead to descend. In an appendix we shall see how intimately intertwined mathematics, mechanics and optics are in Bernoulli's solution.

The second problem turned out to be surprisingly more difficult and to remain so.

Later developments

Since then, research on oscillations has continued steadily and expanded. One direction of interest was the study of sound and light in terms as vibrational phenomena. In the 19th century the electromagnetic oscillations ensuing from the theory of James Clerk Maxwell (1831-1879) form a milestone in this development. At each occasion new aspects were discovered. In the 20th century the development of electronics surfaced all kinds of questions. This period often is referred to as the *radio time*. One of the pioneers in this direction is the Dutch physicist Balthasar van der Pol (1889-1959), a long time member of the Philips Research Laboratories.

The discipline of dynamical systems, which includes the study of oscillators in networks of other dynamical agents, has been growing in complexity over the last century. New phenomena that showed up were *multi- or quasiperiodicity* and *chaos*. The development was further stimulated by the use of numerical methods and the upcoming of electronic computers.

In a couple of appendices we touch on a few of these newer aspects.

Outline of what follows

We conclude this preamble with an outline of what follows. In the first chapter *It oscillates by itself* we are led by the second and third problem of Huygens. We present the pendulum as an example of an oscillator without friction and deal with such oscillations in a geometric fashion. In the second chapter *It oscillates in resonance* also frictional and external forces come into play. By means of a number of mechanical and electronic examples we encounter the phenomenon of *resonance*. The third chapter *Oscillations in daily life* gives some examples of oscillations as they occur in a string, in sound, water, etc. These phenomena have a more complex nature than the previous ones, since apart from motion in time also spatial configurations like *waves* become important. All chapters are closed by a number of exercises the solutions of which are sketched in an appendix.

The book closes with a number of appendices which may be of interest to the reader, but where often somewhat more advanced mathematics is being used. The first appendix is devoted to Bernoulli's brachistochrone problem, where mathematics, mechanics and optics are nicely intertwined. The second appendix *Small oscillations and the Foucault problem* deals with the theory of small oscillations as these occur in linearizations of coupled oscillators. As one 19th century application we deal with the Foucault experiment, designed to demonstrate the rotation of the earth, and also reveal the phenomenon of spherical precession which complicates this set-up. A third appendix *Chaos in periodically forced oscillators* treats aspects of the more recent chaos theory as this occurs in the present context. Here we shall meet the partly experimental *Benedicks-Carleson Ansatz* which forms a structuring element. The fourth appendix *More on resonance* expands Chapter 2 in various ways and discusses another problem of Huygens, concerning synchronization of weakly coupled pendulum clocks, as a leading example. It turns out that

Contents

fractal sets form an intrinsic component of the theory. Finally we also reveal part of the extremely rich subject of *celestial resonances*. The book closes with an appendix *Solutions of selected exercises*.

1. It oscillates by itself

In this chapter we only consider frictionless motions. As we shall see, this means that the energy remains preserved during the motion.

1.1. The pendulum, the spring and some other examples

1.1.1. The pendulum

The pendulum consists of a weight of mass m attached to a rigid rod of length ℓ which is suspended from a pivot. For simplicity, we assume that the weight is a point mass (or material point) and that the rod is massless.

We assume that the motion occurs in a vertical plane, under the influence of a constant gravitational acceleration g . As we know from elementary mechanics, the gravitational force acting on the material point then is mg pointing in the downward direction. This force can be decomposed into two components, one parallel to the motion of the material point and one orthogonal to it, see

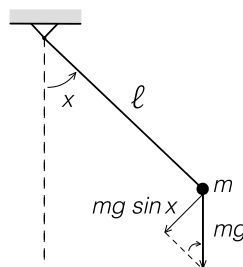


Fig. 1.1: Pendulum

1. It oscillates by itself

Figure 1.1. A simple trigonometric observation shows that the parallel component is given by $-mg \sin x$, where x denotes the angle between the rod and its equilibrium position, increasing from left to right. This is the force acting on the material point in the angular direction.

By the rigidity of the rod, the point mass is constrained to move on a circle arc. If the angle x is expressed in radians, the distance between the material point and its equilibrium position along the circle is given by the arclength ℓx .

It is our aim to describe the motion of the pendulum. Therefore we need to find out how the angle x changes with respect to the time t . In other words, the motion is going to be a function $t \mapsto x(t)$. The relation between the force acting on a system and its motion is provided by Newton's well-known law

$$F = m a, \quad (1.1)$$

where F denotes the force, m the mass of the material point, and a its acceleration [104]. Due to the rigidity of the rod, no motion takes place in the radial direction, and therefore Newton's law will only effect the angle x . By definition, the acceleration is the rate of variation of the velocity, which in turn is the rate of variation of the position. This mathematically translates to

$$a = \frac{d^2(\ell x)}{dt^2} = \ell \frac{d^2x}{dt^2},$$

where $\frac{d^2x}{dt^2}$ denotes the second derivative of the function $t \mapsto x(t)$.

Replacing F and a in Newton's law we obtain

$$-mg \sin x = m\ell \frac{d^2x}{dt^2}$$

or, more concisely,

$$\frac{d^2x}{dt^2} = -\frac{g}{\ell} \sin x. \quad (1.2)$$

- Remark 1.**
1. Note that we already tacitly used Newton's law when we said that the gravitational force equals mg , where indeed g is the constant gravitational acceleration.
 2. Observe that in equation (1.2), which completely determines the motion of the pendulum, the mass m plays no role. As mentioned in the Preamble, the independence of the motion of the pendulum from its mass m , was already established experimentally by Galileo.

Newton himself uses the notation \dot{x} and \ddot{x} for differentiation. So

$$\dot{x} = \frac{dx}{dt} \quad \text{and} \quad \ddot{x} = \frac{d^2x}{dt^2}. \quad (1.3)$$

Many authors have adopted this dot-notation, and from now on we will also do this.

Equations like (1.2) are called *differential equations*. To solve this equation we have to find an unknown function $t \mapsto x(t)$ that satisfies the equation (1.2), that is

$$\ddot{x}(t) = -\frac{g}{\ell} \sin x(t)$$

for all t .

1.1.2. The spring

A point mass with weight m is attached to a wall by a spring. We assume that the point can move on the horizontal plane without friction; in this way its motion is not affected by gravity. Compare Figure 1.2. Furthermore, we denote by x the distance of the point mass from the equilibrium position: the position in which the spring is

1. It oscillates by itself

neither compressed nor extended. As before, if we know x as a function of time t , we can describe completely the motion of the point mass.

The force acting in this new setting is the restoring force of the spring, in the opposite direction of the deviation from the equilibrium. According to Hooke's law, this force is proportional to the deviation

$$F = -kx,$$

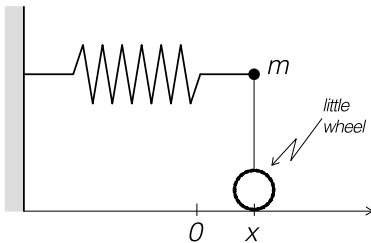


Fig. 1.2: Spring

where the positive proportionality constant k , called the *spring constant*, is a property of the spring in question. Newton's law again provides the connection between force and motion:

$$-kx = m\ddot{x},$$

or

$$\ddot{x} = -\frac{k}{m}x. \quad (1.4)$$

Remark 2. We like to point out that we kept gravity out of the game by assuming that the motion was horizontal. In Exercise 1.6.1 we shall discuss what happens when the spring is mounted vertically so that gravitation also plays a role.

Equation (1.4) can be explicitly solved by

$$x(t) = A \cos(\omega t) + B \sin(\omega t) \quad \text{where} \quad \omega = \sqrt{\frac{k}{m}}. \quad (1.5)$$

Here A and B are arbitrary. We can just consider them as generic constants and check that all the functions of the form (1.5) satisfy

the equation (1.4). The actual choice of A and B depends on position and velocity of the system at time $t = 0$, or at any other fixed time for the matter. For convenience one normally uses $t = 0$. Computing the velocity out of (1.5)

$$\dot{x}(t) = -A\omega \sin(\omega t) + B\omega \cos(\omega t), \quad (1.6)$$

then using (1.5) and (1.6) we conclude

$$A = x(0) \quad \text{and} \quad B = \frac{1}{\omega} \dot{x}(0).$$

When taking, for instance, $x(0)$ and $\dot{x}(0) = \left. \frac{dx}{dt} \right|_{t=0}$ both equal to 0, the system remains at rest. Indeed, this implies $A = B = 0$ and by (1.5) we find that $x(t) = 0$ for all t .

By a simple geometric consideration one can rewrite (1.5) in the more compact form

$$x(t) = R \cos(\phi - \omega t), \quad (1.7)$$

where R and ϕ have taken the role of A and B . Indeed, we can mimic the previous computation of $x(0)$ and $\dot{x}(0)$ as

$$x(0) = R \cos \phi \quad \text{and} \quad \dot{x}(0) = R\omega \sin \phi.$$

Figure 1.3 shows the graph of the function (1.7). The maximal extension R is called the *amplitude* of the vibration or oscillation. As one can also see from the picture, the *period* or *vibration time* or the *period of oscillation* is $2\pi/\omega$ and thus its *frequency*, i.e., the number of oscillations per second, is $\omega/2\pi$. We call ω the circular or angular frequency.

Remark 3. 1. The frequency of all the oscillations is $\omega/2\pi$ and therefore independent of R .

1. It oscillates by itself

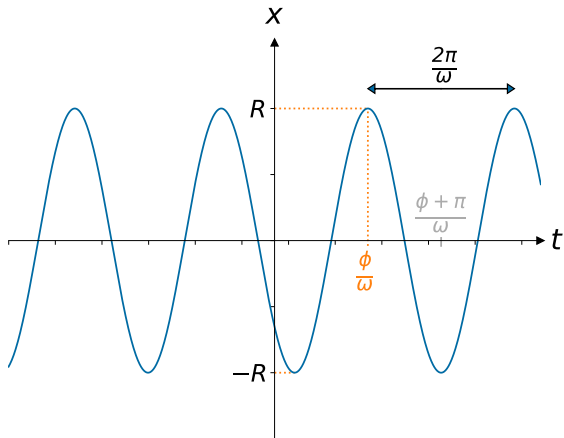


Figure 1.3: Vibration (1.7) of the spring

2. The definition $\omega = \sqrt{\frac{k}{m}}$ implies that ω is larger if the mass is smaller and the spring stiffer: loose springs with large masses are slower than stiff springs with small masses. Does that reflect your experience?

1.1.3. The U-pipe

In this example we consider a U-shaped pipe of constant section containing some liquid, see Figure 1.4. The pipe is open above, allowing the fluid to move freely. By the principle of communicating vessels, when the liquid is at rest, it will be at the same height in both pipes.

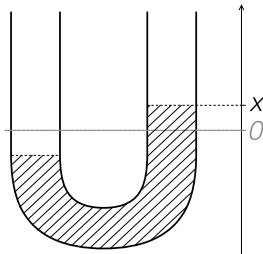


Fig. 1.4: U-pipe

Denote by x the height of displacement of the liquid from its equilibrium position as depicted in Figure 1.4.

Also in this case, we want to apply Newton's law and describe the motion of the liquid level.

Let ρ be the specific weight of the liquid and O the surface area of the horizontal cross-section of the pipe legs. Then, the restoring force is given by the extra weight of the liquid in the column. If M denotes the total mass of the liquid, then

$$M \frac{d^2x}{dt^2} = -2 O \rho g x.$$

We end up with an equation that is of the same type as (1.4), which we just derived for the spring! Therefore, the motion is again of the form (1.7) where

$$\omega^2 = 2 \frac{O \rho g}{M}.$$

1.1.4. The L-C circuit

This final example comes from electricity theory. Suppose you have a circuit with a capacitor of capacitance C and an inductor coil with inductance L . A current with intensity I flows through the circuit, as depicted in Figure 1.5.

Let V_L denote the voltage across the inductor and V_C the voltage across the capacitor. By Kirchoff's law, the sum of the voltages across the elements in the circuit equals 0:

$$V_C + V_L = 0. \quad (1.8)$$

Moreover, the constitutive relations for the circuit elements provide the following ad-

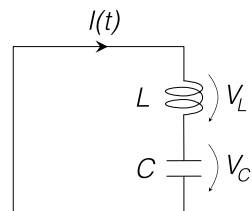


Fig. 1.5: *L-C circuit*

1. It oscillates by itself

ditional relations:

$$I = C \frac{dV_C}{dt} \quad \text{and} \quad V_L = L \frac{dI}{dt}. \quad (1.9)$$

Differentiating (1.8) gives

$$\frac{dV_C}{dt} + \frac{dV_L}{dt} = 0,$$

which, by (1.9), can be rewritten as

$$\frac{I}{C} + L \frac{d^2 I}{dt^2} = 0,$$

or, again adopting the dot-notation (1.3),

$$\ddot{I} = -\frac{1}{CL} I.$$

And again, this equation is of the same type as equation (1.4), and once more the motion is of the form (1.7) with $\omega^2 = 1/LC$.

Remark 4. Kirchoff's law (1.8) is stricter than

$$\frac{dV_C}{dt} + \frac{dV_L}{dt} = 0.$$

This is not a problem here, since $I = C dV/dt$ implies that V_C is only determined up to an additive constant. Therefore it is always possible to ensure that (1.8) holds true.

For general physics background we refer to [119].

1.1.5. On modeling

In the four examples of this section we obtained equations of motions, under assumptions that do not hold for real systems. To be-

gin with, in all the examples we neglected frictional forces: air resistance, friction at the suspension points, electrical resistance, surface friction in the pipes, etc. We will return to this in the next chapter, in particular we will see how friction will cause all oscillations to die out.

Another problem in our hypotheses is the following. The pivot of most pendulums cannot constrain them to only vertical oscillations. Small perturbations can make the motion considerably more complicated than the one described by equation (1.2). The same applies when reducing material bodies with a physical dimension to point masses.

However, all this does not diminish the usefulness of our considerations. In general one should understand this in the following way. Our equations of motion describe idealized *models* of the physical reality. They only describe reality to a certain extent: by approximation or by the representation of only certain aspects.

1.2. The pendulum as a spring: linearization

In Section 1.1.1, we derived the equation of motion for the ideal pendulum (1.2) in a form that, to some extent, resembles the equation of motion of the spring (1.4):

$$\begin{aligned}\ddot{x} &= -\omega^2 \sin x, & \omega &= \sqrt{g/\ell} && \text{(pendulum),} \\ \ddot{x} &= -\omega^2 x, & \omega &= \sqrt{k/m} && \text{(spring).}\end{aligned}$$

However, while the latter admits solutions in closed form as (1.5) or (1.7), this is not so straightforward for the former.

We now introduce an approximation of the pendulum equation as follows. Observe that the line $y = x$ at $(x, y) = (0, 0)$ is tangent to the

1. It oscillates by itself

curve $y = \sin x$, a statement also expressed by the famous limit

$$\lim_{x \rightarrow 0} \frac{\sin x}{x} = 1.$$

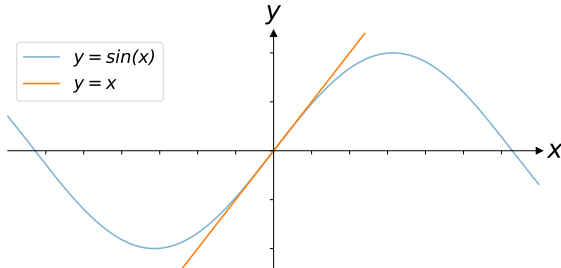


Figure 1.6: $\sin x \approx x$

Therefore, in a small neighborhood of the origin, the function $x \mapsto \sin x$ is well approximated by $x \mapsto x$. For x small, we can approximate the equation of motion of the pendulum (1.2) by

$$\ddot{x} = -\frac{g}{\ell}x.$$

Since this has the same form as the spring equation (1.4), its solutions are given by (1.7):

$$x(t) = R \cos(\phi - \omega t) \quad \text{where} \quad \omega = \sqrt{\frac{g}{\ell}}.$$

In other words, for *small oscillations*, the pendulum oscillates like a spring with stiffness $k = g/\ell$ and mass $m = 1$.

Remark 5. As already observed for the spring, we see that in the small oscillations approximation all the solutions have the same frequency

$$\frac{1}{2\pi} \sqrt{\frac{g}{\ell}},$$

independent of the amplitude of the oscillation.

This again corresponds to an experimental fact already known to Galileo, as mentioned in the Preamble: the oscillation time of a pendulum with small oscillations is approximately independent of their amplitudes.

The technique presented in this section is called *linearization*: we replaced the curve $y = \sin x$ by the straight line $y = x$. Such approach is widely applied in practice to attack a large variety of problems. We will get back to this in Chapter 3 and in Appendix B.

1.3. The phase plane and the line element field

Until now we focused on two types of differential equations, namely

$$\ddot{x} = -x \quad \text{and} \quad \ddot{x} = -\sin x, \quad (1.10)$$

where, for simplicity, all the constants have been normalized to 1. For the first type, we could easily compute all the solutions in dependence of the time t , but for the second one we are not so lucky; below we shall return to this particular problem. This is why other means have been developed to say something about the behavior of the solutions, even without having an explicit formula for them. As we will see, these means have a strong geometric character.

1.3.1. The phase plane

Instead of considering a differential equation involving a second derivative, we can view the equations of motion as a system of dif-

1. It oscillates by itself

ferential equations in which only first derivatives occur.

We then try to find to solve for two unknown functions x and y of the time t , where $x(t)$ denotes the *position* of the point particle at time t and $y(t)$ its *velocity* at that time. In the case of our examples in (1.10) we get

$$\begin{cases} \dot{x} = y \\ \dot{y} = -x \end{cases} \quad \text{and} \quad \begin{cases} \dot{x} = y \\ \dot{y} = -\sin x \end{cases} \quad (1.11)$$

recalling the dot-notation (1.3). The top equation is always the same, it is just the definition of velocity. We can further reduce these systems to a single differential equation by eliminating time and taking y as a function of x . This can be done with the help of the chain rule

$$\frac{dy}{dt} = \frac{dy}{dx} \frac{dx}{dt} \quad \text{or, in other words,} \quad \frac{dy}{dx} = \frac{\frac{dy}{dt}}{\frac{dx}{dt}}.$$

This reduces the systems in (1.11) to

$$\frac{dy}{dx} = -\frac{x}{y} \quad \text{and} \quad \frac{dy}{dx} = -\frac{\sin x}{y}. \quad (1.12)$$

Both of these equations can be solved fairly easily by quadrature, i.e., in terms of integrals. Indeed, just writing

$$y dy = -x dx \quad \text{and} \quad y dy = -\sin x dx$$

and integrating, for the former we obtain

$$x^2 + y^2 = C, \quad (1.13)$$

where $C \geq 0$ is an arbitrary constant, and for the latter

$$y^2 = 2 \cos x + C, \quad (1.14)$$

where $C \geq -2$ is also arbitrary.

The (x, y) -plane that contains the solution curves of a system of differential equations like (1.11), is called the *phase plane*. Below, we shall see that we are developing a method to describe situations that are far more general than the pendulum or the spring.

Determinism. Indeed, the phase plane is an extremely important tool in the study of physical phenomena such as oscillations. The reason for this is the following. For the general theory, the solution curve $(x(t), y(t))$ for systems like the one in (1.11) is uniquely determined by the state $(x(0), y(0))$ at $t = 0$. In more mundane terms, if for a system like the spring or the pendulum the position *and* the velocity at any given moment is known, then position and velocity are determined for the entire future of the system. This is a consequence of Newton's law, which says that to describe the motion of a system we only need to look at its acceleration

$$a = \ddot{x} = \dot{y}$$

and that higher derivatives of x with respect to t are not needed. The mathematical background of this is the Theorem of Existence and Uniqueness of solutions of *first order* differential equations [81].

- Remark 6.**
1. *You can check for yourself that such determinism of the future does not apply if you only look at the position $x(0)$: $x(t)$ for $t > 0$ can not be determined by the mere position $x(0)$ alone.*
 2. *In general we call systems of the form (1.11) deterministic: the state at one moment determines the entire evolution. Here it is important that the system is autonomous, i.e., that the right hand side does not explicitly depend on t . In Appendix C we shall come back to this.*

This is a characterisation as opposed to, for instance, stochastic, in which case randomness comes into play.

Motion in the phase plane. In the remainder of this section we study the motion of systems in the phase plane. Here we have to bear in mind, that the actual (physical) motion that we observe is

1. It oscillates by itself

only the first component $x(t)$, i.e., the position. To visualize also the velocity component $y(t)$, we would need the help of a more technical tool such as, for instance, the tachometer of a car.

The motion in the phase plane is propagated by the *velocity vector*

$$\begin{pmatrix} \dot{x} \\ \dot{y} \end{pmatrix} = \begin{pmatrix} \frac{dx}{dt} \\ \frac{dy}{dt} \end{pmatrix}$$

as a function of t . On the one hand, there is the *velocity* of the motion

$$\dot{x} = y,$$

while on the other we have the *acceleration* of the above motion

$$\dot{y} = \ddot{x}.$$

In the equations in (1.12) we have eliminated the time t . The advantage of this is that we could easily determine the integral curves of those systems in the phase plane, particularly in the cases (1.13) and (1.14). We have to realize that this came with a cost: by eliminating time we have lost the time parametrization of the integral curves.

In the next section we will relate our observations with the *conservation of energy*. However, before moving on we look at our examples one more time.

The spring

We start recalling the relevant equations:

$$\ddot{x} = -x \quad \text{or} \quad \begin{cases} \dot{x} = y \\ \dot{y} = -x, \end{cases}$$

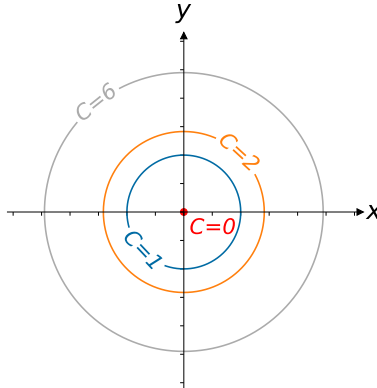


Figure 1.7: Integral curves of the spring

with integral curves $x^2 + y^2 = C$, $C \geq 0$, see (1.13). This is a family of circles centered at the origin $(x, y) = (0, 0)$ and parametrized by C (i.e., with radius \sqrt{C}). What can we learn from this?

To begin with, each solution $t \mapsto (x(t), y(t))$, of the system of differential equations moves in the (x, y) -plane along one of these circles. Position and velocity at a particular moment, say at $t = 0$, uniquely identify this circle: after all, only one circle in the family of circles passes through the point $(x(0), y(0))$. But there is more.

We can also reconstruct *how* the point $(x(t), y(t))$ moves along the circle as a function of t , this despite the fact that we have apparently eliminated time from our problem. The answer lies in the fact that $y = \dot{x} = \frac{dx}{dt}$, so $y(t)$ is the x -component (i.e., the horizontal component) of the velocity vector

$$\begin{pmatrix} \dot{x} \\ \dot{y} \end{pmatrix} = \begin{pmatrix} \frac{dx}{dt} \\ \frac{dy}{dt} \end{pmatrix}$$

at time t , and that the velocity vector has to be tangent to the circle, thereby completely fixing this velocity vector.

1. It oscillates by itself

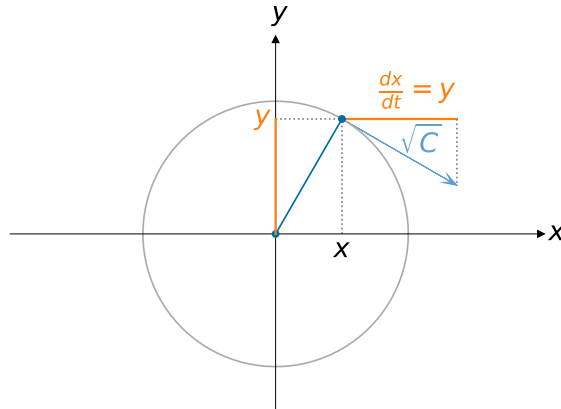


Figure 1.8: Reconstructed velocity vector of the spring

To illustrate this, in Figure 1.8 we have fixed an arbitrary point (x, y) on a circle $x^2 + y^2 = C$. The velocity vector points along the tangent to the circle at the point (x, y) and its x -component is equal to y . We now see two congruent triangles rotated over 90° with respect to each other. Therefore, the length of the velocity vector has to be equal to the circle radius, which in this case is \sqrt{C} . This means that the point $(x(t), y(t))$ moves clockwise with uniform velocity \sqrt{C} along the circle $x^2 + y^2 = C$ (you could also say that it moves with uniform angular velocity -1).

When comparing these observations with the explicit solutions (1.7) for this case

$$\begin{aligned} x(t) &= R \cos(\phi - t) \\ y(t) &= \dot{x}(t) = R \sin(\phi - t) \end{aligned}$$

we also see that the point $(x(t), y(t))$ moves clockwise at uniform velocity R along the circle $x^2 + y^2 = R^2$. As you can see, both descriptions match exactly if we take $R = \sqrt{C}$.

Remark 7. 1. There is a special integral curve $x^2 + y^2 = C$ with

$C = 0$. What motion of a spring or a (linearized) pendulum does this correspond to?

- We call the oscillations $x = x(t)$ of the spring with equation $\ddot{x} = -x$ harmonic as they are the projection of uniform circular motions. This terminology goes back to the ancient Greeks.

In Exercise 1.6.4 you can see that we can interpret similarly also the oscillations of the more general equation $\ddot{x} = -\omega^2 x$.

In general we shall call any mechanical, electronic or other system described by such an equation of motion a harmonic oscillator. In Figure 1.9 we show how the above picture and the graph of the trajectory are related to each other.

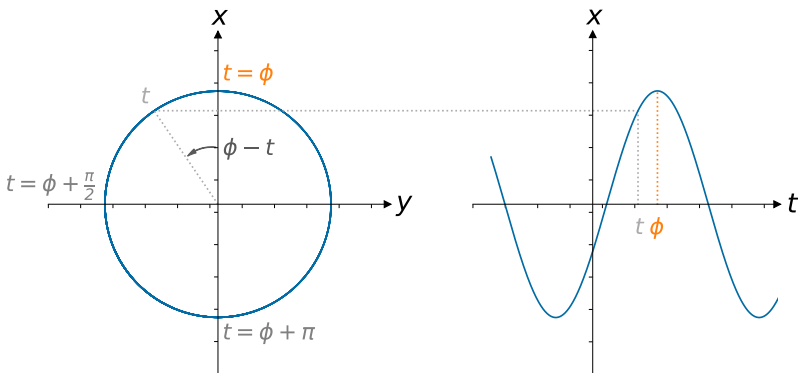


Figure 1.9: Oscillation related to circular motion in the phase plane

The pendulum

Next consider the pendulum equation

$$\ddot{x} = -\sin x \quad \text{or its system form} \quad \begin{cases} \dot{x} = y \\ \dot{y} = -\sin x, \end{cases}$$

1. It oscillates by itself

with integral curves $y^2 = 2 \cos x + C$, $C \geq -2$, see (1.14). By plotting the integral curves $y = \pm \sqrt{2 \cos x + C}$ for various values of C , we find the following, compare with Figure 1.10.

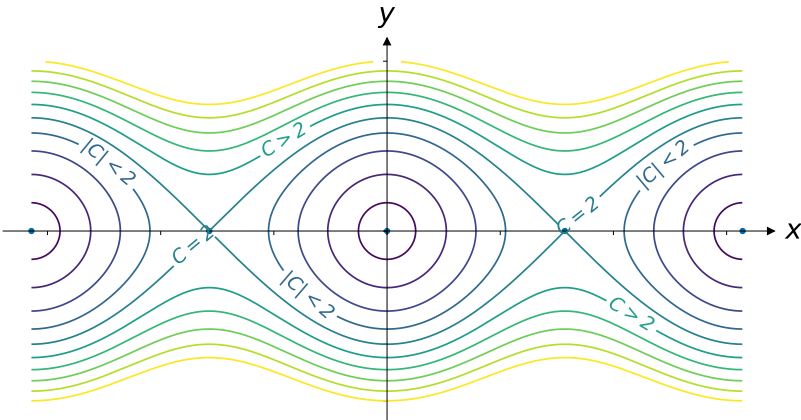


Figure 1.10: Integral curves of the pendulum

1. For $C = -2$ only the points $(x, y) = (2k\pi, 0)$ with integer k , satisfy the equation. Each such point represents a “motion” of the pendulum where constantly $x(t) = 2k\pi$ and, also constantly, $y(t) = \dot{x}(t) = 0$: the pendulum is at rest in its lowest position. These *singular points* therefore correspond to the *stable equilibrium position* of the pendulum.
2. For $-2 < C < 2$, the domain of the functions $\pm \sqrt{2 \cos x + C}$ is constrained by $\cos x \geq -\frac{C}{2}$. At the boundary points the tangent lines are vertical. Together he two graphs describe a closed oval curve centered around the points $(x, y) = (2k\pi, 0)$. Such curves correspond to “ordinary” oscillations of the pendulum around its stable equilibrium point.

You can check that the point $(x(t), y(t))$ traverses the curve in finite time, the *period of oscillation*, also see Section 1.5, after which the pendulum returns to the original position and

velocity: the motion is periodic. You can also see that the amplitude always remains smaller than π .

3. For $C > 2$, the functions $\pm\sqrt{2\cos x + C}$ are defined for all real values of x . Their graph corresponds to motions where the pendulum “has a turnover”. In the equation with the plus sign, $\dot{x} = y > 0$: $x(t)$ is increasing as a function of t and therefore the pendulum moves counter clockwise. Similarly, for the minus sign the motion goes clockwise. As you can see in Figure 1.10, the velocity of the pendulum is maximal at its lowest position $x = 2k\pi$, and minimal at $x = (2k+1)\pi$, when it passes through its upside down position.
4. For $C = 2$ the curves are at the boundary of the regions of ordinary oscillations and of turning over motions. The points $x(t) = ((2k+1)\pi, 0)$ are special here: they are also *singular* but correspond to the *unstable equilibrium* in which the pendulum is at rest in its upside down position.

Moreover, there are two possible motions of the pendulum, both starting and ending in this unstable equilibrium: one going clockwise and the other counter clockwise. A further difference between these motions and the previous ones, is that they last *infinitely long*: the velocity vector $(\dot{x}, \dot{y}) = (y, -\sin x)$ decreases to 0 as it approaches the singular points $((2k+1)\pi, 0)$.

We conclude that the formula $y = \pm\sqrt{2\cos x + C}$, together with the above figure, contains a great deal of information on the motion of the pendulum. We repeat that this is especially important since, as opposed to the harmonic oscillator, for the pendulum there is no explicit time-parametrized solution, like (1.5) or (1.7).

Remark 8. 1. In the case 2 of “ordinary” oscillations, again con-

1. It oscillates by itself

sider the velocity vector

$$\begin{pmatrix} \dot{x} \\ \dot{y} \end{pmatrix} = \begin{pmatrix} y \\ -\sin x \end{pmatrix}.$$

A direct computation shows that its length is always greater than or equal to $\sqrt{1 - C^2/4}$:

$$\begin{aligned} \dot{x}^2 + \dot{y}^2 &= 2 \cos x + C + \sin^2 x \\ &= C + 2 - (1 - \cos x)^2 \\ &\geq C + 2 - \left(1 + \frac{C}{2}\right)^2 = 1 - \frac{C^2}{4}. \end{aligned}$$

This immediately implies that the oval curves are traversed in finite time.

2. The geometric reconstruction of the velocity vector

$$\begin{pmatrix} \dot{x} \\ \dot{y} \end{pmatrix}$$

from the integral curves $y^2 = 2 \cos x + C$, $C \geq -2$, runs exactly as for the spring in Section 1.3.1: indeed, this reconstruction only relies on the fact that $\dot{x} = y$ and that the velocity vector always is tangent to the integral curve.

Pictures like Figures 1.7 and 1.10 are generally called *phase portraits*. These phase portraits depict characteristic integral curves of the systems of differential equations (1.11), with an arrow indicating the direction in which the point $(x(t), y(t))$ moves along the curve.

1.3.2. Line element fields

Let us return to the differential equations (1.12), now written as

$$x \, dx + y \, dy = 0 \quad \text{and} \quad \sin x \, dx + y \, dy = 0.$$

These equations define *line element-* or *direction fields*, in the (x, y) -plane. The direction is given at each point (x, y) by the respective velocity vectors,

$$\begin{pmatrix} y \\ x \end{pmatrix} \quad \text{or} \quad \begin{pmatrix} y \\ -\sin x \end{pmatrix} :$$

the corresponding ratios $-\frac{x}{y}$ and $-\frac{\sin x}{y}$ precisely are the *slopes* of the corresponding integral curve $y = y(x)$ at the point x . See Figure 1.11 below for the case of the spring. This idea can be extended to any

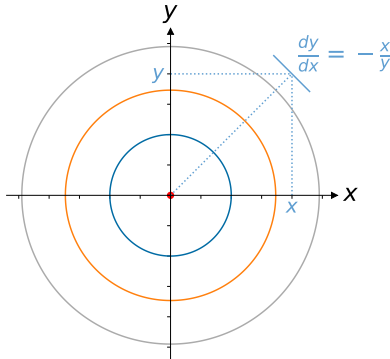


Figure 1.11: Line element related to the spring

differential equation of the form

$$\ddot{x} = F(x), \tag{1.15}$$

where $F(x)$ can be interpreted as the force that “sustains” the motion. Using the familiar formulæ $\dot{x} = \frac{dx}{dt} = y$ and $\dot{y} = \frac{dy}{dt} = F(x)$, we arrive at the line element field

$$-F(x) dx + y dy = 0.$$

How can we perform the geometric reconstruction of the velocity vector from the line element in this general case?

In the next section we develop a general method to describe the integral curves belonging to a differential equation of the form (1.15) or, in other words, to describe its phase portrait.

1.4. Energy

For both the pendulum and the spring almost all motions are periodic: the system returns to a previous state and the motion repeats itself. This suggests that no *energy* is lost throughout the evolution of the system. In what follows we will investigate this conjecture in detail.

1.4.1. Kinetic and potential energy

Let us consider an oscillating system with sustaining force $F = F(x)$. We saw at the end of the last section that its equation of motion is given by (1.15)

$$\ddot{x} = F(x).$$

For simplicity we assume that for the point mass we always have $m = 1$. In the phase plane we get the system of equations

$$\begin{cases} \dot{x} = y \\ \dot{y} = F(x). \end{cases}$$

Because we assumed $m = 1$, the *kinetic energy* of the state (x, y) with velocity $y = \dot{x}$ is given by $\frac{1}{2}y^2$: this is a well-known formula from early mechanics courses, think of “ $\frac{1}{2}mv^2$ ”.

Next, let us look at the *potential energy* of the system. To this end we generally define

$$V(x) = - \int_0^x F(s) \, ds. \quad (1.16)$$

The integral is the total amount of *work* done (or the energy that has to be delivered) to bring the system from the position 0 to the position x . Physically it is important that the variable x (and therefore

also s) describes a *real distance* and not an angle, as for example in the pendulum, compare see Exercise 1.6.11. To fix thoughts let us first consider a few examples.

1. Considering free fall motion of a mass $m = 1$ in a constant gravitational field with acceleration g , the force is $F(s) = -g$ for any height s . The corresponding potential energy $V(x)$ of the point mass at height x then is

$$V(x) = - \int_0^x F(s) \, ds = gx.$$

Again, a well known formula: think of “ mgh ”.

2. One way to obtain the “good” potential energy for the pendulum is to consider it as a special case of the above item 1. In that case, the height can be computed as $\ell(1 - \cos x)$, see Figure 1.12. Therefore

$$V(x) = g\ell(1 - \cos x).$$

See also Section 1.6.11.

3. In the case of the spring, only the sustaining force $F(s) = -ks$ plays a role. Using the definition (1.16), we obtain

$$V(x) = - \int_0^x F(s) \, ds = \frac{1}{2}kx^2.$$

The lower limit 0 in the integral defining the potential (1.16) is not really important, you can just as well take another constant. This is due to the fact that only *differences* in potential energy play a role in the equations of motion. You can immediately see this from the formulas. Indeed, from the definition it immediately follows that

$$F(x) = -\frac{dV}{dx}(x),$$

therefore an additive constant in $V(x)$ will not affect the equation of motion $\ddot{x} = F(x)$.

1. It oscillates by itself

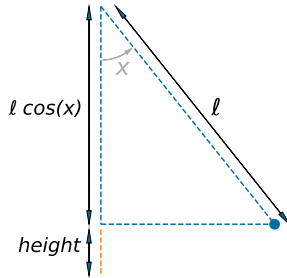


Figure 1.12: The height of the point mass of the pendulum

1.4.2. Conservation of energy

In our case where the mass $m = 1$, the total energy of the system in the state (x, y) is given by

$$H(x, y) = \frac{1}{2}y^2 + V(x). \quad (1.17)$$

The title of this section seems to imply that energy is conserved, but what does that mean?

Suppose that, at some moment $t = t_0$, the system is in the state $(x, y) = (x(t_0), y(t_0))$ with energy $H(x, y) = E$. Then H should have the same value E for all t , i.e.,

$$H(x(t), y(t)) = E \quad \text{for all } t.$$

Note that in an oscillating system like the spring, in general both x and $y = \frac{dx}{dt}$ keep changing all the time, and therefore also both the kinetic energy $\frac{1}{2}y^2$ and the potential energy $V(x)$. The fact that the total energy H is conserved means that there is a continuous conversion of the kinetic energy into potential energy and vice versa. We now mathematically show that energy conservation indeed does apply.

Theorem 1. *The curve determined by the equation $H(x, y) = E$ is an integral curve of the line element field $y \, dy - F(x) \, dx = 0$.*

Proof. We take the equation $H(x, y) = E$ and (1.17) and solve for y :

$$y = \pm \sqrt{2(E - V(x))}.$$

For such a graph we find

$$\frac{dy}{dx} = \pm \frac{\frac{dV}{dx}(x)}{\sqrt{2(E - V(x))}} = \frac{F(x)}{y},$$

which exactly means that it solves the equation $y \, dy = F(x) \, dx$. \square

Without giving a proof, we state that there is at most one integral curve of $y \, dy - F(x) \, dx = 0$ passing through each point of the (x, y) -plane. Theorem 1 then tells us exactly what these integral curves are: they are formed by all the possible curves with equation $H(x, y) = E$. A curve $H(x, y) = E$ is called the *energy level* with energy E .

But why is the entire plane filled by energy levels? In the above proof we have been a bit sloppy with the case $y = 0$. See the Exercises 1.6.3 and 1.6.4 and the corresponding parts in Appendix E. We will also come back to this in Section 2.2.2.

1.4.3. Energy conservation and the phase portrait

We can now use Theorem 1 to determine the phase portrait of our system.

For the spring with spring constant $k = 1$ we have $F(x) = -x$. We can take as potential $V(x) = \frac{1}{2}x^2$, to get total energy $H(x, y) = \frac{1}{2}y^2 + \frac{1}{2}x^2$.

1. It oscillates by itself

The energy level with energy E is therefore the curve

$$\frac{1}{2}y^2 + \frac{1}{2}x^2 = E.$$

And again we find the circles that we already met in the previous section.

In exactly the same way we can find the integral curves of the pendulum, taking m, ℓ and g all equal to 1. After all, now $F(x) = -\sin x$ and we can choose $V(x) = 1 - \cos x$, obtaining $H(x, y) = \frac{1}{2}y^2 + 1 - \cos x$. The energy level $H(x, y) = E$ is then described by

$$y = \pm \sqrt{2(E - \cos x - 1)},$$

again see above.

The general case

Returning to the general case, from the relation $y = \pm \sqrt{2(E - V(x))}$ we can graphically determine the integral curves for any given potential energy V .

Suppose the function V , around some minimum, is given by the graph in Figure 1.13. For E we fix some value. The function V attains this value for $x = x_{\min}$ and $x = x_{\max}$. Since $\frac{1}{2}y^2 \geq 0$ for any value of y , we know that the motion with energy E must be confined to the interval $x_{\min} \leq x \leq x_{\max}$: after all we must always have $V(x) \leq E$. Moreover, the formula also implies that at x_{\min} and x_{\max} we have $y = 0$ and at the minimum V_{\min} we have $y = \pm \sqrt{2(E - V_{\min})}$.

In Figure 1.13 we presented a schematic sketch of the integral curve. In Exercise 1.6.6, you can experiment yourself with a number of potential energy functions (also known as *potentials*) and with the corresponding phase portraits. In the same exercise you are also asked

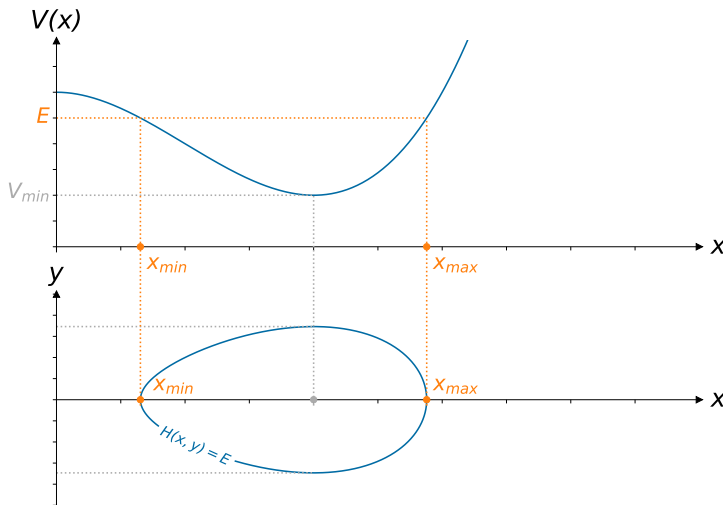


Figure 1.13: Potential V with a minimum and a corresponding integral curve

to derive a number of general characteristics of the phase portrait from the shape of the graph of V .

Let us briefly return to the idea of the bead that slides frictionless along a wire (or the marble rolling in a gutter); also compare one of Huygens's problems mentioned in the Preamble.

There is a very pictorial way to imagine motion of a system with potential function $V = V(x)$, as the one outlined in Figure 1.14 and energy E .

You can think of this as the motion of a bead that slides back and forth along a wire shaped as the graph of the function $x \mapsto V(x)$. You can then imagine that the bead is

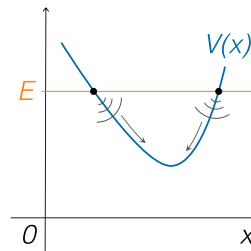


Fig. 1.14: Sliding or rolling in a potential well

1. It oscillates by itself

released at some height E , falls down – thereby gaining velocity and therefore kinetic energy – and then again climbing the wire, slowing down until the height E is reached again.

However nice this thought may be, we have to keep in mind that this is only approximately correct: unless you use the arclength parameter along the wire instead of the variable x , the shape of the wire and that of the graph of the function $x \mapsto V(x)$ do not exactly match.

For instance, for the pendulum the shape of the wire is circular, but $V(x) = 1 - \cos x$. In Exercise 1.6.8 we will return to this, as well as to the problem of designing a wire the potential energy of which is exactly equal to $V(x) = \frac{1}{2}\omega^2 x^2$, i.e., of the harmonic oscillator. This will be the way to solve Huygens's problem of finding an isochronous curve as described in the Preamble. Also see the comments in Remark 5.

Two examples

We conclude this section with two examples of a given graph $V = V(x)$, where we sketch the corresponding phase portraits. See the Figures 1.15 and 1.16. Note that the scales on the x -axis and y -axis are not equal.

1.5. Period of oscillation

Although we can compute at any point (x, y) the velocity vector $(y, F(x))$, we still have effectively lost the ability to determine the global behaviour of the system as a function of time. However, when studying oscillatory motion it is useful to have an expression in terms of

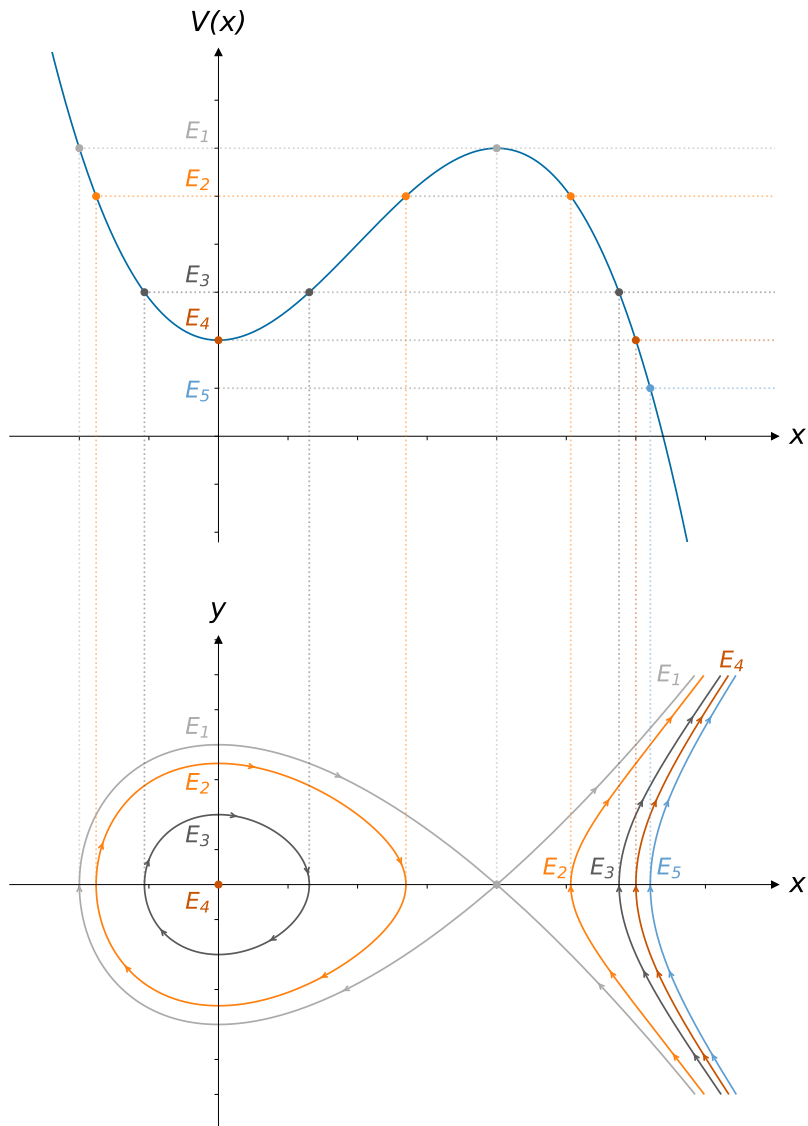


Figure 1.15: *Phase portrait of a potential V with a minimum and a maximum, the corresponding singularities are called center and saddle point; can you imagine what the term “saddle point” refers to?*

1. It oscillates by itself

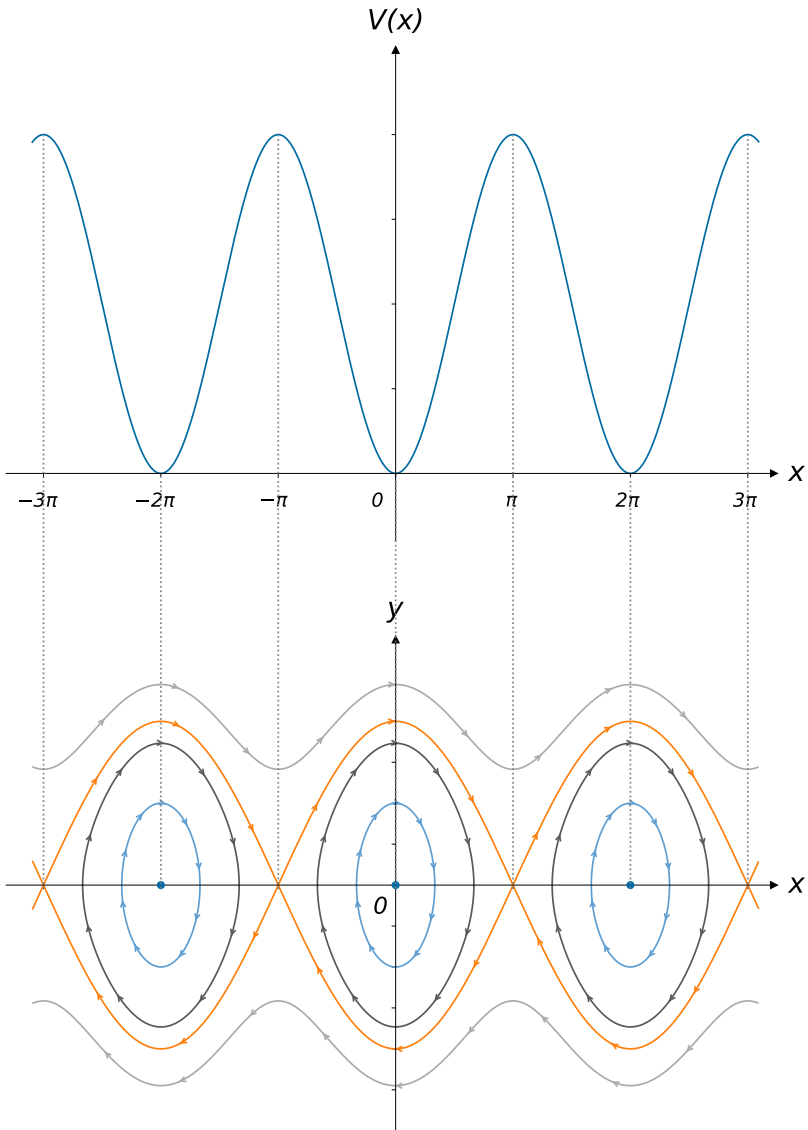


Figure 1.16: Phase portrait of the pendulum with potential $V(x) = 1 - \cos x$

the potential V for the *period of oscillation*. This is a classical issue, compare Huygens's problems mentioned in the Preamble. This problem will be addressed now.

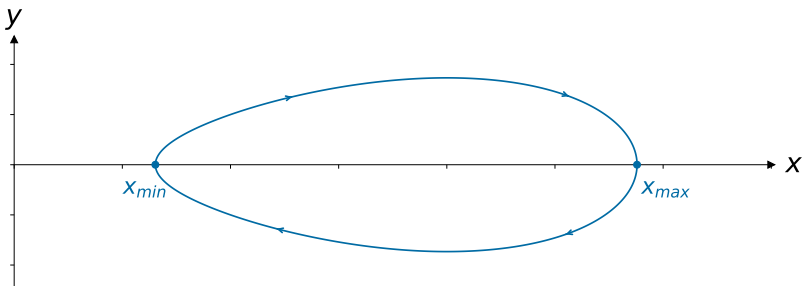


Figure 1.17: One oscillatory motion

1.5.1. A general expression for the period of oscillation

Let us assume that the oscillatory motion occurs in the energy level E with $x_{\min} \leq x \leq x_{\max}$, see Figure 1.17. As before, we can rewrite the equation $H(x, y) = E$ as $y = \pm\sqrt{2(E - V(x))}$. Using the fact that $y = \frac{dx}{dt}$, we get

$$dt = \frac{dx}{y} = \pm \frac{dx}{\sqrt{2(E - V(x))}}.$$

Putting the pieces together and integrating from x_{\min} to x_{\max} , we get the *half period*

$$\frac{1}{2}P(E) = \int_{x_{\min}}^{x_{\max}} \frac{dx}{\sqrt{2(E - V(x))}}.$$

The fact that the integral is half of the period follows from a symmetry consideration: indeed, the motion is symmetric under reflection in the x -axis, compare Exercise 1.6.2.

1. It oscillates by itself

1.5.2. Spring and pendulum

Again consider the example of the spring

$$\ddot{x} = -x,$$

where we choose $V(x) = \frac{1}{2}x^2$. Then for $E > 0$ we find

$$x_{\min} = -\sqrt{2E} \quad \text{and} \quad x_{\max} = +\sqrt{2E},$$

which implies

$$P(E) = 2 \int_{-\sqrt{2E}}^{\sqrt{2E}} \frac{dx}{\sqrt{2E - x^2}}.$$

This integral can be explicitly computed with some knowledge of elementary calculus, from which we recall that

$$\frac{d}{dx} \arcsin x = \frac{1}{\sqrt{1-x^2}}.$$

This directly gives

$$P(E) = 2\pi,$$

which is independent of the energy E . This *isochrony* is not new: we already observed this in Remark 1.

The pendulum case

$$\ddot{x} = -\sin x,$$

we find, together with Huygens, far more interesting. In this case, given the energy E , we have

$$P(E) = 2 \int_{x_{\min}}^{x_{\max}} \frac{dx}{\sqrt{2\cos x + 2E - 2}}. \quad (1.18)$$

This integral turns out to be very difficult to compute. It has even been *proven* that the integral cannot be expressed in terms of “elementary” functions. Such integrals also emerge when one tries to

find a general solution for the pendulum in terms of time parametrization. It turns out that similar integrals occur in the computation of the arclength of an ellipse, reason why one speaks of *elliptic integrals*. Also compare Exercise 1.6.10.

Remark 9. 1. *Be that as it may, but having a closed expression (1.18) at our possession is convenient. Indeed, it enables us to approximate the period of oscillation, for instance by numerical means.*

2. *Elliptic integrals have kept mathematicians busy throughout the centuries, and even today they remain a subject of active research – in particular their algebraic and geometric properties.*

We conclude this section with a comment on the period of the pendulum which follows without any calculation. Choosing again the potential energy $V(x) = 1 - \cos x$, the oscillating motions take place in energy levels E for $0 < E < 2$, see Section 1.3.1. The closer E is to 2, the closer the corresponding integral curve passes along the unstable equilibrium of the upside down pendulum. This equilibrium indeed occurs exactly at the energy level $E = 2$.

Since the velocity vector $(y, -\sin x)$ near the equilibrium gets smaller, the motion of the point $(x(t), y(t))$ on the integral curve gets slower. As a result, the period of oscillation $P(E)$ increases as E approaches 2. In fact, one can show that

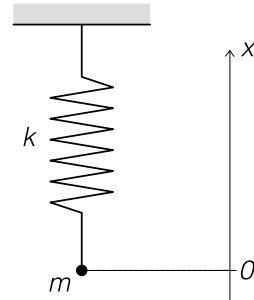
$$\lim_{E \nearrow 2} P(E) = \infty.$$

One immediate consequence of this is that the period of oscillation of the pendulum varies with the energy (and therefore the amplitude) of the oscillation, and is not constant as with the spring. We express this by saying that the pendulum is an *anisochronous* oscillator.

1.6. Exercises

1.6.1. The vertical spring

Given is a point particle with mass m at the end of a vertically suspended spring. We indicate its position of by x : the x -axis therefore is vertical. The point $x = 0$ corresponds to the position at which the spring is at rest: the spring is stretched to compensate the gravity $-mg$ acting on the mass. We assume that, according to Hooke's law, the spring exerts a force that is proportional to deviation:

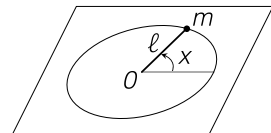


$$F(x) = -kx.$$

1. At what height is the point mass at rest?
2. Find the equation of motion for $x(t)$.
3. Determine the solutions of the equation of motion.

1.6.2. The horizontal pendulum

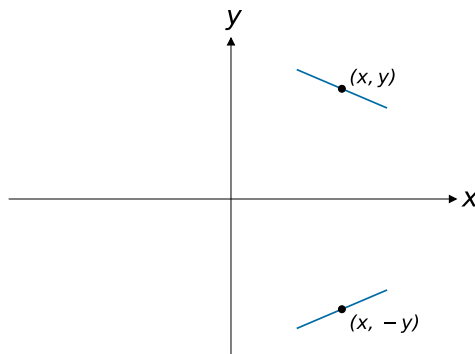
Consider a pendulum with length ℓ and mass 1 in the horizontal plane. The pendulum can rotate without friction around a fixed point O . If x denotes the displacement angle with respect to a given axis, give the equation of motion for $x(t)$ and determine all its solutions.



Sketch a phase portrait. In what way can this pendulum be interpreted as a limit of the usual vertical pendulum?

1.6.3. Symmetries of the line elements field

Show that the line elements field $y \, dy - F(x) \, dx = 0$ is symmetric with respect to reflections in the x -axis. I.e., if the direction of the field at a point (x, y) is (ξ, η) , its direction at the point $(x, -y)$ is given by $(\xi, -\eta)$. What does this imply for the directions at points of the x -axis? What does this imply for the integral curves?



1.6.4. Ellipses and time rescalings on the spring

Consider a point particle of mass $m = 1$ attached to a spring with stiffness k . The potential (or potential energy) of the spring is $V(x) = \frac{1}{2}kx^2$.

1. Determine the equation of the energy level E in the phase plane, give a sketch.

1. It oscillates by itself

2. Show that the energy level becomes a circle if you replace y with $z = y/\sqrt{k}$.
3. Check that by rescaling the time with $\tau = t\sqrt{k}$, the equation of motion becomes $\ddot{x} = -x$. How is this related to the previous point?

1.6.5. Amplitudes and energies

Consider a spring with potential $V(x) = \frac{1}{2}kx^2$ and a pendulum with potential $V(x) = -\frac{g}{\ell} \cos x$. In both cases, compute the amplitude of the oscillation in terms of the energy. (The amplitude is half of the difference between the maximum and minimum value that the x coordinate assumes throughout the periodic motion.)

1.6.6. Phase portraits

A number of potential functions are outlined in Figure 1.18. Sketch the corresponding phase portraits and discuss the effect of (local) maxima and minima and of horizontal asymptotes on how the level curves fill up the phase plane.

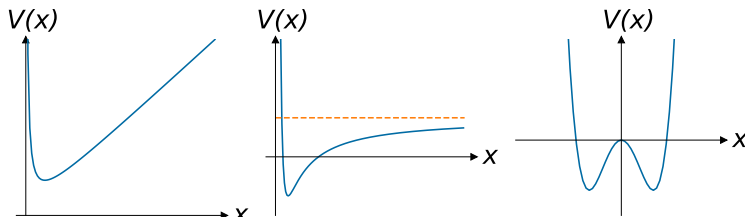
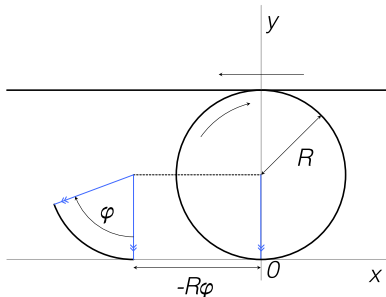


Figure 1.18: Potential energy profiles. From left to right: $V(x) = x + \frac{1}{x}$, $V(x) = \frac{4}{x^2} - \frac{8}{x} + 2$ and $V(x) = x^4 - 2x^2$

1.6.7. The cycloid

If one rolls a bicycle wheel on the ground, ensuring that it always moves in the same vertical plane, then its valve describes a curve that is called *cycloid*. Here we will study the case of a bicycle wheel rolling along the ceiling. You can see the latter depicted on the right: R denotes the radius of the wheel and φ the angular displacement of the valve from the vertical direction. The position of the valve on the circle is indicated by a double arrow.



1. Use the figure to show that the following is a parametrization of the cycloid

$$\begin{cases} x(\varphi) = -R(\varphi + \sin \varphi) \\ y(\varphi) = R(1 - \cos \varphi). \end{cases}$$

In the sequel we shall refer to R as the *radius* of the cycloid and to φ as its *rolling angle*, see Appendix A.

2. Sketch the cycloid in the (x, y) plane for $-\pi \leq \varphi \leq \pi$. Does this curve have any symmetries? Where does it have a horizontal tangent? And where a vertical one?
3. Let $s(\varphi)$ be the arclength of the cycloid, measured from $\varphi = 0$. Show that $s(\varphi) = R\sqrt{2(1 - \cos \varphi)} = 4R \sin\left(\frac{1}{2}\varphi\right)$.
4. Finally, show that

$$y(\varphi) = \frac{1}{8R}s^2(\varphi).$$

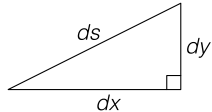
Hint for 2: in general, one can use the Pythagorean Theorem to

1. It oscillates by itself

compute the length of an infinitesimal piece of curve parametrized by some parameter ϕ .

Referring to the figure on the right we get

$$ds = \sqrt{\left(\frac{dx}{d\varphi}\right)^2 + \left(\frac{dy}{d\varphi}\right)^2} d\varphi.$$



If we now fill in the values for x and y from the first item of the exercise, we get

$$ds = R \sqrt{2(1 + \cos \varphi)} d\varphi = 2R \cos\left(\frac{1}{2}\varphi\right) d\varphi.$$

It then follows that $s(\varphi) = 4R \sin\left(\frac{1}{2}\varphi\right)$. Note that this is an arclength 'with sign' which can serve as a real coordinate with $\varphi = 0$ as the origin.

1.6.8. Huygens's isochronous and tautochronous curve

In the text we have seen that a bead that slides along a circular wire (or a marble that rolls into a circular gutter) corresponds to a potential $V(x) = 1 - \cos x$. Which potential corresponds to a bead that slides along a wire, bent according to a cycloid as in the previous exercise?

1. Show that the cycloid is an isochronic curve.
2. A *tautochronous* curve is defined by the fact that, from whatever height the bead is dropped, the the down time is always the same.

Show that the cycloid also is tautochronous.

1.6.9. Period and surface

Consider an oscillator with potential $V(x)$ as depicted in Figure 1.19. Let $A(E)$ be the area in the phase plane that is enclosed by the energy level $H(x, y) = E$ (shaded in the figure). Let $P(E)$ be the period of the oscillation with energy E . Show that the following holds

$$P(E) = \frac{dA(E)}{dE}.$$

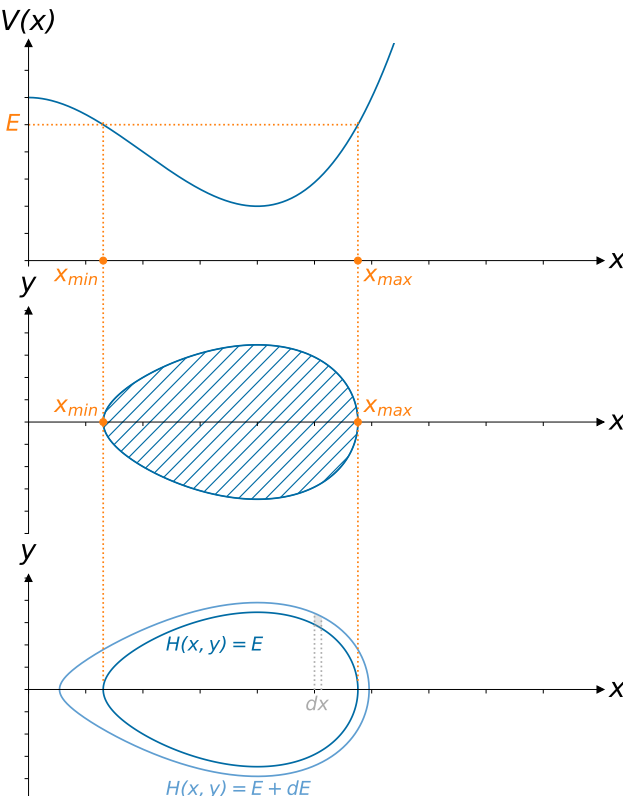


Figure 1.19: Phase portrait of an oscillator

1. It oscillates by itself

Hint: in the figure we indicated the energy level $H(x, y) = E$ along-side with $H(x, y) = E + dE$. Try to prove that the shaded area is equal to dE multiplied by the time that the oscillator needs to move from x_0 to $x_0 + dx$.

1.6.10. Elliptic integrals

When studying the period of oscillation of the pendulum we encountered elliptical integrals. By definition an elliptical integral is any expression of the form

$$\int R\left(x, \sqrt{P(x)}\right) dx$$

where $P(x)$ is a polynomial of degree 4 and where $R(x, y)$ is a rational function of x and y . I.e., $P(x)$ is a polynomial of the form $P(x) = \alpha + \beta x + \gamma x^2 + \delta x^3 + \epsilon x^4$ and $R(x, y)$ is the quotient of two polynomials in x and y , e.g.,

$$R(x, y) = \frac{x^2 - xy - y^3}{1 - x^2 + y^2}.$$

Show that the expression

$$\int \frac{dx}{\sqrt{2 \cos x + C}},$$

from Section 1.5.2 to describe the period of the pendulum, can be transformed into an elliptical integral by a substitution.

Show that calculating the arclength of a piece of ellipse (also) gives rise to an elliptical integral.

Hint: An ellipse is a curve that can be described by the equation

$$\frac{x^2}{a^2} + \frac{y^2}{b^2} = 1.$$

1.6.11. The potential energy of the pendulum

Derive the potential energy of the pendulum with length ℓ by using a variable u which, unlike the angle x , corresponds to a real distance and then applying

$$V(x) = - \int_0^x F(s) ds.$$

What happens if you directly compute the potential energy out of the equation of motion

$$\ddot{x} = -\frac{g}{\ell} \sin x,$$

so neglecting the fact that x is not a real distance?

2. It oscillates in resonance

If you look around, you will notice that almost nothing vibrates all “by itself” in the sense of the previous chapter. That is because, in reality, energy is always lost to frictional forces. Air resistance, friction at suspension points, electrical resistance: all possible causes for energy loss. In many cases the lost energy is converted into heat. If we do not exert any external forces on such a system with friction to keep the oscillation going, it will eventually “die out” and end up remaining in an equilibrium position. To prevent this, a pendulum clock is driven or forced by gravity – via the “weights” – or by a wound coil spring.

We will successively involve these two new effects into our story by introducing *friction* and *external forcing*, where our main interest goes to *forced oscillations* with or without friction.

2.1. Friction

2.1.1. A friction directly proportional to the velocity

How do we fit the frictional force into our mathematical description? In general, friction increases with increasing velocity: just think of air resistance. The easiest way to express this is to assume that the strength of the frictional force is directly proportional to the

2. It oscillates in resonance

velocity, i.e.,

$$W = -c\dot{x}, \quad c > 0. \quad (2.1)$$

From which the name of *Linear* or *Rayleigh* friction. The minus sign here is to indicate the “opposing” character of W . With help of Newton’s law we get the equation of motion

$$\ddot{x} = F(x) - c\dot{x}, \quad (2.2)$$

recalling that $\dot{x} = \frac{dx}{dt}$ and $\ddot{x} = \frac{d^2x}{dt^2}$. Here $F = F(x)$ is the usual sustaining force from the previous chapter. For the *pendulum* and the *harmonic oscillator* (e.g., the spring) this gives the following equations of motion

$$\ddot{x} = -\omega^2 \sin x - c\dot{x}, \quad \text{and} \quad (2.3)$$

$$\ddot{x} = -\omega^2 x - c\dot{x}. \quad (2.4)$$

Recall from Chapter 1 that for a pendulum of length ℓ in the constant gravitational field with acceleration g we have $\omega^2 = g/\ell$ and for a spring with mass m and stiffness k we have $\omega^2 = k/m$.

Remark 10. *A very different type of friction, the so-called Coulomb- or dry friction, looks like this*

$$W = \begin{cases} a & \text{if } \dot{x} < 0 \\ -a & \text{if } \dot{x} > 0 \end{cases}.$$

Of course there are more ways than (2.1) to translate into mathematics an increase in frictional force with velocity. From the physics point of view, (2.1) is not always a good choice: for instance, air resistance increases much faster at high velocities than in direct proportionality to the velocity.

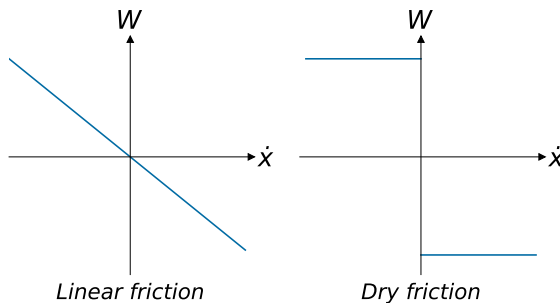


Figure 2.1: Linear versus dry friction

There are two reasons behind our choice of (2.1): firstly, it is not a bad description in many *practical* situations, and secondly, it is mathematically relatively easy to use.

Dry friction is briefly discussed in Chapter 3, also see Exercise 2.6.3.

2.1.2. The R-L-C circuit

This is another example from electronics. As we will see, in this case the “choice” (2.1) naturally follows from Ohm’s law. In the L-C circuit from Chapter 1, the resistance of the wires was neglected. Instead of ignoring it, we will now assume that the circuit contains a resistor with resistance R , which may also include separate additional resistors. According to Ohm’s law, the voltage difference V_R across the resistor is given by

$$V_R = IR$$

where, as before, I is the current. Kirchhoff’s law, then requires that

$$V_R - V_L + V_C = 0,$$

2. It oscillates in resonance

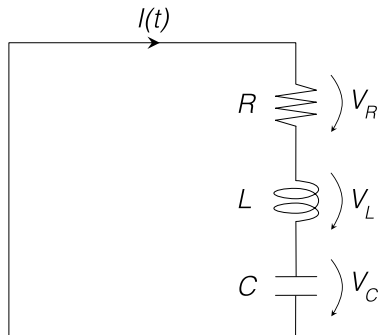


Figure 2.2: *R-L-C circuit*

which in this case, by a similar calculation as in the previous chapter, implies that

$$R \frac{dI}{dt} + L \frac{d^2I}{dt^2} + \frac{I}{C} = 0,$$

or

$$L \frac{d^2I}{dt^2} = -R \frac{dI}{dt} - \frac{1}{C} I.$$

Due to Ohm's law, the friction term now indeed is

$$W = -R \frac{dI}{dt},$$

which is of the form (2.1). The equation of motion thus becomes of type (2.2).

Remark 11. *In the present context friction takes on a different shape only in special physical conditions, such as with very high intensity of the current I or with superconductivity.*

2.2. Loss of energy due to friction

We have already mentioned the experimental fact that friction causes the motions to die out in equilibrium states. Instead of “friction” and “extinction”, people often say *damping*. We will study a mathematical description of damping and give phase pictures of the damped harmonic oscillator and of the damped pendulum.

In the previous section, we met the general equation

$$\ddot{x} = F(x) - c\dot{x} \quad (c > 0).$$

For a damped oscillator, special cases are (2.3) and (2.4) from Section 2.1.1: the pendulum and the harmonic oscillator, both with damping.

First again considering the phase plane, the equations of motion take the form

$$\begin{cases} \dot{x} = y \\ \dot{y} = F(x) - cy. \end{cases} \quad (2.5)$$

In analogy to Chapter 1, we set $F(x) = -\frac{dV}{dx}(x)$. Then, the total energy is $H(x, y) = \frac{1}{2}y^2 + V(x)$. Eliminating time t from (2.5) as before, we end up with the line element field

$$\frac{dy}{dx} = \frac{F(x)}{y} - c,$$

or

$$(cy - F(x))dx + ydy = 0.$$

Mathematically, we can translate that energy is lost during the motion into saying that for a solution $(x(t), y(t))$ of (2.5), the function $H(x(t), y(t))$ decreases with t . We will show that this is indeed the case (except at the equilibrium points), by looking at the line element field. Recall that the integral curves of this line element field correspond precisely to the integral curves $(x(t), y(t))$ of (2.5), see Section 1.3.

2.2.1. When the undamped motion oscillates

We first consider the following special situation: there is a value of the energy for which $H(x, y) = E$ is a closed curve in which the *undamped* motion oscillates (all values of E slightly above a local minimum in the potential function V have this property).

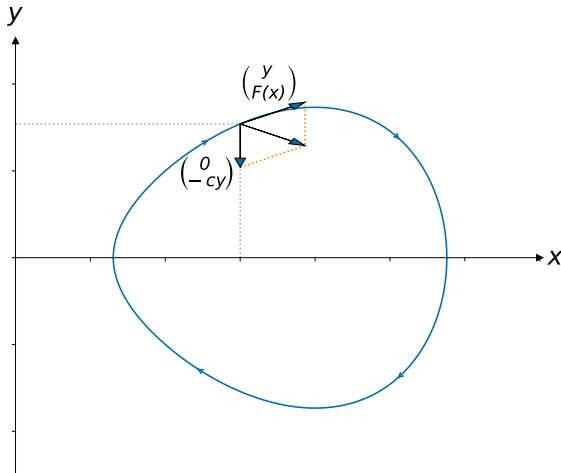


Figure 2.3: Integral curve of an oscillation

In a point (x, y) on the energy level with energy E , the line element is determined by the velocity vector $\begin{pmatrix} y \\ F(x) - cy \end{pmatrix}$. Now observe that

$$\begin{pmatrix} y \\ F(x) - cy \end{pmatrix} = \begin{pmatrix} y \\ F(x) \end{pmatrix} + \begin{pmatrix} 0 \\ -cy \end{pmatrix}.$$

Here $(y, F(x))$ is the velocity vector of the undamped system and therefore it is tangent to the curve $H(x, y) = E$; compare Section 1.4. The vector $(0, -cy)$ is vertical and points towards the x -axis (unless $y = 0$). This means that their sum points towards the inner area of the curve $H(x, y) = E$, see Figure 2.3, i.e., to the area in the phase

plane with *lower* energy. In turn this means that H decreases during the evolution of the system. So in case where the undamped motion oscillates, we are done.

Before we consider the general case, let us consider the damped harmonic oscillator

$$\ddot{x} = -x - c\dot{x},$$

so with $\omega = 1$. In the (x, y) -plane, this takes the form

$$\begin{cases} \dot{x} = y \\ \dot{y} = -x - cy, \end{cases}$$

Unless $x = y = 0$, the undamped motion always oscillates and our previous remarks apply. Since now $H(x, y) = \frac{1}{2}(x^2 + y^2)$, the energy levels are concentric circles around $(x, y) = (0, 0)$, see Section 1.4.

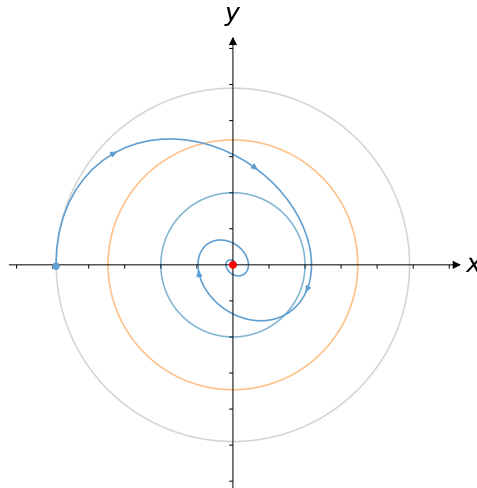


Figure 2.4: A typical damped oscillation in the phase plane

This means that the integral curves of the damped system are *spirals*, see Figure 2.4. (What is the direction on the x -axis? And on the y -axis?)

2. It oscillates in resonance

In this simple case the solution $x(t)$ can be written explicitly as

$$\begin{aligned}x(t) &= e^{-\frac{c}{2}t}(A \cos(\nu t) + B \sin(\nu t)) \\&= e^{-\frac{c}{2}t} R \cos(\phi - \nu t), \quad \text{where} \\v^2 &= 1 - \frac{c^2}{4}.\end{aligned}$$

Compare the formulæ (1.5) and (1.7) from Chapter 1. You can verify this just by substitution into the formula of the differential equation. Calculations can also confirm that the integral curves $(x(t), y(t))$ in the phase plane do have a spiral shape. For $c = \frac{1}{2}$ we gave numerical evidence for this in the Figures in Figures 2.5, 2.6 and 2.7. It is also useful to plot $x(t)$ and see how it changes as c gets larger, see Figure 2.6 and Figure 2.7. The oscillation for large c dampens very quickly.

Remark 12. *In this example we fixed $\omega = 1$. For a generic value of ω we have $v^2 = \omega^2 \left(1 - \frac{c^2}{4\omega^2}\right)$, compare this with an Exercise 1.6.4. Note that always $v \leq \omega$.*

2.2.2. The general case

We shall see that the considerations for the general case do not differ much from the previous ones. Due to the form of the energy function $H(x, y) = \frac{1}{2}y^2 + V(x)$, the vector $\begin{pmatrix} 0 \\ -cy \end{pmatrix}$ always points in the direction of lower energy. Indeed, since the vector $\begin{pmatrix} y \\ F(x) \end{pmatrix}$ is always tangent to the energy level, the sum $F(x) - cy$ necessarily must be always in the direction of lower energy.

Remark 13. *We have included the following calculation for those who know a bit about partial derivatives and the Chain Rule. In-*

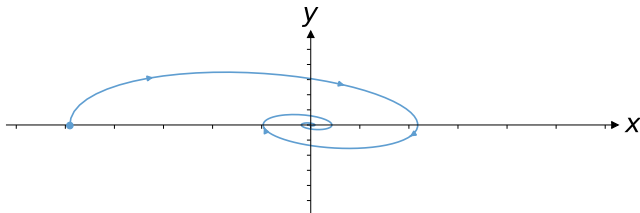


Figure 2.5: Damped oscillation in the phase plane with $\omega = 1$ and $c = \frac{1}{2}$

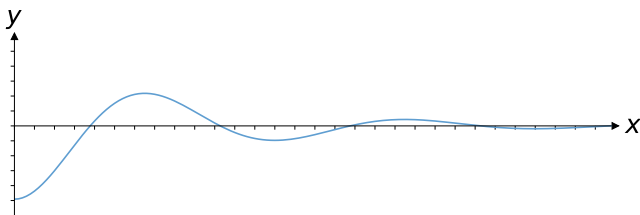


Figure 2.6: Plot of $x(t)$ with $c = \frac{1}{2}$

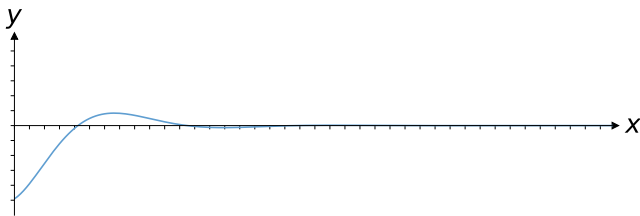


Figure 2.7: Plot of $x(t)$ with $c = 1$

2. It oscillates in resonance

indeed, starting out from the formulæ

$$H(x, y) = \frac{1}{2}y^2 + V(x) \quad (\text{energy})$$

$$F(x) = -\frac{dV}{dx}(x) \quad (\text{relationship between force and potential})$$

$$\begin{cases} \dot{x} = y \\ \dot{y} = F(x) - cy \end{cases} \quad (\text{damped equations of motion}),$$

we aim to investigate the change of H along an integral curve $(x(t), y(t))$ of these equations of motion. In fact we shall prove that

$$\frac{d}{dt} H(x(t), y(t)) = -cy^2(t)$$

which indeed means that the energy H decreases. (Why?)

Proof. The proof consists of a direct computation:

$$\begin{aligned} \frac{d}{dt} H(x(t), y(t)) &= \frac{\partial H}{\partial x}(x(t), y(t)) \frac{dx}{dt}(t) + \frac{\partial H}{\partial y}(x(t), y(t)) \frac{dy}{dt}(t) \\ &= \frac{dV}{dt}(x(t)) \cdot y(t) + y(t) \cdot \frac{dy}{dt}(t) \\ &= -F(x(t))y(t) + y(t)(F(x(t)) - cy(t)) \\ &= -F(x(t))y(t) + F(x(t))y(t) - cy^2(t) \\ &= -cy^2(t), \end{aligned}$$

as was to be proven. □

Note that this formula, applied for $c = 0$, again proves the proposition in Section 1.4.3, namely that in the undamped case the energy is a conserved quantity.

Let us explain our considerations in the case of the damped pendulum, for simplicity taking $g/\ell = 1$.

$$\ddot{x} = -\sin x - c\dot{x},$$

which in the phase plane takes the form

$$\begin{cases} \dot{x} = y \\ \dot{y} = -\sin x - cy \end{cases}. \quad (2.6)$$

As before, we choose as potential energy $V(x) = 1 - \cos x$. Then the

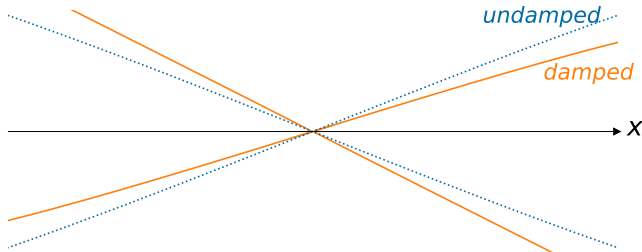


Figure 2.8: The saddle point equilibrium of the undamped and the damped pendulum

following holds.

1. It is easily seen that the equilibrium points (singularities) are the same as in the undamped case: $(x, y) = (k\pi, 0)$ for any integer number k .
2. For $0 < E < 1$ the undamped motion is an ordinary oscillation so, in that area of the phase plane we can apply the reasoning of Section 2.2.1: the integral curves spiral towards the equilibrium points $(x, y) = (2k\pi, 0)$ for integers k .
3. Without proof, we mention that the equilibrium points $(x, y) = ((2k+1)\pi, 0)$, k integer, remain “of the same type” as in the undamped case: these are again called *saddle points*. Compare with Exercise 1.6.6 and its solution in Section E.1.6; also see Section 1.4.3, in particular Figure 1.15

To explain this further we observe the following. These saddle-

points have two *incoming* and two *outgoing* integral curves, which have pairwise the same tangent line at the saddle point itself. The difference with the undamped situation is that these curves are shifted: upwards to the left of the saddle point and downwards to the right. See Figure 2.8.

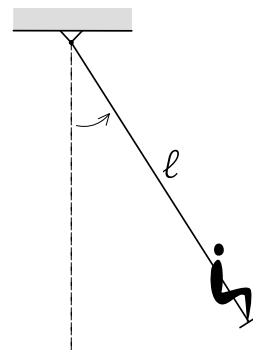
This is exactly the effect of the damping $\begin{pmatrix} 0 \\ -c_y \end{pmatrix}$ which is added to the velocity vector at each point (x, y) of the phase plane.

The consequence of the above considerations are sketched qualitatively in Figure 2.9. It may be clear how the other integral curves move in between.

It is not difficult to see that all solutions are moving towards an equilibrium point. Almost all of them go to $(x, y) = (2k\pi, 0)$ for integer k , corresponding to the stable equilibrium. Apart from periodicity in the x direction, there are *exactly two* integral curves ending up in the unstable equilibrium with the pendulum upside down.

2.3. The damped harmonic oscillator with periodic forcing, resonance

In this section we include external forces in the game that vary periodically in time. Just think of a swing that gets pushed periodically, or rather driven by a person that stands or sits on it while performing periodic motions. You can also think of a pendulum the suspension point of which moves periodically up and down, or of an R-L-C circuit powered by an alternating current generator. In this section we will limit ourselves



2.3. The damped harmonic oscillator with periodic forcing, resonance

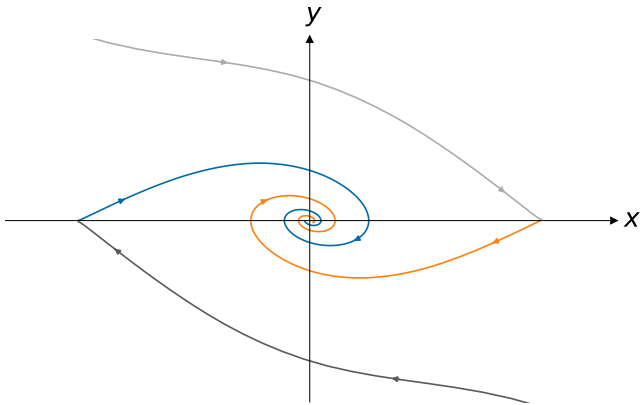


Figure 2.9: Sketch of phase portrait of the damped pendulum

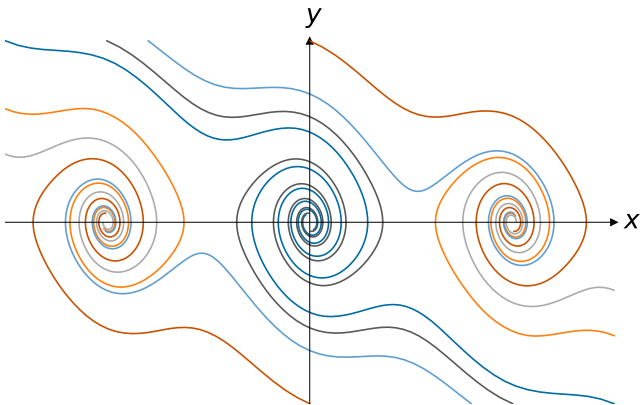


Figure 2.10: Numerical phase portrait of the damped pendulum (2.6) for $c = 0.3$

2. It oscillates in resonance

to the situation where the undamped and non-driven oscillator is harmonic.

2.3.1. “The” solution in the harmonic case

We start by considering the harmonic or linear case

$$\ddot{x} = -\omega^2 x - c\dot{x} + A \sin(\Omega t). \quad (2.7)$$

Here the novelty is the external forcing $A \sin(\Omega t)$, a time-periodic function with frequency $\frac{\Omega}{2\pi}$. In this simple case we can solve the equation of motion (2.7) explicitly and it turns out that it has a periodic solution

$$x(t) = B \sin(\Omega t + \Phi), \quad (2.8)$$

where B and Φ are given by

$$B = \frac{A}{\sqrt{(\Omega^2 - \omega^2)^2 + c^2 \Omega^2}} \quad \text{and} \quad (2.9)$$

$$\tan \Phi = \frac{c\Omega}{\Omega^2 - \omega^2}, \quad -\pi < \Phi < 0.$$

You can check this immediately by substituting this solution in (2.7), also see Exercise 2.6.4. Without proof we mention that this periodic solution, apart from transient phenomena, is the only solution of the equation of motion (2.7). In Figure 2.11 we depicted the graphs of functions $t \mapsto A \sin(\Omega t)$ and $t \mapsto B \sin(\Omega t + \Phi)$. The periodic solution $x(t) = B \sin(\Omega t + \Phi)$ has the same period $\frac{2\pi}{\Omega}$ as the driving force $U(t) = A \sin(\Omega t)$, it is only shifted in time somewhat: the solution lags behind the forcing by $\frac{\Phi}{\Omega}$ units of time. We call Φ the *phase difference* between the two.

Next let us return to the example of the R-L-C circuit, see Section 2.1.2. Suppose that we include in the circuit an Alternating Current (AC)

2.3. The damped harmonic oscillator with periodic forcing, resonance

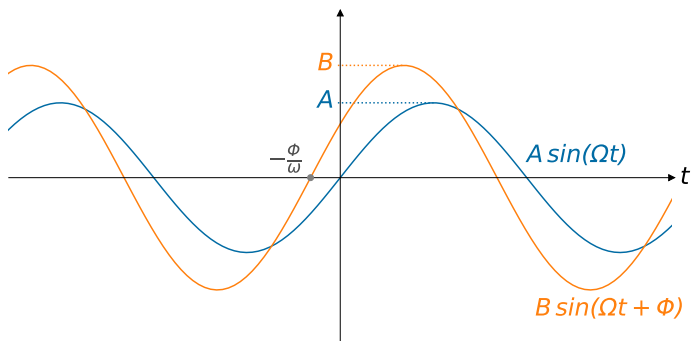


Figure 2.11: Sketch of the periodic solution $B \sin(\Omega t + \Phi)$, see (2.8), together with the external forcing $A \sin(\Omega t)$, see (2.7)

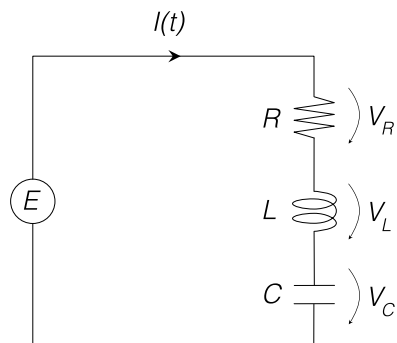


Figure 2.12: RLC circuit with an AC source E

2. It oscillates in resonance

source supplying the voltage

$$E(t) = A \cos(\Omega t).$$

Reasoning as before, Kirchhoff's law gives

$$V_R + V_L + V_C + A \cos(\Omega t) = 0,$$

which in turn leads to

$$L\ddot{I} = -\frac{1}{C}I - R\dot{I} + A\Omega \sin(\Omega t).$$

This is an equation of type (2.7) and therefore all the above results apply.

2.3.2. Resonance in harmonic oscillators with periodic forcing

Note that the amplitude B of the periodically forced equation (2.8) becomes large when the damping c is small and Ω is close to ω , see (2.9). We recall that $\frac{\omega}{2\pi}$ exactly is the frequency of the oscillator without damping and forcing, the so-called *natural frequency*. So when the frequency of the forcing is close to the natural frequency and the damping is small, the amplitude of the generated oscillation may become large: this phenomenon is called *resonance*. In Appendix D we shall also encounter other examples of resonance.

Let's philosophize a bit about the present resonance. Consider the above example concerning the forced R-L-C circuit. Imagine that the AC voltage source gives a "signal" E that combines various frequencies. Then frequencies will be *amplified* that are close to the natural frequency $\frac{1}{2\pi}\frac{1}{\sqrt{LC}}$ of the circuit! Surely this will be the case when the resistance R is small. When tuning a radio this phenomenon is being used to select the signal of the station that one wants to hear.

There are also lots of cases where it is important to avoid the occurrence of resonance. Take a bridge, for example. A bridge has all kinds of parts that can vibrate. Assuming for a moment that these consist of harmonic vibrations, then there is a natural frequency for each of those. If a periodic force now is exerted on the bridge with a frequency close to such a natural frequency, oscillations (deflections) of the material can become very large, possibly with disastrous consequences. Such periodic forces can for instance be supplied by a passing trains or by the wind, or simply groups of people passing by – as notoriously occurred in 2000 during the inauguration of the Millennium Bridge in London. This could also happen when a column of soldiers are marching over the bridge, in which case the “out of step” command will be given.

We conclude this section by a few numerical plots. In Figure 2.13 we depicted solutions of the equation of motion

$$\ddot{x} = -x - c\dot{x} + \sin(\Omega t), \quad (2.10)$$

for different values of c and for $\Omega = 1.2$, together with the plot of the forcing $\sin(\Omega t)$. In Figure 2.14 you can find the corresponding

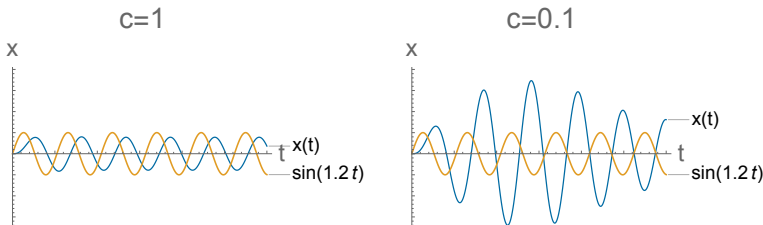


Figure 2.13: Solutions of (2.10) for $\Omega = 1.2$ and $c \in \{1, 0.1\}$ together with the periodic forcing term

integral curves in the phase plane. Why can these curves in this case intersect?

Finally, Figure 2.15 shows the amplitude B as formula (2.9), of the

2. It oscillates in resonance

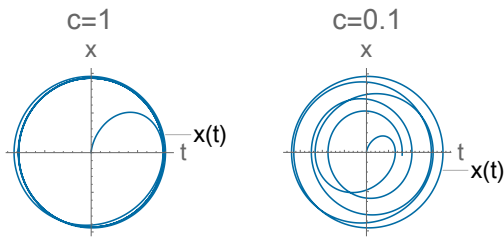


Figure 2.14: Phase curves of equation (2.10) for $\Omega = 1.2$ and $c \in \{1, 0.1\}$

solution of (2.10) with $c = 0.1$ as a function of Ω . We here speak of a

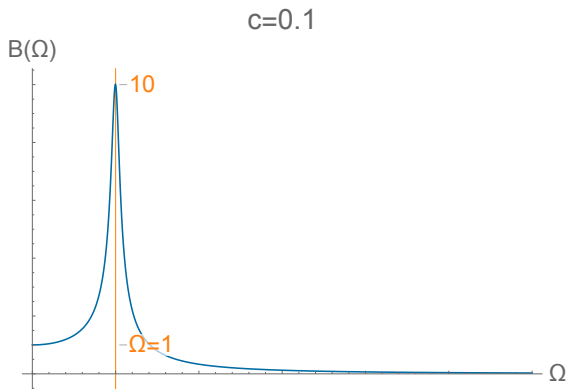


Figure 2.15: Resonance peak: amplitude B (2.9) as function of Ω for equation (2.10) with $c = 0.1$

resonance peak. If in the radio receiver the peak is narrow and high, it is possible to tune sharply to the corresponding frequency. If the peak is wide and low, sharp tuning is impossible.

2.4. Resonance in non-harmonic oscillators with periodic forcing

Harmonic or linear oscillators, with or without damping, already form an incredible source of mathematical insights. They also play a tremendous role in all kinds of physical or engineering applications. If we let go of the harmonic character, as with the pendulum, things become far much more difficult; this is especially true for resonance phenomena. Active mathematical research is still being carried out on this, for more information see Appendix D. Below we give two examples, both based on the pendulum, and give an impression of the kind of motions you can expect.

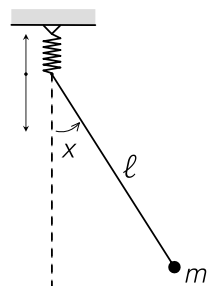
2.4.1. Parametric resonance

In the introduction to Section 2.3 we already mentioned the example of an undamped pendulum the suspension point of which moves up and down periodically.

If we first assume that the oscillation of the suspension point is harmonic, then we can model this system with the following equation of motion

$$\ddot{x} = -\omega^2(1 + A \cos(\Omega t)) \sin x, \quad \omega^2 = \frac{g}{\ell}, \quad (2.11)$$

where the suspension point oscillates with frequency $\frac{\Omega}{2\pi}$ and amplitude A .



For $A = 0$, that is when the suspension point is at rest, we have already seen in Chapter 1 that the pendulum generally oscillates around the lower, stable equilibrium. If we linearize the oscillation, applying the approximation technique for small oscillations

2. It oscillates in resonance

described in 1.2, we replace $\sin x$ by x so obtaining the *Mathieu equation*

$$\ddot{x} = -\omega^2(1 + A \cos(\Omega t))x$$

to which we shall return in Appendix D.

We state the following without proof. When A is small and Ω is close to an integer multiple of $\omega/2$, the oscillations are no-longer confined around the equilibrium point $(x, \dot{x}) = (0, 0)$: the equilibrium loses stability. The shaded regions in Figure 2.16 form a schematic representation of the regions of instability in the (Ω, A) -plane. Moreover it turns out that in these shaded regions, the upside-down equilibrium point $(x, \dot{x}) = (\pi, 0)$ of (2.11) can become stable.

Here we speak of *parametric resonance*. We give two examples of how this resonance manifests itself in real life. This particularly concerns the resonance originating from $\Omega = \frac{1}{2}\omega$. The destabilizing effects of this resonance causes ships that go on an increasing wind astern, to start rolling and even capsize. The stabilizing property seems to be used by circus artists to get more stability when performing balancing tricks, compare with Arnold [8, Section 25].

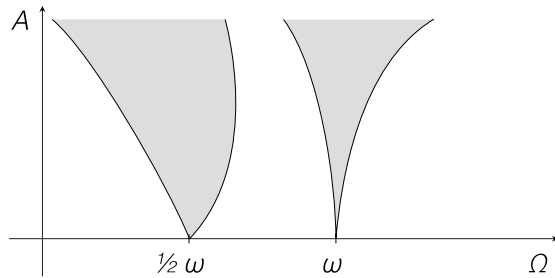


Figure 2.16: Sketch of resonance tongues for the Mathieu equation, for a more realistic picture see Appendix D

2.4.2. Josephson junction

The Josephson junction is an example that plays a role in superconductivity, but unfortunately there is no simple and brief way to explain how. In all previous cases, the types of motions that occurred were quite clear, we will review them for a moment.

1. The system is stationary, there is no motion;
2. The system is in a periodic motion, it oscillates;
3. After some transients, the system ends up in either of the two above situations.

However, let us now consider the pendulum with both damping and forcing:

$$\ddot{x} = -\omega^2 \sin(x) - c\dot{x} + A \cos(\Omega t). \quad (2.12)$$

To fix thoughts, let us set $\omega^2 = 6.4$, $c = 0.6$ and $A = 3.8$, and let Ω vary. With numerical means and a computer you can easily generate images of $t \mapsto x(t)$ for different values of Ω , as shown in Figure 2.17. For $\Omega \in \{1.6, 1.7, 1.8\}$ one can see that the motion is not of the types listed above. More or less oscillating behavior is alternated abruptly by behavior in which the pendulum has a turn over once or several times. Moreover, these are no transient phenomena that eventually disappear and make way for “calmer” motions. Such unpredictable behavior is called *chaotic*. For more about this we refer to the Appendices C and D.

2.5. The stabilization of oscillations

How does a child on a swing slow down the rocking motion?

2. It oscillates in resonance

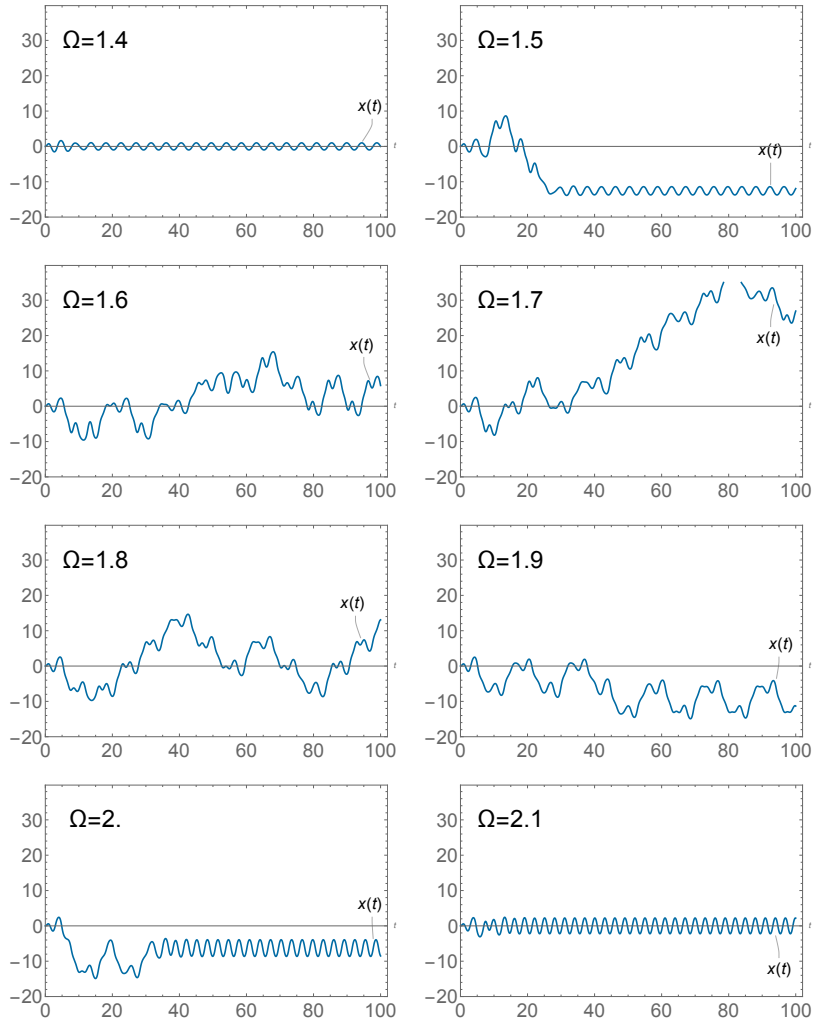


Figure 2.17: Motions of the forced damped pendulum (2.12) for various values of Ω

Almost everyone knows from experience that this is being done by moving one's body in an "appropriate" way. Phenomenologically we may speak of *stabilization*: the "behavior" of the swinger brings the swing into its equilibrium position. It is not that easy to translate this specific behavior into mathematical terms.

Let us thus discuss the following, highly simplified situation. Consider the harmonic oscillator $\ddot{x} = -x$ (think of the swing), on which a force F can be applied (think of the person on the swing). The equation of motion describing the total system (swing with swinger) is quite familiar now:

$$\ddot{x} = -x + F.$$

We are left with the following question. Can we determine a force F such that motions are being stabilized? In other words, if the swing is out of its equilibrium state $(x, \dot{x}) = (0, 0)$, how can we send it back there by the force F . Moreover, this force should be determined by the state of the system itself. This set-up is called *feedback*. To be precise, such an F is a *feedback control*.

2.5.1. First attempt

First, let us try to achieve our objective by letting F be a suitable function of the deviation x alone. For each choice of $F = F(x)$ we get as "total" equation of motion

$$\ddot{x} = -x + F(x).$$

However, this equation is of the kind we already studied in Chapter 1. Namely, by defining

$$V(x) = \int_0^x (\xi - F(\xi)) d\xi,$$

we can rewrite the equation of motion as

$$\ddot{x} = -\frac{dV}{dx}.$$

2. It oscillates in resonance

For these equations, we saw that the energy $E = \frac{1}{2} \left(\frac{dx}{dt} \right)^2 + V(x)$ is a conserved quantity. This means that you can only end up in an equilibrium point if you were there already in the first place. So unfortunately, this first attempt is unsuccessful.

2.5.2. Second attempt

Let us try to take $F = -\frac{dx}{dt}$. In this case we are done: the equation of motion is

$$\ddot{x} = -x - \dot{x}$$

and it only has motions that lose energy and evolve towards $(x, \dot{x}) = (0, 0)$. This is exactly what we want: after the transient phenomena, we are in equilibrium and the motion has stabilized; see Section 2.2.

The practical drawback of this method is that the instantaneous velocity $\dot{x}(t)$ cannot be measured so easily: this control is therefore less feasible. See also comments in Section 1.3.1 with respect to the phase plane.

2.5.3. Third attempt

Finally, let us try to choose a force F that even though it depends on the position x , it does not depend on the position of the swing at the time where F is exerted. Instead, let F depend on the position the swing had some fixed time earlier, say δ . To be more precise we take F of the form

$$F(t) = Ax(t - \delta),$$

where A is some constant. In this case, the “total” equation of motion reads

$$\ddot{x} = -x + Ax(t - \delta). \quad (2.13)$$

For small δ we can use the approximation

$$x(t - \delta) = x(t) - \delta \dot{x}(t),$$

and for $A > 0$ we get roughly the equation of a damped harmonic oscillator: all solutions lose energy and evolve towards $(x, \dot{x}) = (0, 0)$, again see Section 2.2.

Also in this case we have obtained stabilization although we have committed an approximation. That is why it is a good idea to double check the result by numerical means once again, see Figure 2.18. Feedback controls like the one presented in this chapter play an im-

more?

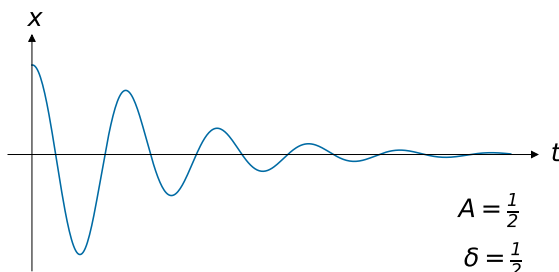


Figure 2.18: Plot of the harmonic oscillator with feedback control (2.13)

portant role in automatic control systems such as automatic pilots, chemical process controllers, etc.

2.6. Exercises

2.6.1. Negative damping

In electronics there are many oscillators with negative damping (or negative friction). Show that a positive-damping oscillator changes into a negative-damping oscillator with the transformation $\tau = -t$ (i.e., by reversing the direction of time). What does this say about the energy and the phase portrait of negative damping oscillators?

2.6.2. Tossing a fair coin

Consider a point particle moving under the influence of the following potential

$$V(x) = x^4 - 2x^2,$$

compare Exercise 1.6.6. Introducing a (small) friction, the equation of motion changes into

$$\ddot{x} = -\frac{dV}{dx}(x) - c\dot{x}, \quad c > 0 \text{ small.}$$

Describe the phase portrait of this system, and find out is the connection with “tossing a fair coin”.

2.6.3. A “controlled” oscillator

Consider a harmonic oscillator the center of which is moving with respect to the velocity as described by the following equation of motion

$$\ddot{x} = -x - a \operatorname{sgn}(\dot{x}),$$

where $a > 0$ and $\text{sgn}(x) = x/|x|$ if $x \neq 0$ and 0 otherwise. Discuss the phase portrait and describe the connection to the “dry friction” introduced in Section 2.1.1.

2.6.4. A damped oscillator with forcing

A harmonic oscillator with friction is driven by an external force. If the external force is $F(t) = A \sin(\Omega t)$, the motion of the oscillator is given by $x(t) = B \sin(\Omega t + \phi)$, after the extinction of the transient phenomenon. Here A, B and Ω are three positive constants. See formula (2.8).

1. How large is the energy supplied to the oscillator by the external force per period?
2. Let the equation of motion of the damped oscillator be given by

$$\ddot{x} = -x - c\dot{x} + F(t), \quad c > 0.$$

For the motion $x(t) = B \sin(\Omega t + \phi)$ as mentioned above, how much energy per period is lost by the oscillator due to the friction?

3. Using the results from the points above, show that $\sin \phi$ is negative.
4. At a time in which $x(t)$ is maximal, that is, when $\Omega t + \phi = (2k + \frac{1}{2})\pi$, the velocity of the point mass is zero and its acceleration is $-B\Omega^2$. At that time, there is no frictional force acting: only the driving force $-B$ of the oscillator and the external force $F(t)$ are affecting its motion. Use this information to show that

$$B(1 - \Omega^2) = A \cos \phi.$$

2. It oscillates in resonance

5. Use the above results to show that

$$\tan \phi = -\frac{c\Omega}{1-\Omega^2} \quad \text{and} \quad B = \frac{A}{\sqrt{c\Omega^2 + (1-\Omega^2)^2}}$$

2.6.5. The Van der Pol-Liénard differential equation

In a few steps we will arrive at describing the phase portrait of the following equation of motion,

$$\epsilon \ddot{x} = -x + \dot{x} - \dot{x}^3,$$

which describes the evolution of an oscillator with non-linear damping. In particular we will focus on the case where ϵ is a small positive number.

Give, in the following order, the phase portraits of

1. $\dot{x} = -x, \quad \epsilon \dot{y} = -y;$
2. $\dot{x} = -x, \quad \epsilon \dot{y} = -(x + y);$
3. $\dot{x} = y, \quad \epsilon \dot{y} = -(x + y);$
4. $\dot{x} = y, \quad \epsilon \dot{y} = -(x + y + y^3);$
5. $\dot{x} = y, \quad \epsilon \dot{y} = -(x - y + y^3);$

Hint: The idea is to make a clear distinction between the so-called slow motion and the fast motion. We here assume that ϵ is very small.

In case 1. we then get the following situation. In the first, very short phase, the x coordinate will hardly change and the y coordinate will

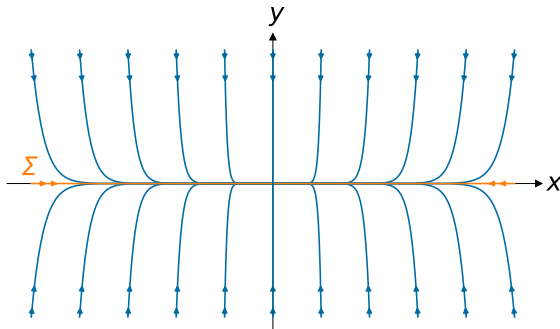


Figure 2.19: Phase portrait of the first case in Exercise 2.6.5

become almost equal to zero: one could say that the equation $\epsilon \dot{y} = -y$ is dominant. In the second phase, the motion will take place at or near the “curve of slow motion” Σ , obtained by setting the right hand side of the second equation equal to zero: in case 1. this is the x -axis. On Σ , the motion is given by the first equation. So we get a picture like in Figure 2.19.

Finally, describe what happens when we “continuously deform” the equations from case 4. to case 5. You can do this by making the equation dependent on a parameter $\mu \in [-1, 1]$:

$$\dot{x} = y, \quad \epsilon \dot{y} = -(x + \mu y + y^3).$$

For what value of μ does the phase picture change most drastically? Describe this change.

3. Oscillations in daily life

Oscillations that we encounter in our daily life, for instance in nature or at the core of our hi-tech devices, are generally of a far more complicated nature than we have seen so far. However, the concepts introduced earlier such as energy, friction, external forces, resonance and the like continue to play an important role. It is also often possible to describe physically complicated phenomena in a simplified manner using examples as we saw in the previous chapters. Obviously, it is important to ensure that simplifications do not throw away the child with the bath water: it remains necessary to trace back enough of the original problem to achieve meaningful conclusions.

In general, every mathematical description of reality will, almost necessarily, lead to some losses. It is therefore important to find *an as good as possible description*. The development of such descriptions is called *modeling*. In this context, we would like to point at a simplification that is often tacit, namely *linearization*, see also Section 1.2. In order not to lose too much in that process, it is important that deviations from equilibrium states do not become too large. Keep these thoughts in mind while reading the present chapter, of which we are now going to outline the contents.

Real life examples. In Section 3.1 we present a few real life examples of oscillations, where some terminology from physics will be needed. The remark about simplifications clearly applies here.

3. Oscillations in daily life

Coupled oscillators. In the Section 3.2 we discuss oscillatory phenomena that can be understood as composed of a *finite* number of oscillations in the sense of the previous chapters. This section has a more mathematical nature with a focus on Lissajous figures, where *two* coupled oscillations in the sense of Chapter 1 play a role. As a further example, we will consider a pendulum the motions of which are not confined to one vertical plane, but where the point mass is allowed to perform spatial motions; we speak of a *spherical pendulum*. The dynamics of such a system again turns out to be a combination of two “ordinary” oscillations. In Appendix B we shall deal more generally with coupled oscillators and also encounter the spherical pendulum in considerations about the Foucault experiment.

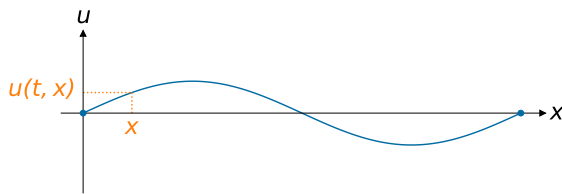


Figure 3.1: *Vibrating string*

Vibrations in continuous media. Next, in Section 3.3 we shall discuss vibrations of *continuous* media. This kind of vibration can be thought of as composed of an *infinite* number of “ordinary” oscillations. Our leading example will be the sound vibration in an *organ pipe*.

To fix thoughts we first briefly start discussing a vibrating string. In Figure 3.1 we depicted such a string that can move in the (x, u) -plane. We assume that the end points of the string are firmly fixed at the points $(x, u) = (0, 0)$ and $(x, u) = (1, 0)$. In addition, we assume that each point of the string can only move in the vertical direction, i.e. the u -direction.

In the idle state, the string coincides with the interval $[0, 1]$ on the x -axis. At a given time t we indicate this (vertical) deviation at a point x with $u(t, x)$. For fixed t , the shape (or configuration) of the string is then given by the graph of the function $x \mapsto u(t, x)$. The question then is how this function changes over time.

Roughly speaking we can say that for every point $x \in [0, 1]$ we consider the evolution of $t \mapsto u(t, x)$, so that its motion is an oscillation in the spirit of Chapter 1. In that sense we have with an infinite number of “ordinary” oscillations. Note that these oscillations are far from independent: indeed, due to the elastic properties of the string, the oscillations are strongly coupled.

Remark 14. *As already noted before, the mathematical treatment of string oscillations, or sound vibrations in an organ pipe, is far more complicated than what we saw earlier. This is due to the fact that we are now dealing with both the spatial variable x and the time t . The equation of motion of the function $x \mapsto u(t, x)$ thereby becomes a so-called partial differential equation, a subject that we shall only briefly touch upon. For an introductory text we refer to Olver [107].*

In Section 3.3 will investigate how such a system of “infinitely many oscillators” can be approximated by (linear) systems consisting of a finite number of point masses, interconnected by massless strings. This is called *discretization* of the continuous system. This discretization is further elaborated in the case of an *organ pipe*: the *longitudinal* air vibrations in the pipe are somewhat easier to deal with than the *transverse* vibrations of the string. At the end of the chapter, we briefly discuss a few other vibration and wave phenomena, including those related to *sound* and *light*.

3.1. Two further examples of oscillators

In this section we deal with two miscellaneous real-life examples of oscillations in the sense of Chapter 1. In both cases some physical principles will be used without further comments.

3.1.1. A plank bridge

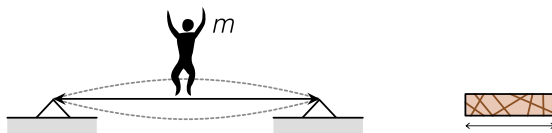


Figure 3.2: Plank bridge over a ditch

A person with mass m stands in the middle of a massless plank lying over a ditch. Due to gravity the plank bends a little. According to the *linear theory*, this sag is equal to $u = mg/k$, where g is the acceleration of gravity and k is the stiffness of the plank, *interpreted as a spring*. See also Exercise 1.6.1. This approach "works" as long as the sag is small.

By performing knee bends in a constant rhythm, someone can easily determine that the plank *resonates* at a frequency $f = \frac{1}{2\pi} \sqrt{\frac{k}{m}}$, compare with Section 2.3. The person is acting here as a *drive* or *forcing*. Furthermore, it turns out that $f = \frac{1}{2\pi} \sqrt{\frac{g}{u}}$, so the larger u , the lower the *natural frequency* f . Does that correspond to your own intuition?

Remark 15. You can also observe such resonance phenomena with a piano, where the dampers are off the strings, or a guitar. An external sound can cause a certain string to resound, or resonate.

3.1.2. Rolling of a ship

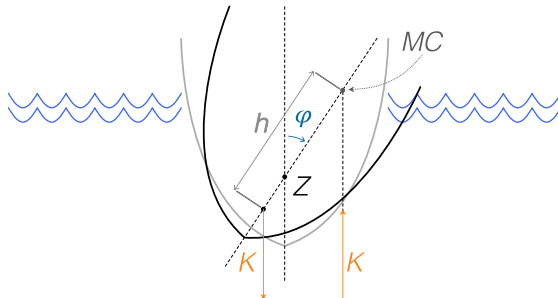


Figure 3.3: Boat rolling about its longitudinal axis

In this example, we consider the *rolling* of a ship, that is, the tilting of the ship about its longitudinal axis, see Figure 3.3. Also within rolling oscillations resonance phenomena can occur. In a small boat we can become aware of this by wiggling it transversally with the correct rhythm or, when the boat responds to waves coming in from the side.

In this case, for the natural frequency we need to replace the formula $\omega^2 = k/m$ from Section 2.3, by $\omega^2 = c/I$: here c represents the revolving torque per unit of angular displacement exerted by the upward force K due to buoyancy and I is the moment of inertia with respect to the longitudinal axis. Again see Figure 3.3. For background we refer to [74, 119].

How does c show up in this game? Well, when the angle $\phi = 0$ then the force K acts exactly in a plane of symmetry. Assuming that the center of gravity Z lies in this plane, we see that K does not exert a torque on Z . If the ship now tilts over angle ϕ , e.g., clockwise as in the figure, then the right part of the ship dives a little deeper into the water, while the left part rises a little. The upward pressure (or buoyancy) increases slightly on the right and decreases on the left.

3. Oscillations in daily life

The resulting upward force K consequently moves to the right. For small angles φ , the working line of K will intersect the axis of symmetry at a fixed point MC , the so-called *metacentre*. The distance h from Z to MC is called the *metacentric height*. Now it holds true that $c = Kh$ (can you see why?). From this it follows that the higher MC , the larger the natural frequency.

We note that h is partly determined by the shape of the ship. For example, a round biscuit can where Z and MC practically coincide has little to no *shape stability* (the ability of a vessel to staying up right due to its shape). How about a submarine? And a manned rowing boat with a fairly high center of gravity? Keep this in mind if you ever try to stand up in a small rowing boat.

Remark 16. *The history of buoyancy and shape stability studies goes back at least to Archimedes of Syracuse (287–212 BC). His famous law, part of his two volumes on hydrostatics entitled “On floating bodies”, marked a turning point in the understanding of floating stability. Archimede’s law states that the buoyancy force on a body is an upward force with magnitude equal to the weight of the fluid displaced by the body. This law lies at the core of the above discussion. For general background information again compare with [74, 119].*

3.2. Coupling finitely many oscillations

All the examples that we have seen so far involved only one position variable, in a more fancy language: the *configuration space* was always one-dimensional. Another way of saying the same, is that these are systems with one *degree of freedom*. In engineering these cases are referred to as *1-mass-spring systems*, where tacitly the model is assumed linear.

We now turn to oscillatory phenomena the description of which requires a finite number of position variables, the so-called number of *degrees of freedom* of the system in question.

The considerations to follow require a bit more of mathematics and a more thorough treatment is postponed to Appendix B.

3.2.1. Lissajous figures

Both in the Preamble and in Section 1.4.3 we encountered the idea of conceiving an oscillator as a bead sliding along a wire or as a marble in a gutter (disregarding friction and the rolling motion). Now, to formalize the current ideas, we replace the gutter by a bowl. Each point on the bowl is a possible position of the marble. The bowl is considered as a two-dimensional surface and hence the number of degrees of freedom of such a system equals two. The problem in this section is what kind of figures can be described by the marble on this surface. This can be even more interesting when the bowl is not exactly rotationally symmetrical, but say, oblong.

In part III of Minnaert's *The Nature of Light and Colour in the Open Air* [97] there is a discussion of a tree branch swaying in the wind. This system generally has a different stiffness in the vertical and in the horizontal direction, and the end of the branch will describe figures similar to ones of the marble in an oblong bowl. If you would tie a flashlight to the branch at dark, you could observe what these figures look like.

The *linear* theory of this type of motion is mathematically well known under the name of *small oscillations*. Compare with Section 1.2 and also Appendix B. With the aid of linear algebra (vector geometry), we can show the following. With an *appropriate choice* of position variables y_1 and y_2 , the system will look like a set of two *uncoupled*

3. Oscillations in daily life

(i.e., independent) harmonic oscillators

$$\begin{cases} \ddot{y}_1 = -\omega_1^2 y_1 \\ \ddot{y}_2 = -\omega_2^2 y_2. \end{cases}$$

In our example of the marble in the oblong bowl, the variables y_1 and y_2 could describe the direction of the length resp. width of the bowl. In that case we would have $\omega_1 < \omega_2$. (Why?) Oscillations of the system occurring along the line $y_2 = 0$, so only in the y_1 variable, are called *characteristic*. As known from Chapter 1 all oscillations have the same frequency $\omega_1/2\pi$, which is a *characteristic frequency*. The same can be said of oscillations along the line $y_1 = 0$, which have characteristic frequency $\omega_2/2\pi$. We can now easily present all possible solutions using (1.7) from Section 1.1:

$$\begin{pmatrix} y_1(t) \\ y_2(t) \end{pmatrix} = \begin{pmatrix} R_1 \cos(\phi_1 - \omega_1 t) \\ R_2 \cos(\phi_2 - \omega_2 t) \end{pmatrix}$$

where the constants R_1, R_2, ϕ_1, ϕ_2 are determined by the *state* of the system at any given time, say at $t = 0$. The curves in the (y_1, y_2) -plane described by such solutions are called *Lissajous figures*. Their shape is largely determined by the ratio ω_1/ω_2 of the characteristic frequencies. We give some examples in Figure 3.4.

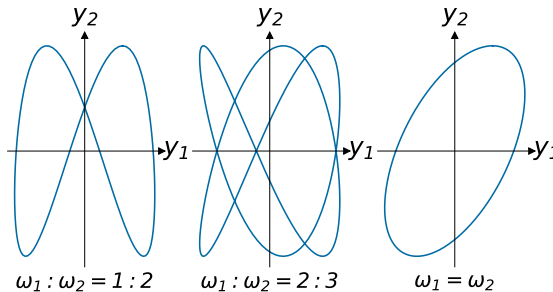


Figure 3.4: Lissajous figures

Remark 17. When $\omega_1 = \omega_2$, such as in the case of a rotationally symmetrical bowl or for the spherical pendulum mentioned before, the

Lissajous figures are ellipses (or degenerates ellipses in the form of straight-line segments). For details on small oscillations of the spherical pendulum we refer to Appendix B.

1. *The non-linear theory of problems of two (or more) degrees of freedom is also particularly rich. In connection with the spherical pendulum, we mention the phenomenon of spherical precession. The motion of the pendulum in this case is not an ellipse, but a rosette. You can think of it as (almost) an ellipse that slightly rotates during each swing, again see Appendix B.*
2. *The spherical pendulum is still pretty tame. In more general examples, the motions can become so complicated that one speaks of chaos, compare with Section 2.4. In such cases, the mathematical theory is still quite unexplored. For certain impressions see Appendix C.*

We conclude with a few questions and comments.

- As said before the shape of the Lissajous figure is “largely” determined by the ratio ω_1/ω_2 . It can be shown that degenerations into straight-line segments are *always* possible by choosing R_1, R_2, ϕ_1, ϕ_2 appropriately. Do you have any idea what happens when the ratio ω_1/ω_2 is irrational (e.g., if $\omega_1/\omega_2 = 1/\sqrt{2}$)?
- In Section 1.3.1 we encountered the phase plane. It is important to stress that the (y_1, y_2) -plane occurring here should not be confused with this. What are the differences?

If in this context we perform the construction of Section 1.3, we obtain a four dimensional *phase space* or *state space* with similar properties as the phase plane. The most important of these again is *determinism*: the future of the evolution is fully

3. Oscillations in daily life

determined once we know at any given time at which point of the phase space the system is located, in other words, what is the state of the system.

Note that such a point in the phase space is composed of the *positions* y_1 and y_2 and the *velocities* $\dot{y}_1 = \frac{dy_1}{dt}$ and $\dot{y}_2 = \frac{dy_2}{dt}$ (compare (1.3)): these four coordinates $(y_1, y_2, \dot{y}_1, \dot{y}_2)$ exactly describe the state of the system.

3.2.2. Beats

Beats as we know them. We probably all know the phenomenon of *beat tones*: it happens when we hear the sound of two tones that are close to each other in frequency, the result is a sound that pulses continuously, decreasing and increasing.

Besides in the context of musical instruments, you can hear it in the sound of a twin-engine aircraft. A primitive way to explain this phenomenon is the following: two sound waves reach our eardrum of our ear and deflect the membrane by quantities proportional to $\sin((\omega - \delta)t)$ and $\sin((\omega + \delta)t)$. Here we assume that δ is small and,

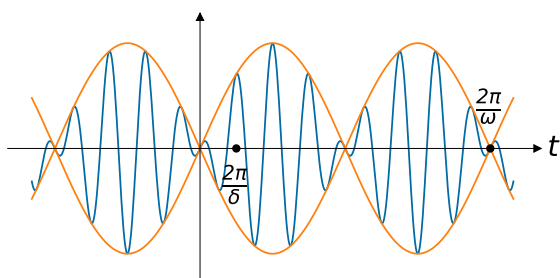


Figure 3.5: A (schematic) beat tone

for the sake of convenience, we also assume that the amplitude is

the same in both cases, say 1. The *superposition* of both deflections yields, according to a known formula from the trigonometry

$$\sin((\omega - \delta)t) + \sin((\omega + \delta)t) = 2 \cos(\delta t) \sin(\omega t).$$

We hear the pitch corresponding to the frequency $\frac{\omega}{2\pi}$; while the process of mutually reinforcing and quenching of the wave has the frequency $\frac{\delta}{\pi}$. What happens when the amplitudes of the two signals are not equal?

Beats in coupled oscillators

We next discuss a problem that shows a certain similarity with the above: also here beats occur. As we shall see this occurrence has to do with an *exchange of energy*. Let us come to the point at once.

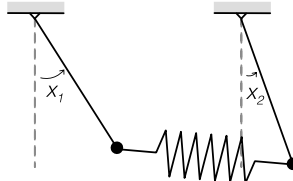


Figure 3.6: Two pendulums coupled by a spring

Two identical pendulums are linked by a spring as shown in Figure 3.6. All motions take place in one vertical plane. For simplicity we fix the masses, the lengths of the pendulums and also the acceleration of gravity, all to equal to 1. Furthermore, the length of the unloaded spring is equal to the distance between the suspension points. We will denote by k the spring constant. In the course of the story that unfolds now, we will choose k small, which is why one speaks of *weak coupling*.

3. Oscillations in daily life

Here we recognize a system with 2 degrees of freedom: the configuration of the system is determined by the angular positions x_1 and x_2 . In what follows, we are going to investigate the behavior of the system in the vicinity of the equilibrium solution $x_1 = x_2 = 0$.

First, let's describe the type of behavior that of interest to us. If we let one of the pendulums, say the left one, be at rest in the lower equilibrium and let the other, the right one, perform small oscillations, the following happens. After a while the right pendulum will come to rest in its lower equilibrium while the left one “takes over” the motion. Now left and right switch roles: after about the same time, the left pendulum is at rest and the right one is moving. This process is repeated for ever, the kinetic energy is always transferred from one pendulum to another. This can be demonstrated in a test set-up, although the “everlasting” character cannot really exist due to the ever-present friction ...

Remark 18. *Let us for a while consider the left pendulum on its own. In a somewhat one-sided view of the case, you could say that it is forced by the right pendulum in a rather complicated way. Somehow, the motion of the left pendulum is very reminiscent of the vibration of the eardrum in the example of sound beats. This is one reason to speak of beats also in this case.*

In the above we used the term “small oscillations”. This means that for a proper mathematical description we first switch to a linear model: as in Section 1.2, we approximate $\sin x_1 \approx x_1$ and $\sin x_2 \approx x_2$. Without proof, we claim that the resulting linear system completely falls within the theory of small oscillations; for a more complete and detailed description see Appendix B. As said earlier, the main point of this theory is that for a suitable choice of position variables the system completely decouples. It should be clear at this point that these variables cannot be x_1 and x_2 : the entire description above with the energy transfer indicates that these are strongly coupled.

As it turns out, in this case we have to use the new variables y_1 and y_2 defined by

$$y_1 = \frac{1}{\sqrt{2}}(x_1 + x_2) \quad \text{and} \quad y_2 = \frac{1}{\sqrt{2}}(x_1 - x_2). \quad (3.1)$$

With this choice, one can check that the system decouples to

$$\begin{cases} \ddot{y}_1 = -\omega_1^2 y_1 \\ \ddot{y}_2 = -\omega_2^2 y_2, \end{cases}$$

where $\omega_1 = 1$ and $\omega_2 = \sqrt{1+2k}$. What do the characteristic oscillations look like now? From the above we can directly obtain the sketch in Figure 3.7. We further describe Figure 3.7 as follows.

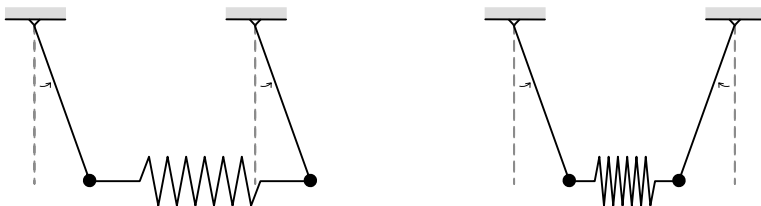


Figure 3.7: *Characteristic oscillations of the coupled pendulum system*

Left $y_2 = 0$: Characteristic oscillations of the y_1 -variable with frequency $\omega_1/2\pi$; this means that $x_2 = x_1$ and the pendulums move in phase.

Right $y_1 = 0$: Characteristic oscillations of the y_2 -variable with frequency $\omega_2/2\pi$; this means that $x_2 = -x_1$ and the pendulums move in anti-phase.

Why does the spring constant k play no role in the value of ω_1 and how can one see that $\omega_1 < \omega_2$ without explicit computation? Here comes another analogy to the sound beats: we are apparently dealing with two uncoupled oscillators with frequencies that, for small

3. Oscillations in daily life

k , are close together. The *tones* in the sound example here correspond to *characteristic oscillations*.

Let us first try to understand the beat phenomenon without calculations. It is an important property of the linear theory that any motion of both pendulums can be written as a *superposition* (addition) of the characteristic oscillations just described. This is schematically depicted in Figure 3.8. During the first few periods, the mo-

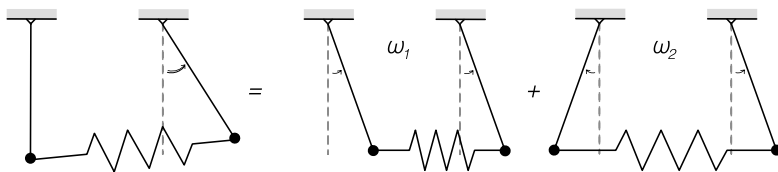


Figure 3.8: *The superposition principle*

tion is largely restricted to the right pendulum, the left one remains approximately at rest. This happens because ω_1 and ω_2 are almost equal. However, ω_2 is *slightly* larger than ω_1 , so the oscillation with ω_2 is *slightly* faster than that with ω_1 . Therefore, if we wait long enough, the ω_2 -motion has a “phase” that becomes 180° ahead of the ω_1 -motion. The superposition of both these oscillations, sketched in Figure 3.9, shows that now the right pendulum has become stationary, while the left one is swinging with the initial amplitude. And so on. Therefore this reasoning gives a solid qualitative description of the motion.

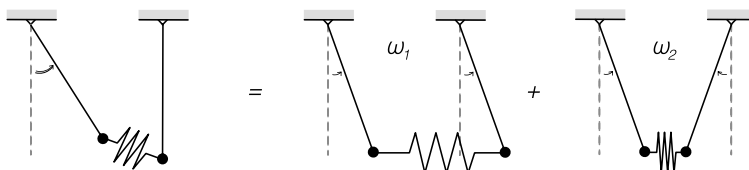


Figure 3.9: *The superposition principle continued*

Now let us compute a few things. To this end, we first write out the characteristic oscillations in the x_1 and x_2 variables. Using equation (3.1) one can simply verify that this is equivalent to

$$x_1 = \frac{1}{\sqrt{2}}(y_1 + y_2) \quad \text{and} \quad x_2 = \frac{1}{\sqrt{2}}(y_1 - y_2).$$

As we saw in Section 3.2.1, the formulas for the characteristic oscillations in the y variables are

$$\begin{aligned} y_1(t) &= R_1 \cos(\phi_1 - \omega_1 t), & y_2(t) &= 0 \quad \text{and} \\ y_1(t) &= 0, & y_2(t) &= R_2 \cos(\phi_2 - \omega_2 t). \end{aligned}$$

In the x variables these correspond to

$$\begin{aligned} x_1(t) &= x_2(t) = \frac{1}{\sqrt{2}}R_1 \cos(\phi_1 - \omega_1 t) \quad \text{and} \\ x_1(t) &= -x_2(t) = \frac{1}{\sqrt{2}}R_2 \cos(\phi_2 - \omega_2 t). \end{aligned}$$

As said before, in the linear theory you can interpret all motions as the sum of characteristic oscillations. It follows that we now have the general solutions

$$\begin{pmatrix} x_1(t) \\ x_2(t) \end{pmatrix} = \frac{1}{\sqrt{2}} \begin{pmatrix} R_1 \cos(\phi_1 - \omega_1 t) + R_2 \cos(\phi_2 - \omega_2 t) \\ R_1 \cos(\phi_1 - \omega_1 t) - R_2 \cos(\phi_2 - \omega_2 t) \end{pmatrix}$$

where R_1, R_2, ϕ_1, ϕ_2 depend on the state of the system at any fixed time, say at $t = 0$.

The kind of motion of interest to us now, so where the beats (should) occur, has the property that $R_1 = R_2$ and $\phi_2 = \pi - \phi_1$. Here we recall that ϕ_1 is measured in radians and the π radians correspond to 180° . Substituting these values and after possibly applying a translation in the t variable, we can safely assume that $\phi_1 = 0$. This means that we are left with

$$x_1(t) = \frac{1}{\sqrt{2}}R(\cos(\omega_1 t) - \cos(\omega_2 t)), \quad x_2(t) = \frac{1}{\sqrt{2}}R(\cos(\omega_1 t) + \cos(\omega_2 t)),$$

3. Oscillations in daily life

where $R = R_1 = R_2$. Again applying some trigonometry we obtain

$$x_1(t) = -R\sqrt{2} \sin\left(\frac{1}{2}(\omega_1 + \omega_2)t\right) \sin\left(\frac{1}{2}(\omega_1 - \omega_2)t\right)$$

$$x_2(t) = R\sqrt{2} \cos\left(\frac{1}{2}(\omega_1 + \omega_2)t\right) \cos\left(\frac{1}{2}(\omega_1 - \omega_2)t\right).$$

Recall that $\omega_1 = 1$ and $\omega_2 = \sqrt{1+2k}$. Using the fact that k is small, we have that *approximately* $\omega_2 \approx 1+k$. Can you see why this is true? (Hint: we found it helpful to remember that for small $k > 0$ one has $k^2 \ll k$.) The motion then gets the form

$$x_1(t) = R\sqrt{2} \sin\left((1 + \frac{1}{2}k)t\right) \sin\left(\frac{1}{2}kt\right) \quad \text{and} \quad (3.2)$$

$$x_2(t) = R\sqrt{2} \cos\left((1 + \frac{1}{2}k)t\right) \cos\left(\frac{1}{2}kt\right),$$

depicted in Figure 3.10. This computation clearly confirms what we

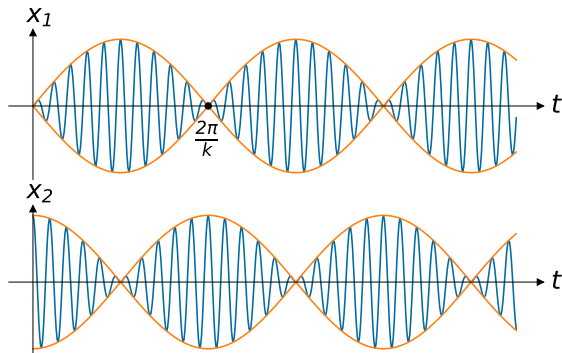


Figure 3.10: *Beats of the weakly coupled oscillators*

saw before; evidently we now get more detailed information, such as the frequencies of oscillation and of beating, the maximum amplitudes, and so on. It is good to think a bit about the similarities and differences between this example of the weakly coupled pendulums and that of the sound beats.

To complete the story, in Figure 3.11 we give the Lissajous figure that belongs to the motion described in formula (3.2). Find a practical

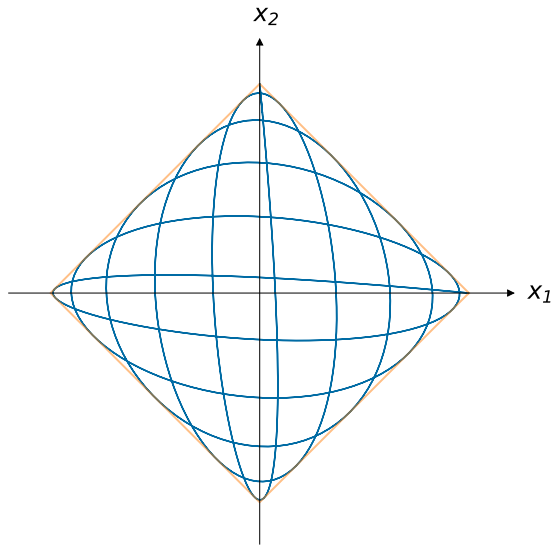


Figure 3.11: *Lissajous figure of the weakly coupled oscillators*

difference between this Lissajous figure and those in Section 3.2.1, particularly paying attention to the observability.

That is all concerning the weakly coupled pendulums. This kind of beats may occur in many variations. Think of two identical springs, weakly coupled by a third and below we will briefly discuss the so-called Wilberforce pendulum. It is also quite easy to device test setups to try out for yourself. However, it is more difficult to find these beat phenomena in everyday life.

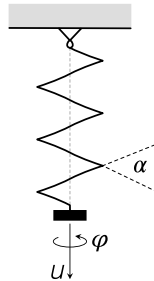
Nevertheless, we suggest the following experiment. The main ingredient for this is a well-tuned piano. Detach the dampers from the strings and find a tone where the string is doubled once. As in Section 1.6.1, we view these two strings, as 1-mass-spring systems, with exactly the same spring constant (pitch). The string suspension, the soundboard and the air create a weak coupling between

3. Oscillations in daily life

the two. Now excite one of the strings with your hand, leaving the other at rest. What do you expect to hear and what do you hear? Note that this set-up is different from one where you would aim to demonstrate sound beats.

Wilberforce. To conclude the discussion on beats consider the Wilberforce spring: a system consisting of a rather long vertical coil spring attached to a rigid cylindrical-shaped body at the bottom, compare with the figure to the right.

In first approximation, we observe two types of oscillation: vertical motions (in the u direction) and rotations about the vertical axis (in the φ direction), also called torsional oscillations.



After linearization around the equilibrium state where the system is at rest, we can speak about the frequencies of these two oscillators. These depend on the elastic properties of the spring, the mass and the moment of inertia of the cylinder about the vertical axis. We here assume that these two frequencies are equal.

On closer inspection, both oscillators turn out to be weakly coupled. Indeed, since we are dealing here with a coil spring (spiral), a weak torsional force occurs when moving in the vertical direction; the spring will tend to slightly coil or uncoil itself depending of the compression or extension. In this case, the pitch angle α of the spiral spring plays a role. On the basis of the above, we would expect beats in which energy in the vertical oscillator is exchanged with energy in the torsion pendulum. And, indeed, you can observe these beams in physical realizations of this pendulum. It is also useful to consult with the internet.

3.2.3. More than two degrees of freedom

Whether or not we are dealing with two or more degrees of freedom is not very important for the linear theory. Mutatis mutandis, the above story concerning small oscillations can now be told again. The important point is that with a suitable choice of position variables such a system reduces to a finite number of *decoupled* systems of one degree of freedom oscillators, compare Appendix B.

Regarding the non-linear theory, we only want to add the following to what has already been said at the end of Section 3.2.1: the complexity of the systems increases somewhat if we consider three or more degrees of freedom instead of only two.

We conclude this section with an example of the motions of a *tugboat* that we conceive of as a rigid body. In Section 3.1 we already met with the *rolling motion* of a boat. Similar considerations also apply to so-called *yawing*, a rotational motion about the transverse axis, see Figure 3.12.

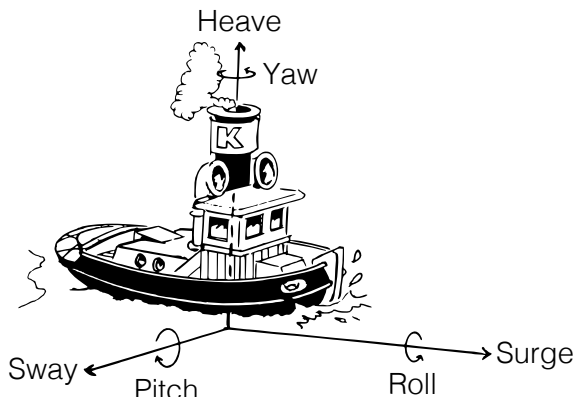


Figure 3.12: Superposition of oscillations in a boat; the tugboat is called De Kraak [131]

3. Oscillations in daily life

It goes without saying that the metacentric heights for both motions will generally not be the same. A third oscillation that a ship can perform is called *heaving*: it concerns vertical motions of the ship.

In general, a *rigid body* can perform six motions, three translations and three rotations: the system has six degrees of freedom. This also applies to a boat, as long as we consider it as a rigid body. We have added the nautical names relating to these motions in Figure 3.12. If we restrict ourselves to the oscillatory motion that the ship can perform in more or less calm water, that is, rolling, pitching and yawing, then we have a system of three degrees of freedom.

3.3. Vibrations of continuous media

In the introduction to this chapter we already met the vibrating string. Further examples of systems that involve a continuum of oscillations are membranes, beams, air, water, ... We already mentioned the partial differential equations that here act as equations of motion. In general these equations lend themselves badly for the kind of mathematical analysis we have seen so far. In part, the required theory has not *yet* been developed. In many practical problems, people use numerical analysis that often provides sufficiently useful answers.

3.3.1. Discretizing the continuum

The discretization of the vibrating medium is one approach that can be used for a numerical treatment of vibrating continua, but also for deriving partial differential equations to model them. As said before, the organ pipe is going to be our leading example.

The organ pipe

We consider an organ pipe as a cylindrically-shaped tube. For simplicity we assume that the pipe is closed at both openings, see Figure 3.13. Note that a real organ pipe is always open, at least at one end where the air is blown in.

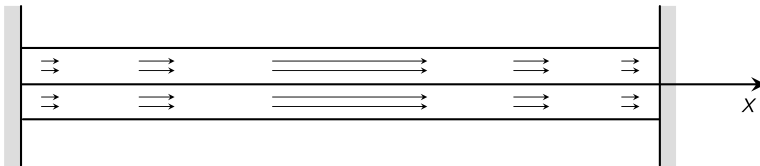


Figure 3.13: *Schematic organ pipe*

We also make the following assumptions:

1. Gravity does not effect the motion;
2. The air particles can only move in the x -direction (longitudinal);
3. The motion of each air particle is determined only by its x -coordinate, i.e., the motion is parallel. This means that we neglect any friction at the pipe wall.

An air particle that at rest has x -coordinate x_0 now moves in the x -direction that we denote by

$$t \mapsto x_0 + u(t, x_0).$$

So here $u(t, x_0)$ corresponds to the x -displacement of the particle at time t . Finally, since both ends $x_0 = 0$ and $x_0 = L$ of the pipe are closed, for all t we have $u(t, 0) \equiv 0 \equiv u(t, L)$; compare our comments on the vibrating string at the beginning of this chapter.

3. Oscillations in daily life

Remark 19. The length L of the organ pipe is important for the pitch. For the moment we simply can take $L = 1$, but later will come back to this.

In a discrete approach, we replace the above by a system of n equal point masses, joined by identical massless springs, see Figure 3.14. Again all motion occurs in the x -direction.

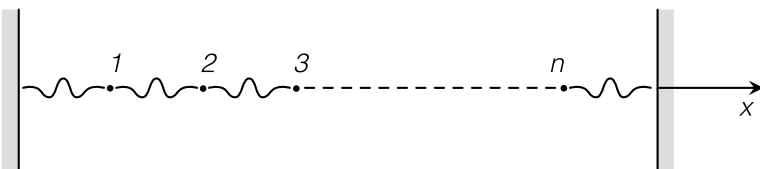


Figure 3.14: Discretized organ pipe

The idea is that as n gets ever larger, this system will become an increasingly better approximation of the organ pipe. Let us clarify this somewhat vague statement. For this we must first determine the size m of the masses and the spring constants. Since the springs are massless, we distribute the total air mass M equally over the point masses, that is, we could choose $m = \frac{M}{n}$. If we do this, however, we penalize unevenly the extrema of the n -pipe relative to the center. This problem is avoided if we always take $m = \frac{M}{n+1}$. The “residual” mass m then is distributed in two halves over the two extrema. For the rest of the story, we stick to this last choice.

Next, we consider the spring constant k . We start by noting the following: If a spring with stiffness k is cut into two equal pieces, each of the two halves will have stiffness $2k$. Check that out for yourself. Now suppose that K is the return force of the air column in the pipe which is (adiabatically) “pressed” or “stretched”. Recalling that the length of the pipe equals $L = 1$, the pressure difference thus occur-

ring is multiplied by the area of the cross-section of the pipe. So it turns out to be natural to give each of the $n + 1$ springs the stiffness constant $k = (n + 1)K$.

In what sense can we now speak of a good approximation? At this point it should be clarified that an organ pipe can produce more than one tone. The lowest of these is the so-called *fundamental (tone)*: all air particles oscillate with the frequency $f_0 = \frac{1}{2} \sqrt{\frac{K}{M}}$. The motion in the pipe corresponding to this fundamental, is shown in Figure 3.13. In addition to the fundamental, there are the so-called *harmonics* consisting of *overtones*.

The first overtone is produced by the configuration in Figure 3.15, where the center of the pipe is at rest. Here, all air particles oscillate with the frequency $f_1 = 2f_0 = \sqrt{\frac{K}{M}}$, this overtone sounds an *octave* higher than the fundamental. Similarly, you also have second, third, etc. overtones: the frequency of the ℓ^{th} overtone is $f_\ell = (\ell + 1)f_0$. What you hear in practice is always a combination (superposition)

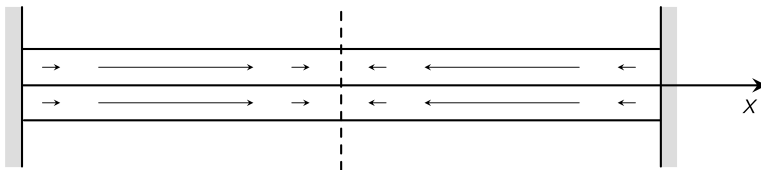


Figure 3.15: *The first overtone*

of fundamental and overtones. In our approximate model, fundamental and harmonics correspond to *characteristic* oscillations. Recall from Section 3.2 that all possible motions are (linear) combinations of characteristic oscillations, also see Appendix B. In the first approximation $n = 1$ we have only one characteristic oscillation and therefore the pipe can only produce the analogon of the fundamental. For $n = 2$ there are two characteristic oscillations that we already

3. Oscillations in daily life

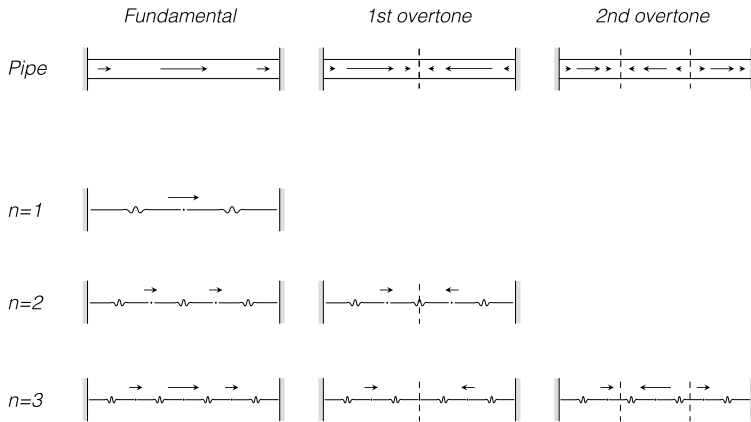


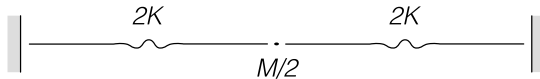
Figure 3.16: *The fundamental and other harmonics as n increases*

know from Section 3.2.2. They correspond to the fundamental and the first overtone respectively, etc.

Below we will compute the characteristic frequencies for $n = 1, 2$ and 3 and see that these differ from the frequencies of the corresponding overtones. However, these differences become smaller as n gets larger, we aim to show this in more details in the case of the fundamental. It is in this sense that we can speak of an increasingly better approximation of the organ pipe.

Computation of the characteristic frequencies. Now follows the computation of the characteristic frequencies for $n = 1, 2$ and 3 .

Case $n = 1$. Let u denote the deviation of the mass from the equilibrium state. Then one of the springs is extended by the amount $|u|$, while the other is compressed by $|u|$. Therefore, the equa-

Figure 3.17: Case $n = 1$

tion of motion is given by

$$\frac{M}{2} \ddot{u} = -2K(u + u)$$

or

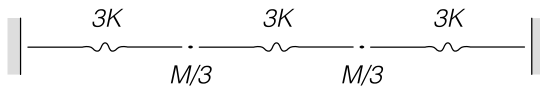
$$M \ddot{u} = -8Ku.$$

From Chapter 1 we know that solutions are oscillating with $\omega = 2\sqrt{2}\sqrt{\frac{K}{M}}$ and the corresponding frequency of oscillation is

$$\frac{\omega}{2\pi} = \frac{\sqrt{2}}{\pi} \sqrt{\frac{K}{M}} \approx 0.450 \sqrt{\frac{K}{M}}.$$

Comparing this to the fundamental frequency $f_0 = 0.5\sqrt{\frac{K}{M}}$, we see a rather crude though not unreasonable approximation.

Case $n = 2$. As said before, we already met this system in Section 3.2.2, also compare Appendix B. In complete analogy to the case

Figure 3.18: Case $n = 2$

$n = 1$, if let u_1 and u_2 denote the deviations of the left and right air masses from equilibrium, then we get the equations of motion

$$\begin{cases} \frac{M}{3} \ddot{u}_1 = -3K(2u_1 - u_2), \\ \frac{M}{3} \ddot{u}_2 = -3K(2u_2 - u_1). \end{cases}$$

3. Oscillations in daily life

From these, we immediately get the characteristic oscillations (also see Figure 3.16) and their corresponding frequencies

1. $u_1 = u_2$:

$$M\ddot{u}_1 = -9Ku_1 \Rightarrow \frac{\omega_1}{2\pi} = \frac{3}{2\pi}\sqrt{\frac{K}{M}} \approx 0.477\sqrt{\frac{K}{M}};$$

2. $u_1 = -u_2$:

$$M\ddot{u}_1 = -27Ku_1 \Rightarrow \frac{\omega_2}{2\pi} = \frac{3\sqrt{3}}{2\pi}\sqrt{\frac{K}{M}} \approx 0.827\sqrt{\frac{K}{M}}.$$

Comparing $\frac{\omega_1}{2\pi}$ with $f_0 = 0.5\sqrt{\frac{K}{M}}$, we see that the approximation has improved. We also recover the next harmonic, even though the distance between $\frac{\omega_2}{2\pi}$ and $f_1 = 1.0\sqrt{\frac{K}{M}}$ is still quite large.

Case $n = 3$. This is our first serious encounter with a system of 3 degrees of freedom. We follow the same strategy as before. If



Figure 3.19: Case $n = 3$

u_1 , u_2 and u_3 are the deviations from the equilibrium of the left, middle and right masses, respectively, then the equations of motion are

$$\begin{cases} \frac{M}{4}\ddot{u}_1 = -4K(2u_1 - u_2), \\ \frac{M}{4}\ddot{u}_2 = -4K(2u_2 - u_1 - u_3), \\ \frac{M}{4}\ddot{u}_3 = -4K(2u_3 - u_2). \end{cases}$$

Also here, we can compute the characteristic oscillations (also see Figure 3.16) and their frequencies:

1. $u_1 = u_3$, $u_2 = \sqrt{2}u_1$:

$$M\ddot{u}_1 = -16(2-\sqrt{2})Ku_1 \Rightarrow \frac{\omega_1}{2\pi} = \frac{2\sqrt{2}}{\pi} - \sqrt{2}\sqrt{\frac{K}{M}} \approx 0.487\sqrt{\frac{K}{M}};$$

2. $u_1 = -u_3, u_2 = 0$:

$$M\ddot{u}_1 = -32Ku_1 \Rightarrow \frac{\omega_2}{2\pi} = \frac{2\sqrt{2}}{\pi} - \sqrt{\frac{K}{M}} \approx 0.900\sqrt{\frac{K}{M}};$$

3. $u_1 = u_3, u_2 = -\sqrt{2}u_1$:

$$M\ddot{u}_1 = -16(2+\sqrt{2})Ku_1 \Rightarrow \frac{\omega_3}{2\pi} = \frac{2\sqrt{2}}{\pi} + \sqrt{2}\sqrt{\frac{K}{M}} \approx 1.176\sqrt{\frac{K}{M}}.$$

Let us compare these with the fundamental the the first harmonics. Both $\frac{\omega_1}{2\pi}$ and $\frac{\omega_2}{2\pi}$ respectively provide better approximations of $f_0 = 0.5\sqrt{\frac{K}{M}}$ and $f_1 = 1.0\sqrt{\frac{K}{M}}$ with respect to the case $n = 2$. We also recover the harmonic $f_2 = 1.5\sqrt{\frac{K}{M}}$ even though $\frac{\omega_3}{2\pi} = 1.176\sqrt{\frac{K}{M}}$ is still a rather poor approximation.

On the length L of the organ pipe. We now come to the discussion of the length L of the organ pipe as announced in Remark 19, noting that L is not explicitly showing in the expression $\frac{K}{M}$. To solve this problem we first introduce some new constants.

So, if L is the length of the pipe, we further introduce σ as the area of its cross section, ρ as the density (specific weight) of the air in the pipe and κ the “stiffness constant” of a pipe of unit length and unit cross section area.

Then $M = \sigma L \rho$ and $K = \frac{\sigma \kappa}{L}$. The first identity is quite obvious and the second follows by a similar reasoning as the one used above when determining the spring constant of the springs in the approximation with n masses and $n+1$ springs. It then follows that $\frac{K}{M} = \frac{1}{L^2} \frac{\kappa}{\rho}$, so that, for example, the fundamental becomes

$$f_0 = \frac{1}{2L} \sqrt{\frac{\kappa}{\rho}}. \quad (3.3)$$

3. Oscillations in daily life

Note that σ does not appear in (3.3). Moreover, the role of L may now become clear: doubling it gives a halving of the fundamental frequency and thus a reduction of the fundamental by 1 octave. Hence the classical custom of dividing organ registers into 2-foot, 4-foot, 8-foot, 16-foot and 32-foot registers. Here, the number of feet stands for the length of the longest pipe in that register. Here the fundamental is always one octave lower than in the previous register.

Towards a partial differential equation

Let us further speculate for a while about our approach to the organ pipe by an n degrees of freedom system. As before, let u_1, u_2, \dots, u_n

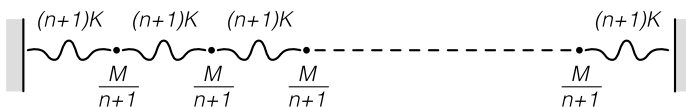


Figure 3.20: Case of arbitrary n

denote the deviation of the n masses from their equilibrium. The usual reasoning, completely analogue to the case $n = 3$, leads to the equations of motion

$$\begin{cases} \frac{M}{n+1} \ddot{u}_1 = -(n+1)K(2u_1 - u_2), \\ \frac{M}{n+1} \ddot{u}_j = -(n+1)K(2u_j - u_{j-1} - u_{j+1}), \quad 2 \leq j \leq n-1, \\ \frac{M}{n+1} \ddot{u}_n = -(n+1)K(2u_n - u_{n-1}), \end{cases}$$

compare the above case $n = 3$. We are no longer concerned in computing the characteristic frequencies $\omega_1 < \omega_2 < \dots < \omega_n$, but instead we want to arrive at the equation of motion of the continuous system by means of an infinitesimal consideration. Let $x = \frac{jL}{n+1}$ and $\Delta x = \frac{L}{n+1}$. Then, for $2 \leq j \leq n-1$, the j^{th} mass has position x and

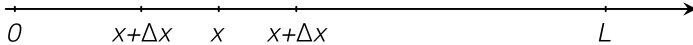


Figure 3.21: Infinitesimal consideration

surrounded by the $(j - 1)^{\text{th}}$ and $(j + 1)^{\text{th}}$ masses respectively at the positions $x - \Delta x$ and $x + \Delta x$. Then we compute

$$\begin{aligned} M\ddot{u}_j &= -(n+1)^2 K(2u_j - u_{j-1} - u_{j+1}) \\ &= (n+1)^2 K[(u_{j+1} - u_j) - (u_j - u_{j-1})]. \end{aligned}$$

With a slight abuse of notation we write $u(x) = u_j$, $u(x - \Delta x) = u_{j-1}$ and $u(x + \Delta x) = u_{j+1}$ and observe that $L = (n+1)\Delta x$. The latter expression then can be rewritten as

$$\begin{aligned} &(n+1)^2 K[(u_{j+1} - u_j) - (u_j - u_{j-1})] \\ &= \frac{L^2 K}{(\Delta x)^2} [(u(x + \Delta x) - u(x)) - (u(x) - u(x - \Delta x))] \\ &= \frac{L^2 K}{\Delta x} \left[\frac{u(x + \Delta x) - u(x)}{\Delta x} - \frac{u(x) - u(x - \Delta x)}{\Delta x} \right] \\ &\approx \frac{L^2 K}{\Delta x} \left[\frac{du}{dx} \left(x + \frac{\Delta x}{2} \right) - \frac{du}{dx} \left(x - \frac{\Delta x}{2} \right) \right] \\ &= L^2 K \frac{du}{dx} \left(x + \frac{\Delta x}{2} \right) - \frac{du}{dx} \left(x - \frac{\Delta x}{2} \right) \Delta x \\ &\approx L^2 K \frac{d^2 u}{dx^2}(x). \end{aligned}$$

In the transitions \approx we approximate the expression by a differential quotient: this becomes more precise as n gets larger. Gradually u has become a function of x , while at the same time, u is also still a function of t . As in the introductory treatment of the vibrating string we write $u = u(t, x)$. Now, we change slightly the notation, writing

$$\frac{\partial^2 u}{\partial x^2} \text{ instead of } \frac{d^2 u}{dx^2} (= u'') \quad \text{and} \quad \frac{\partial^2 u}{\partial t^2} \text{ instead of } \frac{d^2 u}{dt^2} (= \ddot{u}),$$

3. Oscillations in daily life

and speak about *partial derivatives* of u with respect to t and x . In summary, we have arrived at the equation of motion

$$M \frac{\partial^2 u}{\partial t^2} = L^2 K \frac{\partial^2 u}{\partial x^2},$$

or, using the constants introduced earlier,

$$\frac{\partial^2 u}{\partial t^2} = \frac{\kappa}{\rho} \frac{\partial^2 u}{\partial x^2}. \quad (3.4)$$

This is a so-called *partial differential equation*. The fact that the pipe is closed at both ends is expressed by the boundary conditions

$$u(t, 0) \equiv 0, \quad u(t, L) \equiv 0.$$

Equation (3.4) is known as *wave equation*. The reason for this is that for a suitably chosen positive number v , all solutions have the form

$$u(t, x) = g(x + vt) \quad \text{and} \quad u(t, x) = g(x - vt).$$

Here g is a (rather) arbitrary function, which has to be chosen in accordance with the boundary conditions, which are generally different from problem to problem. See below for more details. A solution of the above form is called a *traveling wave*. Why would one have chosen this name? The number v is called the (*wave*) *propagation speed* or *phase speed*. Justify this (first) name as well. In our case, $v = \sqrt{\frac{\kappa}{\rho}}$ and v is exactly the speed of sound. Let us examine the above above in more detail.

First we discuss the fact that necessarily $v = \sqrt{\frac{\kappa}{\rho}}$. This can be seen by replacing the traveling wave $u(t, x) = g(x \pm vt)$ in the wave equation. By the chain rule

$$\frac{\partial^2 u}{\partial t^2} = v^2 g'' \quad \text{and} \quad \frac{\partial^2 u}{\partial x^2} = g'',$$

which reduces the wave equation to

$$\nu^2 g'' = \frac{\kappa}{\rho} g''.$$

The latter equation, with the unknown function g , then is soluble exactly when $\nu^2 = \frac{\kappa}{\rho}$.

It may now be clear that traveling waves with propagation speed $\nu = \sqrt{\frac{\kappa}{\rho}}$ are indeed solutions of the wave equation. Our second observation is that sums (superpositions) of such running wave solutions are again solutions of the wave equation themselves. (This has to do with the linearity of the differential equation, also see the analogous comments in Section 3.2). So we find that for (rather) arbitrary functions g_1 and g_2

$$u(t, x) = g_1(x + \nu t) + g_2(x - \nu t) \quad (3.5)$$

satisfies the wave equation. The word “rather”, which has been used here twice, refers to the differentiability conditions that the relevant functions (g or g_1 and g_2) must satisfy. It can be shown that, apart from this issue, equation (3.5) represents the most general solution of the wave equation. For further background see [107].

Back to the organ pipe. In the above discussion, we disregarded the boundary. Now let us consider solutions of the above general type (3.5) that also satisfy the boundary conditions $u(t, 0) \equiv 0 \equiv u(t, L)$. To this purpose we first take the solutions

$$g_1(x) = \frac{1}{2} \cos\left(\frac{k\pi}{L} y\right), \quad g_2 = -g_1, \quad k = 1, 2, 3, \dots$$

then, after some trigonometric manipulations, we obtain

$$u_k(t, x) = \sin\left(\frac{k\pi}{L} y\right) \sin\left(\frac{k\pi}{L} \nu t\right), \quad k = 1, 2, 3, \dots$$

3. Oscillations in daily life

If, on the other hand, we choose

$$g_1(x) = \frac{1}{2} \sin\left(\frac{k\pi}{L} y\right), \quad g_2 = g_1, \quad k = 1, 2, 3, \dots,$$

we obtain

$$u_k(t, x) = \sin\left(\frac{k\pi}{L} y\right) \cos\left(\frac{k\pi}{L} v t\right), \quad k = 1, 2, 3, \dots.$$

You can check see that the boundary conditions are satisfied for both of these choices u_k . Such a solution u_k is often called k^{th} harmonic; for understanding the reasons for a such name, also see the remarks in Section 1.3.1. In fact, the first harmonics form the fundamental of the pipe, while for $k > 2$ the k^{th} harmonics form the $(k-1)^{\text{th}}$ overtone. To elaborate a bit more on this, we define

$$\lambda_k = \frac{2L}{k} \quad \omega_k = \frac{k\pi}{L} v, \quad k = 1, 2, 3, \dots,$$

and obtain

$$u_k(t, x) = \begin{cases} \sin\left(\frac{2\pi}{\lambda_k} x\right) \sin(\omega_k t) \\ \sin\left(\frac{2\pi}{\lambda_k} x\right) \cos(\omega_k t) \end{cases} \quad k = 1, 2, 3, \dots.$$

Now observe that $f_{k-1} = \frac{\omega_k}{2\pi}$ is the frequency of oscillation of the air particles in the solutions u_k . The constant λ_k is called *wavelength* of the solution: the larger k , the shorter the wavelength and the higher the frequency (pitch) of the corresponding tone. Intuitively, sound waves all travel at about the same speed, the speed of sound, and the wavelength measures the distance between consecutive 'maxima' of the wave: in the same time interval, waves with a shorter wavelength will reach your hear more often than the ones with longer wavelength, thereby leading to the higher pitch.

Before we started to discretize the organ pipe, we observed that the tone you hear is a combination of the fundamental and overtones.

Mathematically, this means that any solution $u(t, x)$ can be written as an (infinite) sum, or series,

$$u(t, x) = \sum_{k=1}^{\infty} \sin\left(\frac{2\pi}{\lambda_k} x\right) (a_k \sin(\omega_k t) + b_k \cos(\omega_k t)),$$

for certain numbers $a_1, b_1, a_2, b_2, \dots$ called *amplitudes*. In fact these amplitudes determine the *timbre* of the tone.

Conclusive digression and questions. How long is the pipe in terms of the wavelength λ_1 of the fundamental? Recalling that v denotes the speed of sound, check that $v = f_{k-1} \lambda_k$ for all $k = 1, 2, \dots$ and give a simple interpretation of this formula.

Earlier we said that real organ pipes are open at at least one end. Consider the case of a pipe that is open at exactly one end: this is where the air is blown on, the other end is “covered”. The equation of motion is again

$$\frac{\partial^2 u}{\partial t^2} = v^2 \frac{\partial^2 u}{\partial x^2}, \quad v = \frac{\kappa}{\rho},$$

but now the boundary conditions are

$$u(t, 0) \equiv 0 \quad \text{and} \quad \frac{\partial u}{\partial x}(t, L) = 0,$$

where $x = L$ is the open end. Treat this problem in analogy to this chapter. What are the differences with the above derivation? Finally, consider a possible discretization of the semi-open pipe.

3.3.2. Strings, beams, etc.

The organ pipe is an illustrative example of all kinds of vibrations, e.g., longitudinal vibrations of an elastic rod, but also of transverse

3. Oscillations in daily life

string vibrations and even, albeit as a rough approximation, transverse ship vibrations, where the idea that a ship is a rigid body has to be abandoned; compare with the Sections 3.1.2 and 3.2.3.

First we return to the string, also see the introduction to this chapter. In the discretization, we replace the string by a finite number of points of equal mass, connected by identical, massless springs. The difference with the organ pipe is that now the masses may only move transversely, i.e., perpendicular to the line connecting them when they are at rest, see Figure 3.22.

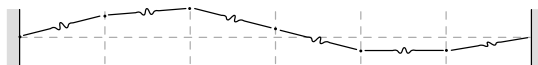


Figure 3.22: *A discretized string*

We can literally repeat the story about fundamental, overtones and characteristic oscillations that we developed for the organ pipe and summarize the result in Figure 3.23. Although these the computations of these characteristic oscillations are somewhat more involved than for the organ pipe, there is actually no mathematical difference between the two situations.

If for a fixed t , the deviation of the string is given by the function $x \mapsto u(t, x)$ as indicated in the introduction, then the equation of motion is again the wave equation

$$\frac{\partial^2 u}{\partial t^2} = v^2 \frac{\partial^2 u}{\partial x^2},$$

where now $v^2 = \frac{s}{\rho}$. Here s is the tension of the string and ρ the mass density. If the string has length L (in the introduction we took $L = 1$), then the boundary conditions are $u(t, 0) = 0 = u(t, L)$. Compare this with our treatment of the organ pipe: both ends of the string are fixed. We can now literally repeat the computations from

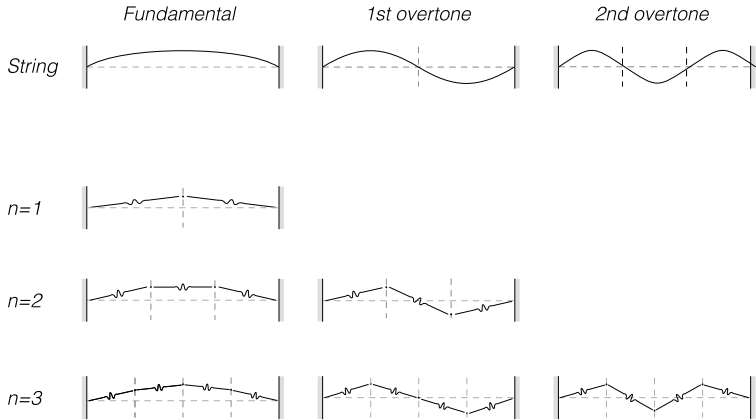


Figure 3.23: *Characteristic oscillations of a discretized string for different values of n*

Section 3.3.1. Graphs of the functions $x \mapsto u_n(t, x)$, for t fixed and $n = 1, 2$ and 3 are depicted in Figure 3.23. What are the frequency f_0 and wavelength λ_1 of the fundamental? Note that, in principle, the waves in the string propagate at a speed different from the sound waves in air.

Next we turn to the oscillations of a boat. In the analysis there is, at least *in principle*, no difference with the string.

Also bars or beams containing longitudinal or transverse vibrations can be treated entirely according to the above recipe. The assumption is always that there is only one space variable at stake. Two-dimensional continua such as plates and shells like the floor of a bridge or the wings and body of an airplane, follow an analogous albeit somewhat more complicated theory. Discretizations always play an important role in both practical computations and in more theoretical considerations.

3. Oscillations in daily life

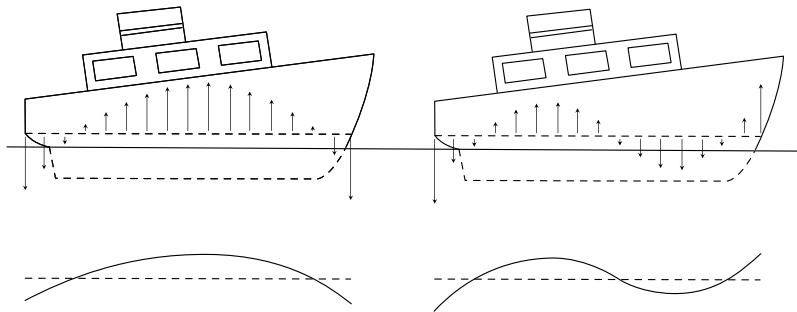


Figure 3.24: *Oscillations of a boat*

Remark 20. *In practice, it is often not enough to rely solely on computations, however accurate. This is because we are always working within a model, in which all kinds of more or less essential matters are not included; compare remarks made earlier in Section 1.1.5 and in the introduction to the present chapter. These often cannot be included in the model for mainly two reasons: Firstly, because certain effects are not known well enough, e.g., precise effects of energy losses due to something like friction. Secondly, because otherwise the model becomes unmanageably complicated, e.g., by certain nonlinear effects.*

In many cases one has to resort to experimental measurement data. In some cases such data can be obtained using scaled models such as a wind tunnel or a gutter. Often however, such data only become available when the construction in question (e.g. a ship) has already been completely built. In the latter case, constructive retrospective changes, the desirability of which is determined on the basis of measurements, can not always be realized or only at very high costs.

3.3.3. Other vibrational phenomena

Finally, we will discuss a number of separate topics. We will use a less mathematical style than and also recommend you to consult with an additional physics book, e.g., the Feynman Lecture Notes [62] or Minnaert [97].

Sound and light

We already encountered sound as an air vibration extensively in Section 3.3.1 concerning the organ pipe. There we only dealt with one spatial variable, but in general there is a three-dimensional spatial continuum to deal with. Each of us is probably familiar with phenomena associated with the wave character of sound: we only mention *interference* and *Doppler effect*.

Interference and the Doppler effect. Interference phenomena arise from the *superposition* of two or more waves: we have already encountered sound beats in Section 3.2.2. The superposition leads to mutual extinction or amplification of the waves. Spectacular examples of amplification can be met in the well-known whisper galleries, etc. Moreover, blind spots in concert halls can be understood in terms of destructive interference. Doppler phenomena arise from frequency changes due to *relative motions* of the sound source relative to the observer. Think of the bell of the level crossing, which rings higher for the railway passenger when the train approaches the crossing and lower when the train moves away from it.

Remark 21. 1. *It is less evident that light also has a wave character. In this context, there is famous historical controversy in which already Huygens and Newton were involved. Roughly*

3. Oscillations in daily life

speaking, the former proposed a wave theory and the latter a particle theory. Only in the 19th century, Maxwell came up with a theory in which light is understood as an electromagnetic wave phenomenon. In this century, quantum mechanics has yielded a theory for light that includes both wave and particle aspects.

2. *A problem with all this is the following. If light is a wave phenomenon, then what is it that exactly vibrates? For a long time, physicists have thought that there is a medium in space, called ether, in which the light waves move. Nowadays we live in an etherless era.*

Interestingly, in connection with radio and television waves, other special cases of the Maxwell theory, people still speak of the ether. However, whether or not such a thing as this ether exists, leaves mathematics indifferent. The only important thing is that in Maxwell's theory the components of the electromagnetic field satisfy the equation

$$\frac{\partial^2 u}{\partial t^2} = c^2 \left(\frac{\partial^2 u}{\partial x^2} + \frac{\partial^2 u}{\partial y^2} + \frac{\partial^2 u}{\partial z^2} \right),$$

in which a careful reader will immediately recognize the wave equation. Here x , y , and z are the space variables and c is the speed of light.

From the above it may be clear that it is not so easy to find physical phenomena in this context that present the wave character. A large number of the examples to be given below could have not been discovered until the 19th century.

Miscellaneous comments. We conclude this section with a few comments on daily life phenomena that can be explained in terms of the above.

1. *Interference* of light waves may explain well the changing color patterns in oil stains on water. Also the so-called *fading* in short-wave receivers can be understood as an interference phenomenon: radio waves of the same wavelength reach the observer along paths of different length. What one hears is the alteration of extinction and amplification of the sound coming from the radio, just as in the case of beats.
2. The *Doppler effect* can also serve to explain the so-called *redshift* observed in the radiation that reaches us from the distant, *expanding* universe.
3. In wave theory, *dispersion* means dependence of the propagation speed on the wavelength. The refraction of white light through a prism and the associated decomposition in all colors is a well-known phenomenon that can be explained in terms of dispersion. Replacing the prism by a water droplet similarly explains the phenomenon of a *rainbow*. Compare with Arnold [12].
4. In the world of radio and television, the concept of *resonance* is also extremely important, compare with Chapter 2: the incoming electromagnetic radiation forms the external *drive* of the electric circuit attached to a receiver, including the antenna. The resonance peaks then make it possible to select a certain wavelength range upon reception: this is exactly what one does if one *tunes* the receiver to a particular station.
5. Finally, we also mention the *polarization phenomenon* that is being used in sunglasses and LCD screens. This has to do with the so-called *transversality* of the light waves. When waves pass through a material with a certain “crystalline” structure, the vibrations are extinguished in all directions except one, thus obtaining *polarized* light.

3. Oscillations in daily life

Water waves

On water surface waves we will be brief, and just refer to Minnaert's *The Nature of Light and Colour in the Open Air* [97]. It should be noted that this treatment is more involved than with air vibrations, due to the so-called *surface tension*. It is also worth mentioning that in [97] all known wave phenomena mentioned above are beautifully illustrated by means of water waves; this includes the phenomenon of *radiation pressure*.

3.4. Relaxation oscillations

This chapter is concluded by briefly describing *relaxation oscillations*, a group of oscillation phenomena that you may encounter often in everyday life. Here think of the sound of a fiddled violin string, of a chamois that “squeaks” over a glass pane or a “singing” wine glass, or a piece of chalk that “crunches” on a blackboard, but also creaking doors and vibrations of propeller shafts in ships. The physics of such oscillations is quite involved and is still subject of active research. Considerations about energy and forces are central in their mathematical understanding, and *Coulombic* or *dry friction* plays a major role, compare with Section 2.1.

Mathematically speaking, relaxation oscillation can be characterized by saying that deviations as a function of time should alternate periods of *slow* and *fast* variation. Figure 3.25 presents two cases: we consider a variable x as a function of time t . Where does $x = x(t)$ varies slowly and where fast? We will now give some concrete examples.

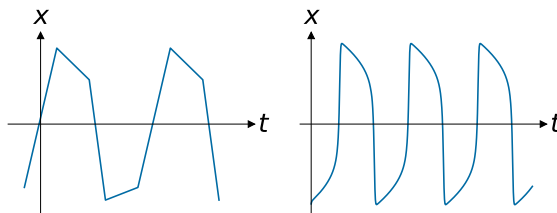
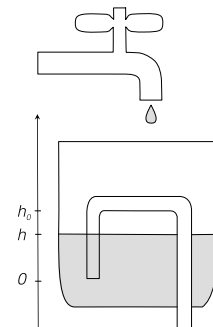


Figure 3.25: Relaxation oscillations

The Tantalus cup. The *Tantalus cup* or *Pythagorean cup* consists of a vessel to which water is continuously added from a tap. A tube that can act as a *siphon* passes through the bottom of the vessel as indicated in the figure on the right. Let h denote the height of the water level in the vessel, then h periodically varies between two extreme values. The lowest value of h is slightly below $h = 0$, see the figure. From this state, h slowly increases as a function of time t : i.e. the vessel is *slowly* filled with tap water.

Once the water level increased slightly above the height $h = h_0$, the pipe is completely filled with water and starts acting as a siphon. The vessel now empties *quickly* to slightly below $h = 0$; with some good will, you could call this phase of motion “relaxating”: the system gives its surplus of potential energy up quite suddenly. Then h slowly increases again, etc.



In Figure 3.26 you see h as function of the time t . (We note however that the dynamics of h above the level h_0 also is more complicated than shown here.) Similar *sawtooth* graphs are common in electronic devices, such as television sets or mobile phones. In such systems, the underlying physics is clear, at least in principle. However, this is not the case at all in the following example.

3. Oscillations in daily life

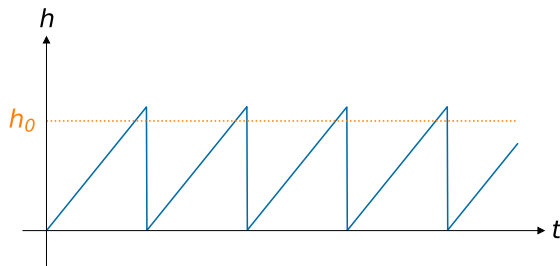


Figure 3.26: *Relaxation oscillations of the Tantalus cup*

Heart beat. Consider the motion of a *muscle fiber* in the human heart. The underlying physiology is particularly complex, but here we are looking for a “simple” mathematical model with the same *qualitative* properties as that of the motion of the muscle fiber. The properties that we have in mind are:

1. The existence of a *stable equilibrium*, a state corresponding to the so-called *diastole*, in which the heart muscle is relaxed;
2. For some electrochemical variable x , there exist a threshold value $x = x_1$, such that once $x > x_1$ an action is triggered: the heart muscle contracts, this is the so-called *systole*. The excitation of the muscle fiber caused by an electromagnetic pulse emitted by a *pacemaker*, forces it to exceed the threshold value $x = x_1$;
3. There is a jump back to the equilibrium state, the heart muscle relaxes again.

If y denotes the length of our muscle fiber, Figure 3.27 schematically shows what the above properties mean. Here x_0 and y_0 are the values of x and y in the diastolic state. The contraction and relaxation are fast motions of y , which are alternated with slow motions in diastole and systole. The dynamics depicted in Figure 3.27 can

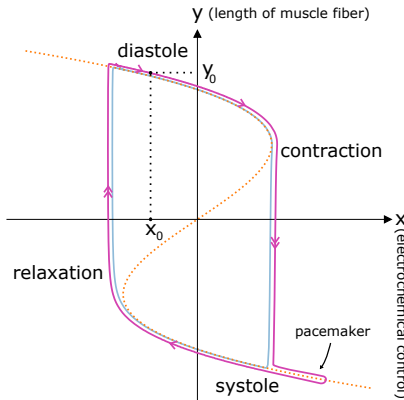


Figure 3.27: Relaxation oscillations for the muscle fiber of the heart

be described rather explicitly using the Van der Pol–Liénard differential equations

$$\begin{cases} \dot{x} = y - y_0 \\ \epsilon \dot{y} = -(x - y + y^3) \end{cases}.$$

Here, $y_0 < \frac{1}{\sqrt{3}}$ and $\epsilon > 0$ is a small constant. Compare this with Exercise 2.6.5 and the discussion in Exercise E.2.5. Give a (rough) sketch of y as a function of the time t .

Remark 22. The latter example stems from E.C. Zeeman's Catastrophe Theory [141], Chapter 3. Zeeman also shows that the above differential equations to some extent forms the simplest mathematical model having the properties 1, 2 and 3 mentioned above. This theory has been developed from the 1970s on, also compare with [113, 10]. In the latter of these references also more recent developments can be found including more recent developments on the more general singularity theory.

The pacemaker of the heart beat is part of the autonomous nervous system. There exists a more general theory of neuronal activity where

3. Oscillations in daily life

increases of voltage can produce cascades of spikes. The leading Hodgkin-Huxley model [78] also lies at the basis of Zeeman [141, Chapter 3].

3.5. Exercises on Hooke's n -body problem

Lissajous figures appears in many different problems. As an interesting example we report here two problems by Bottema, namely problem 673 [22] and problem 683 [23].

Part 1. A particle P of unit mass moves in the plane of a given triangle $A_1A_2A_3$. The force F_i on P is directed towards A_i and is equal to $k\overline{PA}_i$ for $i = 1, 2, 3$, where k is a positive constant and \overline{PA}_i denotes the distance between P and A_i . Prove that there is a motion of P the path of which coincides with the Steiner ellipse S of $A_1A_2A_3$ (the ellipse S that passes through the vertices and whose tangent at any vertex is parallel to the opposite side). Show moreover that P covers the three arcs A_1A_2 , A_2A_3 , and A_3A_1 of S in equal time.

Let us look now at what happens if we allow n points to move under the influence of a similar mutual attraction. In other words, let us investigate the motion under universal Hookian gravitation.

Part 2. The particles A_i with masses m_i ($i = 1, 2, \dots, n$) move in three-dimensional space. Any two distinct particles A_i, A_j attract each other by the force $F = k^2 m_i m_j \overline{d}_{i,j}$, where $k > 0$ and $\overline{d}_{i,j}$ denotes the distance $\overline{A_i A_j}$. We suppose that the motions of A_i and A_j are not disturbed if they pass simultaneously through the same point. Determine the general motion of the particles.

Appendices

A. Johann Bernoulli's brachistochrone

In the Preamble we mentioned a number of problems put forward by Huygens, among which to find the isochronous and the tautochronous curve. We already claimed that nowadays the verification that the cycloid solves both problems has become quite elementary, compare Exercises 1.6.7 and 1.6.8. We also mentioned the brachistochrone problem put forward by Johann Bernoulli, that is, to find the curve of swiftest decent, i.e., with the shortest down time. Surprisingly, here again the cycloid showed up. Since this is a slightly more difficult exercise, we included its solution as an appendix. Although the problem was formulated in the mechanical terms of sliding beads (or rolling marbles), Bernoulli added optics to the picture using the Fermat Principle and Snell's Law, finally obtaining the desired curve as a light ray!

Johann Bernoulli was born in Basel (Switzerland) in 1667 and moved to Groningen in 1695 and back to Basel in 1705, where he died in 1748. Among others, Christiaan Huygens recommended Bernoulli's appointment in Groningen and, like Huygens, he had a great international reputation. From 1699 on he was Associé Étranger of the Académie des Sciences in Paris and from 1712 on he was Fellow of the Royal Society in London. He became also a member of the Academies in Bologna, Berlin and Sankt Petersburg. His most well-known students are his son Daniel (1700-1782) and Leonhard Euler (1707-1783). For an extensive historical account we refer to

A. Johann Bernoulli's brachistochrone

Van Maanen [91].

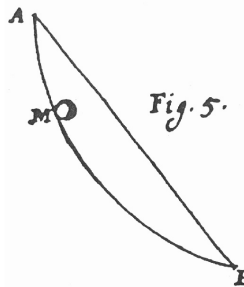


Figure A.1: *The brachistochrone problem: for which profile does the bead M slide in the shortest possible time from A to B? From Opera Johannis Bernoullii, 1742 [20]*

The brachistochrone problem goes as follows. Given two points A and B in a vertical plane, with A higher than B , what is the wire profile along which a bead slides from A to B in the shortest time. The motion takes place under constant vertical gravitation and there is no friction.

A.1. Geometric optics

The present story largely follows [30, Section 4.3.2] and is mimicking Bernoulli's own solution [20]. In analogy with Chapter 3, we are going to discretize the continuum, first dividing it in two layers, and later on in an increasing number of equally thick layers.

Throughout our considerations we restrict in a so-called *flat earth atmosphere* and in one vertical plane. The horizontal coordinate

is denoted x and the vertical coordinate y . The velocity of light is denoted v , depending on the position. Our assumption is that $v = v(y)$ only depends on the vertical co-ordinate y . The *refraction index* is defined as

$$n(y) := \frac{c}{v(y)},$$

where c is the velocity of light in vacuum. For simplicity we take $c = 1$.

Definition 1 (Fermat Principle). *Given two points A and B then a light ray between A and B is the path that takes the shortest time.*

This definition asks for minimality of the traveling time, but often we only ask this time to be extremal and speak of the *weak Fermat Principle*. One of the prime examples is the case where A and B are the focal points of an ellipse, where the light ray reflects in the elliptic curve. In that case the time needed is constant.

A.1.1. Fermat implies Snell

We divide the atmosphere into two horizontal layers numbered 1 and 2, separated by the common boundary $y = 0$, see Figure A.2. The angles with the normal to the boundary are denoted by α_1 for $y \geq 0$ and α_2 for $y \leq 0$. The refraction indices are n_1 for $y > 0$ and n_2 for $y < 0$, with corresponding propagation velocities v_1 and v_2 .

We now formulate

Theorem 2 (Snell's Law). *Under the above circumstances assume that A lies in the upper halfplane $y > 0$, C on the boundary $y = 0$ and*

A. Johann Bernoulli's brachistochrone

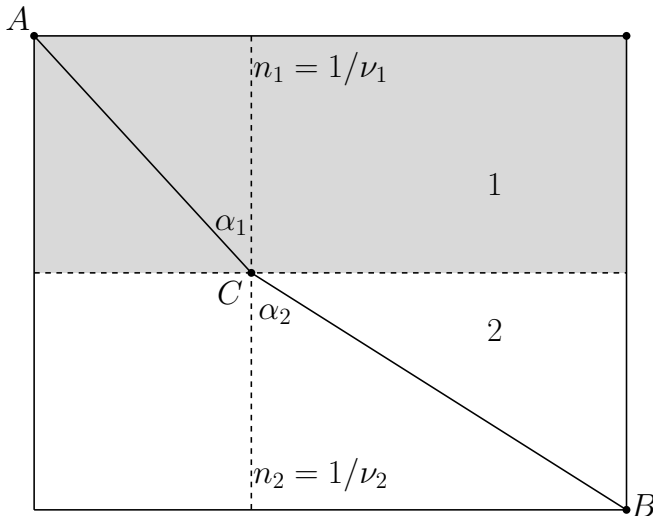


Figure A.2: Snell's law follows from the Fermat Principle

B in the lower half plane $y < 0$. Then the broken straight line ACB is a light ray according to the weak Fermat Principle if and only if

$$n_1 \sin \alpha_1 = n_2 \sin \alpha_2.$$

Proof. Let $x = x_C$ indicate the position of C on the line $y = 0$ that separates both layers. Let t_{AC} denote the time for the light ray needed to travel from A to C and t_{CB} the time needed to travel from C to B . We then have to find an extremum of $t_{AC} + t_{CB}$. The facts that $|A - C| = t_{AC} \cdot v_1$ and that $v_1 = 1/n_1$ yield that

$$t_{AC} = n_1 |A - C|.$$

By the Pythagorean Theorem we know that

$$|A - C| = \sqrt{x^2 + b^2} \quad \text{so} \quad t_{AC} = n_1 \sqrt{x^2 + b^2}.$$

Differentiation with respect to x then gives

$$\frac{d}{dx} t_{AC}(x) = \frac{n_1 x}{\sqrt{x^2 + b^2}} = n_1 \sin \alpha_1.$$

Analogously we find

$$\frac{d}{dx} t_{CB}(x) = -\frac{n_2(a-x)}{\sqrt{(a-x)^2 + c^2}} = n_2 \sin \alpha_2,$$

again see Figure A.2. We may conclude that

$$\frac{d}{dx} (t_{AC}(x) + t_{BC})(x) = 0$$

if and only if

$$n_1 \sin \alpha_1 = n_2 \sin \alpha_2,$$

as was to be proven. \square

- Remark 23.**
1. Reflections in the boundary layer are easily incorporated in this story [30], but since we only consider motions that are monotonic in terms of $y \mapsto x(y)$, for simplicity we exclude reflections.
 2. In this case the extremum also is a minimum as you can verify by inspecting the second derivative.
 3. Leibniz [89] already essentially gave this proof in 1684.

A.1.2. A conservation law

In this subsection instead of two layers, we take many of them in an increasing number, so discretizing the continuum, see Figure A.3. In fact as boundaries we take equidistant horizontal lines separating the layers $1, 2, 3, \dots, N$ where in each layer the speed of light is constant. In layer number j the refraction index is n_j and the angles at the lower boundary boundary of layer j with the vertical direction are α_j from above and α'_j from below ($1 \leq j \leq N$).

As a direct consequence of Theorem 2 we have

A. Johann Bernoulli's brachistochrone

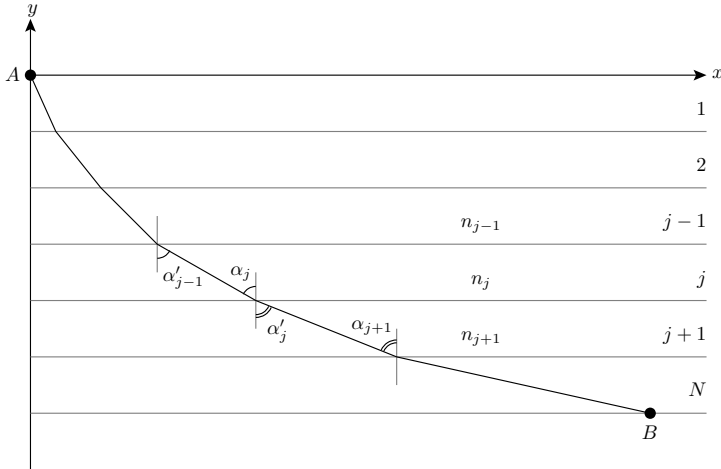


Figure A.3: *Bernoulli's optical set-up: the continuous medium is discretized into layers of constant propagation velocity*

Corollary 1 (Conservation Law). *Under the above circumstances a broken straight line from A to B is a light ray according to the weak Fermat Principle if and only if*

$$n_j \sin \alpha_j = n_{j+1} \sin \alpha_{j+1} \quad (1 \leq j \leq N-1).$$

Proof. According to Theorem 2 always

$$n_j \sin \alpha_j = n_{j+1} \sin \alpha'_j,$$

while from Euclidean geometry it is known that always

$$\alpha'_j = \alpha_{j+1}.$$

From this the assertion follows. \square

We may consider α_j as a parameter along the light ray, which in the continuous limit for $N \rightarrow \infty$ is just called $\alpha = \alpha(y)$: the *inclination* of

the ray. We so have obtained a quantity that is conserved during the propagation of the light:

$$S = n \sin \alpha. \quad (\text{A.1})$$

Remark 24. 1. As said earlier we exclude reflections, otherwise $\alpha(y)$ would be multivalued. The light ray is pointing down, therefore the map $y \mapsto x(y)$ is monotonically decreasing and we have

$$\frac{dx}{dy} = -\tan \alpha$$

2. Note that the form of the light ray is completely determined by the value of S . The propagation along the ray is governed by the refraction index $n = 1/v$.
3. The conservation of S in modern times is related to the invariance of the problem under horizontal translations. In fact, any continuous symmetry of a variational problem is associated to a conserved quantity. This incredible result is known as Noether Theorem [8, 105], from the name of Emmy Noether, probably the most important woman in mathematics in the past century, who proved it in 1918.
4. Snell's law itself is still showing up in modern research, for example it was recently generalized to non-euclidean spaces in order to describe certain problems in celestial mechanics related to central mass galaxies [49, 50].

A.2. The brachistochrone as a light ray

Theorem 3 (The brachistochrone). *Under the above circumstances the brachistochrone curve has the cycloidal form*

$$x(\alpha) = \frac{1}{4S^2g} (2\alpha - \sin(2\alpha))$$

$$y(\alpha) = \frac{1}{4S^2g} (-1 + \cos(2\alpha)),$$

passing through $A = (0, 0)$ for $\alpha = 0$ and where the constant S determines the scale of the curve such that it passes through B .

Before giving a proof we have some comments.

1. Referring back to Exercise 1.6.7, in this case the cycloid has rolling angle $\varphi = 2\alpha - \pi$ and radius $R = 1/(4S^2g)$.
2. There are two conserved quantities. Apart from S , we have the energy H of the motion in a constant gravitational field

$$H = \frac{1}{2}mv^2(y) + mg y.$$

The refraction index $n(y) = 1/\nu(y)$ can now be determined as follows. Since we assume that the bead starts at a height $y = y_0$ at rest, $\nu(y_0) = 0$. It then follows that during the entire motion we have $H = mg y_0$ and, in particular, $H = 0$ when taking $y_0 = 0$. The corresponding falling speed therefore equals $\nu(y) = \sqrt{-2gy}$, where $y \leq 0$. The refraction index then is

$$n(y) = \frac{1}{\sqrt{-2gy}} \quad \text{where} \quad y \leq 0.$$

We now are ready to prove Theorem 3, more or less following Bernoulli [20].

Proof. Since the motion is downward, we have $dx/dy = -\tan \alpha$. In this proof we use both the conserved quantities

$$S = n(y) \sin \alpha \quad \text{and} \quad H = \frac{1}{2}mv^2(y) + mgy.$$

The desired profile will be of the form

$$(x(\alpha), y(\alpha)). \tag{A.2}$$

where α is the inclination with respect to the y -direction. Since H is constant, differentiating the latter of the two above formulæ we get for all y

$$v'(y) = -\frac{g}{v(y)}. \tag{A.3}$$

Rewriting the former formula as $\sin \alpha = Sv(y)$ and differentiating with respect to α gives

$$\cos \alpha = Sv'(y) \frac{dy}{d\alpha}. \tag{A.4}$$

With help of the formulæ (A.3) and (A.4) we can determine the derivatives $dy/d\alpha$ and $dx/d\alpha$ for the parametrized profile (A.2). First we consider $dy/d\alpha$:

$$\begin{aligned} \frac{dy}{d\alpha} &\stackrel{(A.4)}{=} \frac{\cos \alpha}{Sv'(y)} \\ &\stackrel{(A.3)}{=} -\frac{v(y)}{Sg} \cos \alpha \\ &\stackrel{(A.1)}{=} -\frac{1}{2S^2g} \sin(2\alpha). \end{aligned} \tag{A.5}$$

We can then use this expression to determine also the other derivative:

$$\begin{aligned} \frac{dx}{d\alpha} &= -\tan \alpha \frac{dy}{d\alpha} \\ &\stackrel{(A.5)}{=} \frac{v(y)}{Sg} \sin \alpha \\ &\stackrel{(A.1)}{=} -\frac{1}{2S^2g} (1 - \cos(2\alpha)), \end{aligned}$$

A. Johann Bernoulli's brachistochrone

also using some trigonometric gymnastics. Integration then gives

$$y(\alpha) = C_y + \frac{1}{4S^2g} \cos(2\alpha)$$
$$x(\alpha) = C_x + \frac{1}{4S^2g} (2\alpha - \sin(2\alpha)),$$

where we choose the constants of integration C_y and C_x in such a way that $x(0) = 0 = y(0)$, leading to $C_y = -1/(4S^2g)$ and $C_x = 0$. So we end up with

$$x(\alpha) = \frac{1}{4S^2g} (2\alpha - \sin(2\alpha))$$
$$y(\alpha) = \frac{1}{4S^2g} (-1 + \cos(2\alpha))$$

as was to be proven. □

A.3. Scholium

The cycloid has been a subject of general interest in the 17th century, not just in relation with Huygens's or Bernoulli's problems, compare [1, 3, 28, 29, 30, 72, 94, 110, 136, 140]

As we mentioned, Johann Bernoulli put forth his brachistochrone problem in 1696 in a contest published in the journal *Acta Eruditorum* [20]. One year later he published his own solution in the same journal. A number of his contemporaries quickly responded, Newton and Leibniz being two of them. In fact, Newton's solution was sent under pseudonym but Bernoulli recognized the “lion by his paw” (ex ungue leonem). For the mathematical details see Goldstine [70].

The brachistochrone problem and its solutions mark the birth of the long and broad development of the Variational Principle, nowa-

days a cornerstone of many scientific disciplines. In a modern *Variational Calculus* class the brachistochrone problem has become an exercise, see e.g. [86, Exercise 8.20]. For additional discussions see [69, 85, 124, 128].

B. Small oscillations and the Foucault problem

We encountered small oscillations already several times, for instance when linearizing the pendulum in Section 1.2, or in Section 3.2.2 when studying beats. In this section we come back to this by discussing the Foucault pendulum, where small oscillations will again play an important role.

B.1. Beats revisited

There exists a general theory of small oscillations, formulated in terms of linear algebra, for instance see Arnold [8, Section 23]. Instead of fully presenting the theory we illustrate it on the example of beats, as roughly described in Section 3.2.2.

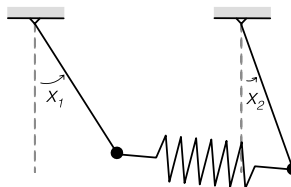


Figure B.1: Two coupled pendulums, compare Figure 3.6

As before, we consider two identical pendulums coupled by a spring.

B. Small oscillations and the Foucault problem

The two deflections (x_1, x_2) describe the configuration of the system, see Figure B.1. To describe the state of the system, we also have to consider the velocities, \dot{x}_1 and \dot{x}_2 , ending up with four variables to work with. The equations of motion are then given by

$$\begin{aligned}\ddot{x}_1 &= -x_1 - 2\kappa(x_1 - x_2) \\ \ddot{x}_2 &= -x_2 - 2\kappa(x_2 - x_1)\end{aligned}$$

where κ is the spring constant of the connection. Observe that we already linearized the pendulum at its lower equilibrium. We are left with a coupled system of differential equation and, as indicated in Section 3.2.2, we aim to decouple it by passing to suitable coordinates.

The kinetic and potential energy of our linear system read

$$T = \frac{1}{2}(\dot{x}_1^2 + \dot{x}_2^2) \quad \text{and} \quad U = \frac{1}{2}(x_1^2 + x_2^2 + \kappa(x_1 - x_2)^2) \quad (\text{B.1})$$

As a small extension of the theory presented in Section 1.4 we now have that

$$\ddot{x}_1 = -\frac{\partial U}{\partial x_1} \quad \text{and} \quad \ddot{x}_2 = -\frac{\partial U}{\partial x_2}. \quad (\text{B.2})$$

We invoke linear algebra by introducing the position and velocity vectors

$$\mathbf{x} = \begin{pmatrix} x_1 \\ x_2 \end{pmatrix} \quad \text{and} \quad \dot{\mathbf{x}} = \begin{pmatrix} \dot{x}_1 \\ \dot{x}_2 \end{pmatrix}$$

and reformulating the expressions for T and U as

$$T = \frac{1}{2}\langle \dot{\mathbf{x}}, \dot{\mathbf{x}} \rangle \quad \text{and} \quad U = \frac{1}{2}\langle B\mathbf{x}, \mathbf{x} \rangle,$$

where B is the matrix

$$B = \begin{pmatrix} 1 + \kappa & -\kappa \\ -\kappa & 1 + \kappa \end{pmatrix}. \quad (\text{B.3})$$

Here $\langle \cdot, \cdot \rangle$ denotes the standard inner product

$$\left\langle \begin{pmatrix} x_1 \\ x_2 \end{pmatrix}, \begin{pmatrix} y_1 \\ y_2 \end{pmatrix} \right\rangle := x_1 y_1 + x_2 y_2.$$

Any expression of the form $U = \langle B\mathbf{x}, \mathbf{x} \rangle$ where B is a real, symmetric matrix, is called a *quadratic form*. The Spectral Theorem [79, Theorem 2.5.6] states that B admits an orthonormal basis of eigenvectors and with respect to such a basis the matrix takes a diagonal form, with the eigenvalues on its diagonal.

Remark 25. *This result mentioned is far more general and surely also holds for all real, symmetric $n \times n$ -matrices.*

That is, in our particular case (B.3) there exists a 2-by-2 matrix C , such that

$$D = CBC^{-1} = \begin{pmatrix} \lambda_1 & 0 \\ 0 & \lambda_2 \end{pmatrix}.$$

The eigenvalues λ_1 and λ_2 are given by the characteristic equation $\det(B - \lambda \text{Id}) = 0$, and the eigenvectors in this case are unit vectors along the diagonals of the (x_1, x_2) -plane. With a direct computation one can find that $\lambda_1 = 1$ and $\lambda_2 = 1 + 2\kappa$, while the matrix C is given by

$$C = \frac{1}{\sqrt{2}} \begin{pmatrix} 1 & 1 \\ 1 & -1 \end{pmatrix}.$$

This means that $\mathbf{y} = C\mathbf{x}$ takes the concrete form

$$y_1 = \frac{1}{\sqrt{2}}(x_1 + x_2) \quad \text{and} \quad y_2 = \frac{1}{\sqrt{2}}(x_1 - x_2),$$

already familiar from formula (3.1), see Figure B.2. Moreover kinetic and potential energy now become of the form

$$\begin{aligned} T &= \frac{1}{2}\langle \dot{\mathbf{y}}, \dot{\mathbf{y}} \rangle = \frac{1}{2}(y_1^2 + y_2^2) \quad \text{and} \\ U &= \frac{1}{2}\langle \mathbf{y}, \mathbf{y} \rangle = \frac{1}{2}(y_1^2 + y_2^2). \end{aligned}$$

Referring back to (B.1) and (B.2), we can find the equations of motion in the new coordinates as

$$\begin{aligned} \ddot{y}_1 &= -y_1 \\ \ddot{y}_2 &= -(1 + 2\kappa)y_1, \end{aligned}$$

B. Small oscillations and the Foucault problem

which now are uncoupled. As in Section 3.2.1 we speak of characteristic oscillations of the coupled pendulum system and we call $\omega_1 = \sqrt{\lambda_1} = 1$ and $\omega_2 = \sqrt{\lambda_2} = \sqrt{1+2\kappa}$ the characteristic frequencies.

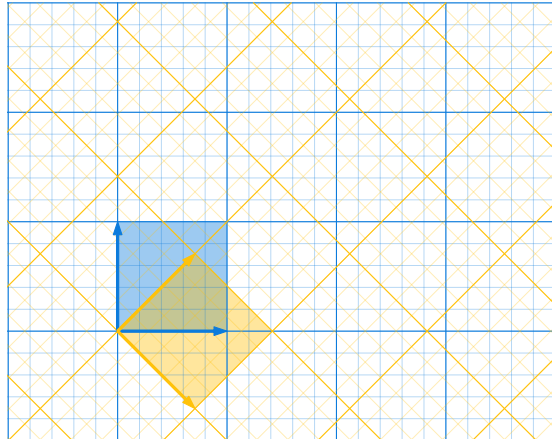


Figure B.2: Transformation of the coordinates by the matrix C). The straight lines identify the standard euclidean coordinates \mathbf{x} , and the skew the new ones $\mathbf{y} = C\mathbf{x}$

Remark 26. 1. The matrix C is orthogonal in the sense that $C^{-1} = C^T$, which means that the transformation C respects the inner product: in other words it is an isometry.

2. The approach delineated above works for any symmetric matrix B in any dimension and gives oscillations in the directions where the eigenvalue λ is positive. We recall that the general solution can be written as a linear combination of characteristic motions.

A slightly more general case occurs when $T = \frac{1}{2}\langle A\dot{\mathbf{x}}, \dot{\mathbf{x}} \rangle$, for a symmetric matrix A that is assumed positive definite. Such A

defines a new inner product that can be normalized by choosing an orthonormal basis and from then on the story runs as above. For more details we refer to [8, Section 23] or [79, Chapter 4, Problem 18].

3. *The general theory is based on the Variational Principle, which in the present case is completely covered by the formulae (B.2). For an elegant presentation of this theory, more details and more applications we again refer to [8, Section 23].*

B.2. The Foucault pendulum

In this section we discuss the *Foucault pendulum*, a spherical pendulum that swings in one vertical plane; this plane itself rotates due to the rotation of the earth. To make this idea more clear, suppose we are setting up the pendulum precisely at the North Pole. In the span of 24 hours the vertical plane, by inertia of the system that is in complete harmony with the fixed stars, should rotate clockwise and make a full turn: the earth just rotates underneath this grandiose device. A success of this experiment would confirm the daily rotation of the earth.

Remark 27. *The vertical plane of the Foucault pendulum positioned on the equator would not rotate at all. Can you explain why and can you also find the amount of rotation in 24 hours as a function of the latitude?*

To understand what is going on we need to look more closely at the spherical pendulum. In particular we have to move from cartesian to spherical coordinates and make use of the concept of *Taylor series*. At the linear level we first meet small oscillations. If we include

B. Small oscillations and the Foucault problem

the quadratic terms we shall then encounter the so-called *spherical precession*, a nonlinear effect that will turn out to substantially complicate the Foucault experiment.

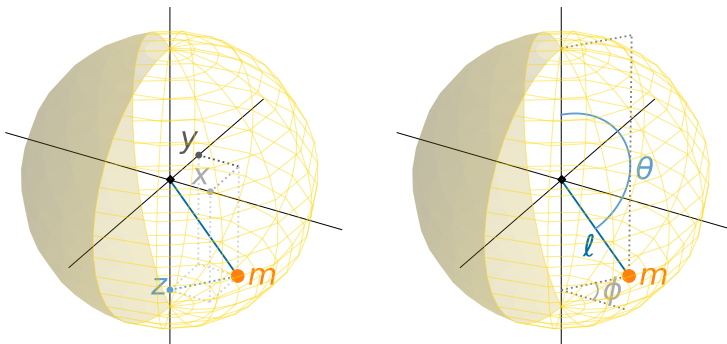


Figure B.3: Configuration of a spherical pendulum in cartesian (left) and spherical (right) coordinates

B.2.1. The spherical pendulum

In this section we investigate the dynamics of the spherical pendulum near its south pole equilibrium. We take a cartesian coordinate system (x, y, z) , where the center of the sphere is at the origin and the z -axis is vertical (pointing upward), see Figure A.3. Passing to spherical coordinates

$$\begin{aligned} z &= r \cos \theta \\ x &= r \sin \theta \cos \varphi \\ y &= r \sin \theta \sin \varphi, \end{aligned}$$

the lower equilibrium occurs at the south pole $(x, y, z) = (0, 0, -\ell)$, corresponding to $r = \ell$ and $\theta = \pi$. The kinetic and potential energy are given by

$$T = \frac{1}{2}m\ell^2\dot{\theta}^2 + \frac{1}{2}m\ell^2\sin^2\theta\dot{\varphi}^2 \quad \text{and} \quad U = mg\ell\cos\theta.$$

We now turn to adapted cartesian co-ordinates that parametrize the southern hemisphere and approximate the system at the south pole's equilibrium. To this end, we define co-ordinates (ξ, η) from the polar coordinates φ and $\varrho = \pi - \theta$ by $\xi = \varrho \cos \varphi, \eta = \varrho \sin \varphi$.

Computational intermezzo

A few computations are in order.

1. A first useful formula turns out to be

$$\dot{\xi}^2 + \dot{\eta}^2 = \dot{\varrho}^2 + \varrho^2 \dot{\varphi}^2. \quad (\text{B.4})$$

To prove this we take derivatives

$$\dot{\xi} = \dot{\varrho} \cos \varphi - \varrho \sin \varphi \dot{\varphi} \quad \text{and} \quad \dot{\eta} = \dot{\varrho} \sin \varphi + \varrho \cos \varphi \dot{\varphi},$$

after which squaring and summing the two equations gives the desired result.

In the same spirit, we have

$$\dot{\varphi} = \frac{\dot{\eta}\xi - \dot{\xi}\eta}{\xi^2 + \eta^2} \quad (\text{B.5})$$

which directly follows from formulæ like

$$\varphi = \arctan \frac{\eta}{\xi}.$$

2. In the approximation at the lower equilibrium we need the first terms of the Taylor-expansions for sinus and cosinus:

$$\begin{aligned} \sin \varrho &= \varrho - \frac{1}{6}\varrho^3 + O(\varrho^5) \\ \cos \varrho &= 1 - \frac{1}{2}\varrho^2 + \frac{1}{24}\varrho^4 + O(\varrho^6), \end{aligned} \quad (\text{B.6})$$

see [4] or any other decent book on calculus.

B.2.2. Small oscillations

We first approximate to second order at the south pole using (B.6):

$$\sin \varrho \approx \varrho \quad \text{and} \quad \cos \varrho \approx 1 - \frac{1}{2}\varrho^2$$

from which we get approximately

$$T = \frac{1}{2}m\ell^2(\dot{\varrho}^2 + \varrho^2\dot{\theta}^2) \quad \text{and} \quad U = -mg\ell(1 - \frac{1}{2}\varrho^2) \equiv \frac{1}{2}mg\ell\varrho^2,$$

where we also used that $\cos \theta = -\cos \varrho$. By formula (B.4) we find

$$T = \frac{1}{2}m\ell^2(\dot{\xi}^2 + \dot{\eta}^2) \quad \text{and} \quad U = \frac{1}{2}mg\ell(\xi^2 + \eta^2),$$

which, again by (B.2), corresponds to a linear system

$$\begin{aligned} \ddot{\xi} &= -\frac{g}{\ell}\xi \\ \ddot{\eta} &= -\frac{g}{\ell}\eta \end{aligned}$$

of two uncoupled harmonic oscillators, in this case with equal frequencies $\omega = \sqrt{g/\ell}$. Referring back to Remark 17 we conclude that the small oscillations consist of all possible Lissajous ellipses with the origin as center.

Remark 28. Notice that we don't need the machinery of Section B.1. Can you identify the matrices A and B here?

B.2.3. Spherical precession

Using one more term in the Taylor expansions (B.6)

$$\sin \varrho \approx \varrho - \frac{1}{6}\varrho^3 \quad \text{and} \quad \cos \varrho \approx 1 - \frac{1}{2}\varrho^2 + \frac{1}{24}\varrho^4$$

gives approximately

$$\begin{aligned} T &= \frac{1}{2}m\ell^2(\dot{\rho}^2 + (\rho - \frac{1}{6}\rho^3)^2\dot{\varphi}^2) \\ U &= -mg\ell \cos \varphi \equiv \frac{1}{2}mg\ell(\rho^2 - \frac{1}{12}\rho^4). \end{aligned}$$

Simplifying further and working mod $\mathcal{O}(\rho^6)$ we get

$$\begin{aligned} T &= \frac{1}{2}m\ell^2(\dot{\rho}^2 + (\rho^2 - \frac{1}{3}\rho^4)\dot{\varphi}^2) \\ &= \frac{1}{2}m\ell^2(\dot{\rho}^2 + \rho^2\dot{\varphi}^2) + \frac{1}{6}\rho^4\dot{\varphi}^2 \\ U &= -mg\ell \cos \varphi \equiv \frac{1}{2}mg\ell\rho^2 - \frac{1}{24}mg\ell\rho^4, \end{aligned}$$

where we added the fourth order terms to the former approximation. The fourth order part of the kinetic energy T reads

$$\frac{1}{6}\rho^4\dot{\varphi}^2 = \frac{1}{6}(\dot{\eta}\xi - \dot{\xi}\eta)^2,$$

where we use formula (B.5). This term corresponds to a slow motion in the φ -direction, in other words, a rotation (= precession) of the system, that roughly deforms any Lissajous ellipse into a rosette, see Figure B.4 and B.5. Again compare Remark 17. This holds at least when the ellipse does not degenerate to a straight line, in which case we would have $\dot{\varphi} \equiv 0$.

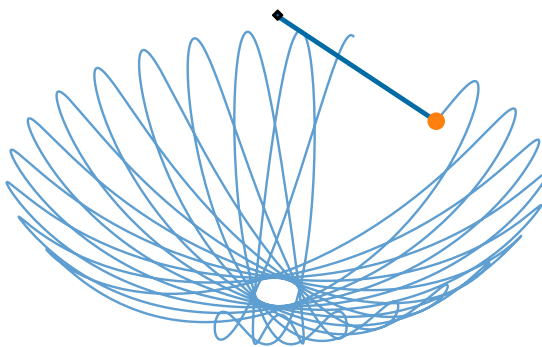


Figure B.4: A trajectory of the Foucault pendulum clearly showing a spherical precession

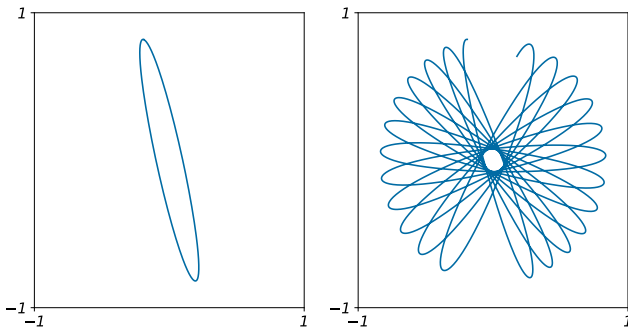


Figure B.5: Left: Lissajous ellipse for the linearization of a pendulum with the same initial condition as the trajectory in Figure B.4 projected on the (x, y) -plane; Right: the trajectory of Figure B.4 projected on the (x, y) -plane

B.3. Scholium

The spherical precession complicates the Foucault experiment, since practically it is impossible to restrict the pendulum motion to one vertical plane. In terms of the Lissajous figures, the ellipses, however narrow, do not completely degenerate to a straight line. This means that the rotation of the pendulum 'plane' may just as well be affected by the precession as by the rotation of the earth. This probably is the case with many of the Foucault pendulums – they do actually exist! – all over the world.

A solution for this problem is to damp out the transversal motion $\dot{\varphi}$ at the maximum of its swings. The physics Nobel laureate Heike Kamerlingh Onnes in 1879 doctorated at Groningen University on the thesis *Nieuwe Bewijzen voor de Aswenteling der Aarde* [84] under the supervision of the mathematical physicist Rudolf Adriaan Mees. For background information also see [42]. In his dissertation Kamerlingh Onnes designs an ingenious construction, where a ring is mounted on the device that performs the damping: the first

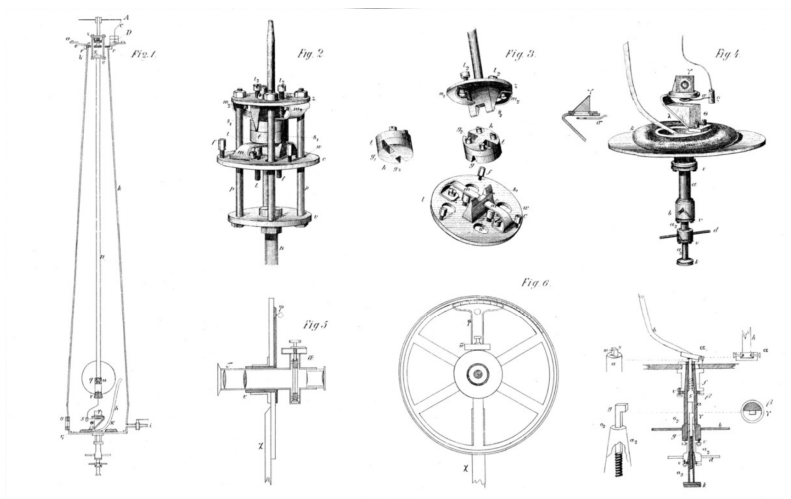
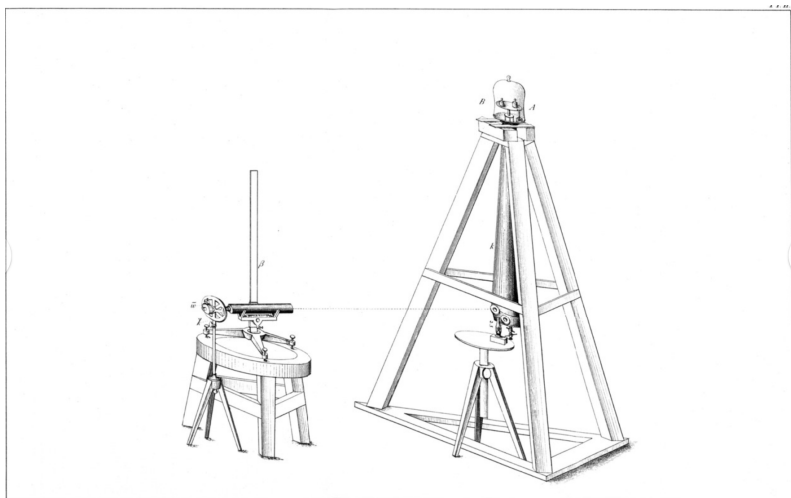


Figure B.6: *Two drawings from Kamerlingh Onnes's thesis [84]*

functioning Foucault pendulum.

Remark 29. *In the above text the spherical pendulum was considered in its own right, and the detected spherical precession already casts serious doubt on the Foucault experiment. In [84] however a deeper understanding of the problem is gained by mounting the spherical pendulum on the rotating earth, compare Figure B.4, alongside a very careful experimental set-up to test the result.*

An interesting mathematical explanation of Kamerlingh Onnes' Foucault pendulum, and its proper mathematical understanding, can be found in [117].

B.4. Another exercise of Bottema

The following exercise is also from Bottema [24].

In Euclidean 3-space, you are given three lines ℓ_i ($i = 1, 2, 3$) which are all passing through the point O . The angle between any of the two lines is α ($0 < \alpha < \pi/2$). Three particles P_i of unit mass move along the lines ℓ_i , respectively. Any two particles P_i, P_j ($i \neq j$) attract each other by the force $k^2 \overline{P_i P_j}$, where $k > 0$ is a positive constant and $\overline{P_i P_j}$ denotes the distance between P_i and P_j . Determine the general motion of the three particles.

C. Chaos in periodically forced oscillators

In Section 2.4.2, when discussing the Josephson junction, we briefly encountered the term “chaotic”. In this appendix we would like to go deeper into the concept of *chaos* as a phenomenon in periodically driven nonlinear oscillators.

In general chaos can be characterized by a lack of predictability. Also when studying the long term dynamics in the phase space we often meet fractal geometry, in particular in the form of Cantor sets [108].

For a better understanding of what is going on, we start with a small detour around the iteration of maps. Systems of differential equations describe dynamical systems with continuous time, whereas the iteration of maps concerns dynamical systems with discrete time. In the latter context one may think for example at the size of a population as it changes at some fixed time interval, say per day or per year. As we will see, in the time periodic case, there is a natural way to pass from continuous to discrete time via the *stroboscopic map*, which will be a helpful tool to observe and clarify chaotic phenomena. A general reference to chaotic systems is [43] which also contains an extensive bibliography.

C.1. The Hénon attractor

In this section we introduce the Hénon map and its attractor. The mathematics here becomes partly *experimental*, in the sense that numerically obtained information will get a partially conjectural mathematical interpretation.

We introduce two maps that are iconic for the development of chaos theory from the 1960's on: the Logistic map and the Hénon map. These systems are given by low degree polynomials, but the mathematics involved in their understanding is very tedious. For an accessible introduction to this matter we refer to Devaney [53].

C.1.1. Iterating a map

Given a map

$$F : M \rightarrow M$$

we consider iterates

$$x_0, x_1, x_2, \dots \quad \text{where} \quad x_{n+1} = F(x_n)$$

for any $x_0 \in M$ and for all $n \in \mathbb{N}$. In the general setting M is just a topological space and F a continuous map. Here $n \in \mathbb{N}$ or $n \in \mathbb{Z}$, depending on whether F is invertible or not, stands for the discrete time. A subset

$$\{x_0, x_1, x_2, \dots\} \subseteq M$$

is called an orbit of F . The interest is the long term behavior of orbits, say, on what subset of M it accumulates on as $n \rightarrow \infty$.

The Logistic map. As a first example we briefly touch on the family of *Logistic* maps

$$\mathcal{L}_a : \mathbb{R} \rightarrow \mathbb{R}, \quad x \mapsto ax(1-x). \quad (\text{C.1})$$

Iterates

$$x_0, x_1, x_2, \dots, \quad \text{with} \quad x_{n+1} = \mathcal{L}_a(x_n),$$

are being used to model population dynamics, in particular of the mayfly (*drosophila melanogaster*). This map is an endomorphism, i.e., non-invertible. Despite the innocent looking form of \mathcal{L}_a , books could (and have been) written on the properties and the dynamics of unimodal maps like (C.1). Here we will limit ourselves to a very basic and superficial discussion, and refer the reader to the references [43, 53, 127] for further details.

In the present context the basic question concerns the long term dynamics of the logistic map. That is, for a fixed parameter value a , what is the behaviour of x_n as $n \rightarrow \infty$?

A numerical experiment. To fix thoughts we perform the following numerical experiment. We take any initial point x_0 and plot the iterates x_{800}, \dots, x_{1000} for various values of the parameter a between 0 and 4. Note that in this way we neglect an initial transient segment of iterates and so can get an idea where the iterates of $\mathcal{L}_a(x_0)$ settle down to, or, in other words, where they are *attracted* to.

In Figure C.1 you can see the result of this experiment. For values of a between 0 and 3.0 we can see that the dynamics settles down in a stable equilibrium point. However at $a = 3.0$ it suddenly bifurcates: the dynamics jumps between two different values, we have an orbit of period 2. When a increases such a period doubling happens more and more often, until at some value it seems that there is an infinity of periodic orbits. For still increasing values of a we get into a chaotic regime interspersed by windows where the behaviour

C. Chaos in periodically forced oscillators

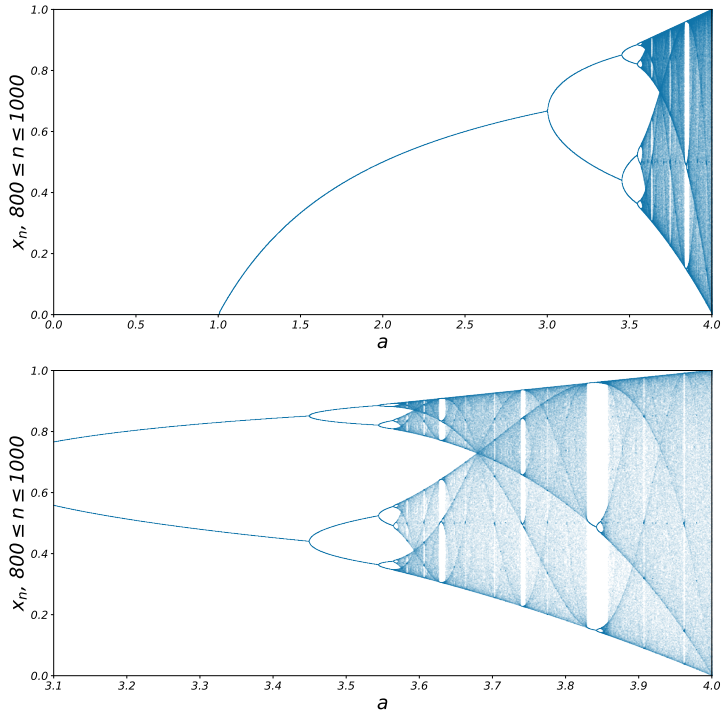


Figure C.1: Bifurcation diagram for the Logistic map or $a \in [0, 4]$ (top) and close to the chaotic region for $a \in [3.1, 4]$ (bottom).

is periodic. The scenario and the diagram described here often are attributed to the well-known physicist Feigenbaum. It turns out to be amazingly difficult to give a solid mathematical explanation of all this, compare with the above references.

The take-home message of this brief example is that plotting the evolution of discrete maps can tell us a lot about their dynamical properties. We will exploit this in the rest of this appendix to describe the concept of certain dynamical attractors.

The Hénon map.

The *Hénon* family of planar maps

$$\mathfrak{H}_{a,b} : \mathbb{R}^2 \rightarrow \mathbb{R}^2, \quad (x, y) \mapsto (1 - ax^2 + y, bx).$$

This map is a diffeomorphism, and also the inverse map is a polynomial. Observe that the line $y = 0$ is an invariant line, and that $\mathfrak{H}_{a,b}$ restricted to this line exactly coincides with the Logistic map \mathcal{L}_a .

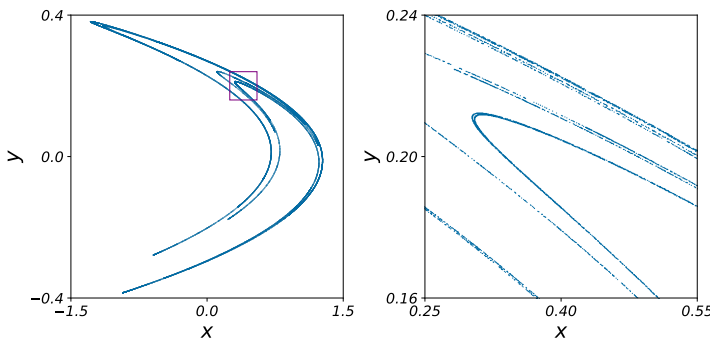


Figure C.2: *The attractor of the Hénon map and a magnification by a factor of 10*

In another numerical experimental it turns out that for the parameter values $a = 1.4$ and $b = 0.3$ all initial positions (x_0, y_0) have or-

C. Chaos in periodically forced oscillators

bits

$$(x_0, y_0), (x_1, y_1), (x_2, y_2) \dots, \quad \text{with} \quad x_{n+1}, y_{n+1} = \mathfrak{H}_{a,b}(x_n, y_n),$$

that, for $n \rightarrow \infty$ tend to the *Hénon attractor* $\mathcal{H} \subseteq \mathbb{R}^2$ as depicted in Figure C.2 (left), where we also showed a magnification (right). The set \mathcal{H} locally has a lot of self-similarity, as it roughly looks like a curve in one direction and a Cantor set in the other.

A first topological digression. A brief topological digression is in order now. A Cantor set is compact set that is both *perfect* and *totally disconnected*. Perfect means that there are no isolated points and totally disconnected that each point of the set has arbitrarily small neighborhoods with empty boundary. Brouwer has proved that all such sets are homeomorphic. For background on this, see Engelking [59].

Cantor sets have a fractal nature. For the box counting dimension of \mathcal{H} the numerical estimate is $\dim_{BC} \mathcal{H} = 1.3$. In general such attractors are called *strange attractors*, a term coined by Ruelle and Takens [115].

C.1.2. The Benedicks-Carleson Ansatz

The Hénon map has a fixed point $p = (.63, .19)$, that turns out to be a saddle point, see Figure C.3, right. Its linearisation (derivative) $D_p \mathfrak{H}_{a,b}$ at p is a matrix with a positive and a negative eigenvalue. The stable and unstable manifolds of p

$$W^s(p) = \left\{ q \in \mathbb{R}^2 \mid H_{a,b}^j(q) \rightarrow p \quad \text{as} \quad j \rightarrow \infty \right\},$$

$$W^u(p) = \left\{ q \in \mathbb{R}^2 \mid H_{a,b}^{-j}(q) \rightarrow p \quad \text{as} \quad j \rightarrow \infty \right\},$$

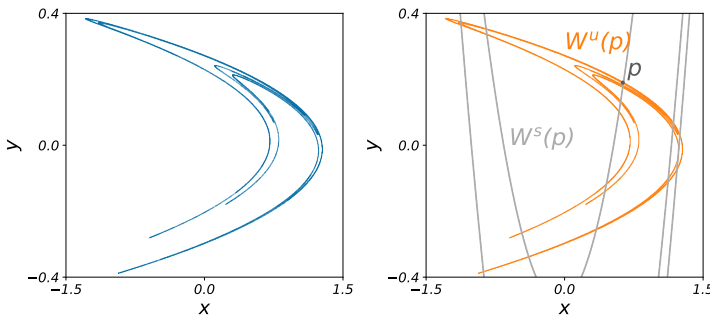


Figure C.3: Left: Hénon attractor, compare Figure C.2; Right: Pieces of the stable and unstable separatrices $W^s(p)$ and $W^u(p)$ of the saddle point $p = (.63, .19)$ of the Hénon map. Note the resemblance between the attractor and $W^u(p)$

turn out to be smooth curves passing through p and at p tangent to the corresponding eigenspaces of $D_p \mathcal{H}_{a,b}$. In Figure C.3 (right) we depicted both $W^s(p)$ and $W^u(p)$ for some length and observe a striking similarity between \mathcal{H} and $W^u(p)$. They cannot be equal because of the difference in dimension, but the general folklore says the following:

Theorem 4 (Benedicks-Carleson Ansatz). $\mathcal{H} = \overline{W^u(p)}$.

In other words that the Hénon attractor \mathcal{H} coincides with the *closure* of the unstable manifold $W^u(p)$. This has been a long standing conjecture that was proven by Benedicks and Carleson [18] for a subset of the (a, b) -parameter plane of positive Lebesgue measure, close to the a -axis. However, the point $(a, b) = (1.4, 0.3)$ does not belong to this subset ...

C.2. The stroboscopic map

In Chapter 2 we met oscillatory systems of the general (smooth) form

$$\ddot{x} = f(x, \dot{x}, t), \quad (\text{C.2})$$

for instance both forced and with or without friction, e.g., compare (2.7) or (2.11) or (2.12). In the present section the time dependence is periodic, i.e.,

$$f(x, y, t + T) \equiv f(x, y, t),$$

for a given period $T > 0$.

C.2.1. Determinism again

In Section 1.3 we turned one second order differential equation in x into a system of two first order differential equations in (x, y) by adding the term

$$y = \dot{x}.$$

We called the (x, y) -plane, phase plane. This is the plane in which the system became deterministic: given any initial point (x_0, y_0) the entire future evolution of the system is completely determined.

However, the case of (C.2) is time-dependent and to obtain again a deterministic system we need to introduce one more variable that represents the time t . As an example we here consider the *swing*

$$\ddot{x} + c\dot{x} + (a + \varepsilon \cos t) \sin x = 0 \quad (\text{C.3})$$

where we take

$$\begin{aligned} \dot{x} &= y \\ \dot{y} &= -cy - (a + \varepsilon \cos z) \sin x \\ \dot{z} &= 1. \end{aligned} \quad (\text{C.4})$$

Note that we included the damping term cy , proportional to the velocity. The general case of (C.2) goes completely similar. Now in the three-dimensional phase space with co-ordinates x, y, z we again have obtained determinism: for any initial point (x_0, y_0, z_0) the entire future evolution is completely determined.

In the former case of Section 1.3, when dealing with an autonomous system, a planar phase portrait gives a quite clear idea of the dynamics. But in the present time dependent case, in the three-dimensional phase space the collection of integral curves forms a kind of spaghetti that in general does not offer too much transparency.

C.2.2. The stroboscopic phase portrait

Fortunately, the time-periodicity helps us to obtain another quite informative two-dimensional picture by constructing a planar map. This is the so-called *stroboscopic map*, that takes a snapshot of the (x, y) -plane at instants $t = 0, T, 2T, \dots$, see Figure C.4.

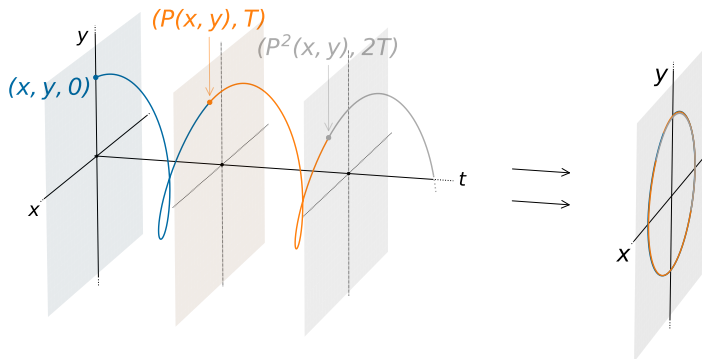


Figure C.4: A solution of (C.4) in the (x, y, t) space with snapshots taken at time instants $t = 0, T, 2T$

C. Chaos in periodically forced oscillators

Consider the integral curve starting at the point $(x, y, 0)$ and follow this till it hits the vertical plane $z = T$. The intersection point is called $(P(x, y), T)$. This defines a map

$$P : \mathbb{R}^2 \rightarrow \mathbb{R}^2.$$

We list a few properties of the map P , without proof, that all follow from the existence and uniqueness theory of ordinary differential equations [81].

Proposition 1.

1. *The map P is a diffeomorphism;*
2. *Extending the integral curve from $(x, y, 0)$ to $(P(x, y), T)$ to the section $z = 2T$ gives the point $(P^2(x, y), 2T)$.*

The latter of the two properties holds for all sections $z = nT$ ($n \in \mathbb{Z}$) and the corresponding iterates P^n of the map P . This means that, by plotting orbits

$$\dots, (x_{-1}, y_{-1}), (x_0, y_0), (x_1, y_1), (x_2, y_2), \dots \quad \text{with}$$

$$(x_{n+1}, y_{n+1}) = P(x_n, y_n)$$

in the (x, y) -plane, we can get a good idea of the dynamics of the system corresponding to (C.2). We now speak of a *stroboscopic phase portrait*.

A fixed point of P corresponds to a periodic solution of the corresponding system. Similarly for a periodic orbit of P . Note, that in the case of the swing (C.4) the origin $(x, y) = (0, 0)$ always is a fixed point. Also other sets that are invariant under iteration of P are of interest.

And another numerical experiment performed on the damped system (C.4), i.e., with $c > 0$, leads to Figure C.5 (left), which surely looks like a strange attractor!

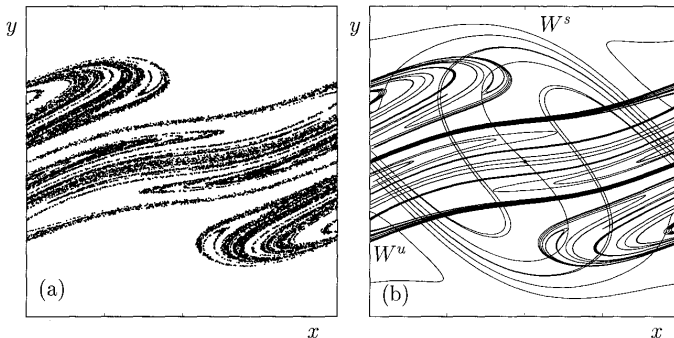


Figure C.5: *Strange attractor for a damped driven swing (left) and the stable and unstable manifolds of the saddle point $(0,0)$ (right)*, [37], p. 48]

C.2.3. Hénon-like strange attractors

Indeed, the attractor of the left hand side in Figure C.5 locally shows a great similarity with the Hénon attractor \mathcal{H} : in one direction we distinguish a curve and transverse to this some kind of Cantor set. Moreover, the origin $(x, y) = (0, 0)$ now is a saddle point and when plotting the stable and unstable manifolds in the right hand side figure, we observe the same phenomenon as before: namely that the attractor strongly resembles the unstable manifold and again we are tempted see the Benedicks-Carleson Ansatz confirmed.

Another example occurs in the context of an optically injected semiconductor laser [37, 135], where the same Ansatz seems to apply, see Figure C.6. In all these cases we speak of *Hénon-like strange attractors*. From this and many other examples it seems that the Benedicks-Carleson Ansatz very well characterizes chaos in two-dimensional diffeomorphisms and therefore also in periodically forced oscillators with damping.

C. Chaos in periodically forced oscillators

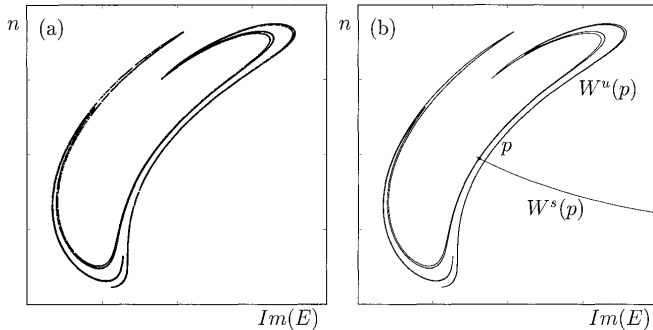


Figure C.6: *Strange attractor appearing in rate equation model of an optically injected semiconductor laser (left) and the stable and unstable manifolds of the saddle point (right), [37], p. 50]*

C.3. Scholium

Please notice the careful formulations used here. According to Wikipedia an Ansatz is nothing but “an educated guess or an additional assumption made to help solve a problem, and which may later be verified to be part of the solution by its results.” And, indeed, the statements are still far from being a mathematical theorem, compare our remarks at the end of Section C.1.2 on the validity of the result in Benedicks-Carleson [18].

The understanding of chaotic dynamics is an ongoing and difficult research program; the difficulty shows already from the fact that such simple models already have such complicated dynamics. One of the pioneers has been the biologist Robert May [95], who studied the mayfly *drosophila melanogaster* in terms of one-dimensional maps related to the Logistic map. Another pioneer was the astronomer Michel Hénon who developed the model named after him. The relationship between the Logistic map and the Hénon map for small values of b has been crucial for the work of Michael Benedicks and

Lennart Carleson and for a lot of ensuing work as well.

C.3.1. Return map and Poincaré map

The stroboscopic map in the present context also is called *return map*. This can be explained as follows. Since the system (C.4) is periodic in the z -direction we can identify all the sections $z = nT$ ($n \in \mathbb{Z}$). So we can change the geometry of the phase space from \mathbb{R}^3 to $\mathbb{R}^2 \times \mathbb{S}^1$, where \mathbb{S}^1 denotes the unit circle. For any $p \in \mathbb{S}^1$, the stroboscopic map then becomes a map from a section $\mathbb{R}^2 \times \{p\} \subseteq \mathbb{R}^2 \times \mathbb{S}^1$ to itself, so indeed as a return map. Fortunately return maps are very suitable for iteration.

A slightly more general concept is that of a *Poincaré map*, a map defined between transversal sections in the flow. In that case iteration is not always an option.

C.3.2. Towards an understanding of chaos

The iterates on the strange attractors we meet here are quite erratic, seemingly almost random, which is related to the unpredictability of the motion.

Ergodicity

This kind of thinking can be formalized in applications of probability theory on dynamical systems; the ensuing theory is called *ergodic theory*. For this we need a probability Borel measure that is invariant under the map $F : M \rightarrow M$ at hand; note that we here returned to the general setting of Section C.1.1. We have to assume

C. Chaos in periodically forced oscillators

that M is metrizable and that we have a countable basis of open sets: properties that hold for all the spaces occurring here. It is common to use the following measure in this context [43, Section 6.5]. For $x \in M$ let $x, F(x), F^2(x), \dots$ be the orbit generated from x , then for any “reasonable” subset $A \subseteq M$ we define

$$\mu(A) = \lim_{n \rightarrow \infty} \frac{\#\{j \mid 0 \leq j \leq n \text{ and } F^j(x) \in A\}}{n},$$

where $\#$ denotes the cardinality. The measure μ assigns to A the average fraction of points of the orbit $\{F^j(x)\}_{j=0}^\infty$ that are in A . If this measure is well-defined it is called the “measure of relative frequencies” of the sequence $\{F^j(x)\}_{j=0}^\infty$. Often we speak loosely of “physical measure”. The property that is essential for this to work is that the measure μ is “ergodic” in the sense that for any continuous function $\psi : M \rightarrow \mathbb{R}$,

$$\lim_{n \rightarrow \infty} \frac{1}{n} \sum_{j=0}^{n-1} \psi(F^j(x)) = \int_M \psi d\mu.$$

In other words, that the orbit $\{F^j(x)\}_{j=0}^\infty$ is well-spread over the attractor.

There is a lot of mathematics hidden in here, and often we don’t get much further than numerically supported conjectures. For classical references see Arnold & Avez [13] and Mañé [93], also see [43, Chapters 4 and 6]. To explore some of the many ramifications of the theory, the interested reader can also consult Einsiedler and Ward [56], which winks towards old and new connections with number theory.

C.3.3. Without friction

All of this works more or less for the strange attractors found in the dissipative situations, i.e., with friction.

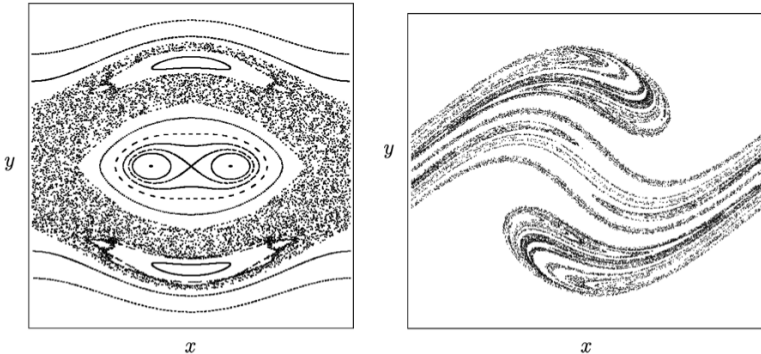


Figure C.7: *Stroboscopic phase portraits of the swing with damping $c = 0$ (left) and with damping $c > 0$ (right)* [43, p. v]; compare with the Figure C.5

Let us briefly discuss the case without friction, where it can be shown that always the stroboscopic map P is area-preserving [8, Section 15]. In other words, the Lebesgue measure is invariant under P . In terms of the above the Lebesgue measure in this case also is the physical measure. To fix thoughts, in Figure C.7 (left) the stroboscopic phase portrait is being shown of the system (C.4) with damping $c = 0$. In this portrait we detect

- A couple of periodic points, where the dots in, e.g., the ‘eye’ correspond to a period 2 orbit.
- A couple of invariant closed curves.
- A cloud of points, which are all part of only a few single orbits.

We shall return to the invariant closed curves in Appendix D, but the present interest is with the cloud, which more or less replaces the strange attractor in the dissipative case. Indeed, the motion inside the cloud seems to be just as chaotic as in the attractors. The question then is what ergodic theory has to say here.

C. Chaos in periodically forced oscillators

It is a long standing conjecture reported in Arnold [13] claiming that the cloud(s) depicted in Figure C.7 (left) densely fill a set of positive Lebesgue measure which is ergodic for the stroboscopic map P . As far as the authors know this conjecture has only been confirmed in a few exceptional cases, compare Chernov and Markarian [48] which focuses on the theory of chaotic billiards. For more or less generic cases as studied here the Arnold conjecture still stands, although folklore has its way of accepting it already as a “fact”.

D. More on resonance

In Chapter 2 we already encountered the phenomenon of resonance in periodically driven oscillators, in particular compare the Sections 2.3.2, 2.4 and 2.4.1. We now also study a somewhat more general setting of systems depending on parameters. Resonance is then considered as the interaction of oscillating subsystems, where the frequencies have a rational relation and where a motion occurs that is compatible with this relation. One of the leading examples concerns Huygens's weakly coupled clocks that are (almost) identical. This is a 1 : 1 resonance and the compatible motion is that both clocks tend to synchronize [82]. Also driven oscillators will again come up for discussion.

One of our interests is the organisation of the parameter space as related to resonance: in the examples this will give rise to so-called resonance *tongues*. For parameter values inside the tongues the actual resonance occurs, but in between the tongues several things may happen that are interesting from both the topological and measure theoretical point of view, see Oxtoby [108]. In fact we shall encounter *fractal sets* here, in the sense of Mandelbrot [92]. In the ensuing nonlinear dynamics we meet a new phenomenon called *quasi-* or *multiperiodicity* but also also chaos may emerge as already met in Section 2.4.2 and in Appendix C.

The appendix is concluded by a discussion on celestial resonances, in particular on orbital and spin-orbit resonances.

Some phenomenology. In Section 2.3.2 we discussed a few occurrences of 1:1-resonances, like the exact tuning of the radio frequency on the incoming signal. Another example is the resonance in the earth-moon system, where the rotation of the moon about its axis occurs with the same period as its revolution about the earth: reason why on earth we always see the same face of the moon. This is a so-called spin-orbit resonance and it can be explained by the tidal force the earth exerts on the moon. For more details see below.



Figure D.1: *Botafumeiro in Santiago de Compostela*

An example of a 1 : 2-resonance is the motion of the Botafumeiro in the cathedral of Santiago de Compostela. This is a large incense container suspended on a long rope mounted over a pully high up in the cathedral and that is kept swinging by a couple of men pulling the rope to and fro over the pully. The Botafumeiro is pulled up each time that it is near its lowest point, which means that the pulling frequency is twice as high as that of the pendulum: the system is in a 1 : 2-resonance. Another example of the 1 : 2-resonance, already mentioned in Section 2.4.1, is the rolling and even capsizing of ships that go astern on an increasing wind.

On methodology. The mathematical programme for understanding phenomena like the above is to provide models in terms of dynamical systems depending on parameters and to study the emerging dynamics. This can vary from periodic to quasi- or multiperiodic and even chaotic. Also we are interested in bifurcations (or phase transitions) between the various types of dynamics. Apart from the examples mentioned above, such approaches are being applied widely in the sciences, in contexts varying from climate change to biological systems.

D.1. Huygens's clocks

Our leading example concerns the following experiment described by Huygens [82], see Figure D.2. A beam is mounted not too rigidly on two chairs and two almost identical pendulum clocks are suspended on the beam. Huygens observed that the clocks tend to synchronize and even that the two pendulums tend to swing in anti-phase. Following [27], we are going to attempt a mathematical description that explains a form of averaged synchronization.

D.2. Arnold resonance tongues and fractal geometry

In Huygens's experiment each pendulum consists of a point mass that moves on a circle. Since we have two pendulums we are dealing with two circles, say with angles (φ, ψ) , which together parametrise a two-dimensional torus: the product of the two circles.

So the dynamics consists of integral curves on this torus, see Figure D.3. Let us assume that a Poincaré map is defined from some

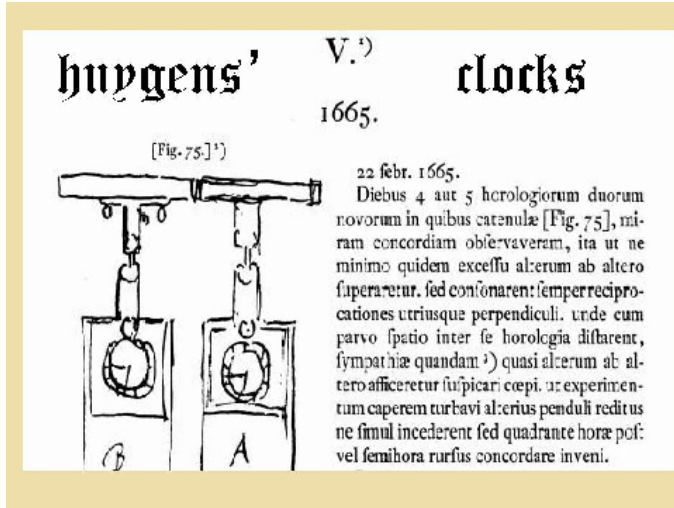


Figure D.2: Huygens's weakly coupled pendulum clocks [82]

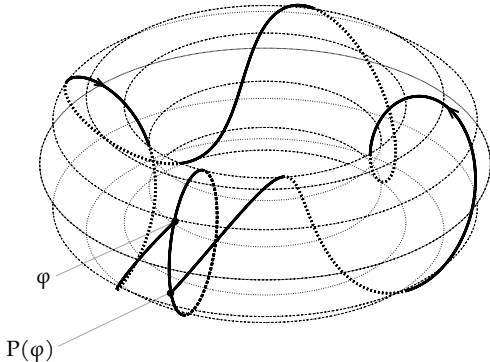
circle $\psi = \text{constant}$ to itself. In terms of Appendix C we may well speak of a return map. Such a map may well take the following form,

$$P : \mathbb{S}^1 \rightarrow \mathbb{S}^1 \quad (\text{D.1})$$

$$\varphi \mapsto \varphi + 2\pi\alpha + \varepsilon f(\varphi),$$

and its iterations, as in Appendix C, would give us a good idea of the long term dynamics. In general we speak of resonance whenever this dynamics is periodic. Our investigation in Huygens's clocks has led us to the theory of circle maps. We now first need some properties of such maps.

Note that meanwhile we have abandoned the context of Huygens's clocks, the study of dynamical systems consisting of iterations of maps like (D.1) has a far wider interest. For details see [9, 43, 53]. At the end of the section we shall come back to Huygens.

Figure D.3: *Poincaré map maps the circle to itself* [43]

D.3. A theoretical digression into circle maps

An important tool is the *rotation number* as this was introduced by Poincaré. Part of the content of this section also is due to Denjoy and Kolmogorov. Let us start with an orientation preserving homeomorphism

$$F: \mathbb{S}^1 \rightarrow \mathbb{S}^1$$

and consider a lift

$$\tilde{F}: \mathbb{R}^1 \rightarrow \mathbb{R}^1$$

defined by the property

$$\Pi \circ \tilde{F} = f \circ \Pi$$

where $\Pi: \mathbb{R} \rightarrow \mathbb{S}$ is the projection

$$x \in \mathbb{R} \mapsto \varphi = e^{2\pi i x} \in \mathbb{S}^1 \subseteq \mathbb{C},$$

and we consider $\mathbb{S}^1 \cong \mathbb{R}/2\pi\mathbb{Z}$. Note that the lift is not unique, but only defined modulo $2\pi\mathbb{Z}$.

We define the *rotation number* of F by

$$\varrho(F) = \frac{1}{2\pi} \lim_{n \rightarrow \infty} \frac{\tilde{F}^n(x)}{n},$$

which is easily shown to be independent of the point x . Moreover, since the lift \tilde{F} is not unique, we take the rotation number modulo \mathbb{Z} . The rotation number measures the average rotation of F . It turns out that the important distinction is whether or not the value of ϱ is rational. We now list a couple of properties.

Proposition 2. *1. If F and G are orientation preserving circle homeomorphisms, and $H : \mathbb{S}^1 \rightarrow \mathbb{S}^1$ is another homeomorphism that conjugates F and G , i.e., such that*

$$G \circ H = H \circ G,$$

then $\varrho(F) = \varrho(G)$.

2. $\varrho(F) \in \mathbb{Q}$ if and only if F has a periodic orbit.

3. Assuming that the map F is sufficiently smooth (say of class C^2), then the fact that $\varrho(F)$ is irrational implies that F is topologically conjugate to a rigid rotation.

We give some comments on Proposition 2. The first statement says that the rotation number is a topological invariant. The second, together with the first, implies that the periodic orbits of F are in correspondence with the given rotation number. The third item is known as the *Denjoy Theorem*. It says that for sufficiently smooth F there is a topological conjugacy with the rigid rotation

$$\mathfrak{R}_{2\pi\varrho(F)} : \varphi \mapsto \varphi + 2\pi\varrho(F).$$

By the way, note that in general

$$\varrho(\mathfrak{R}_{2\pi\alpha}) = \alpha.$$

Moreover, the fact that $\alpha \notin \mathbb{Q}$ implies that every single orbit of $\mathfrak{R}_{2\pi\alpha}$ densely fills the circle, see [43, Lemma 2.4]. The latter property is preserved by the topological conjugacy.

The dynamics of such an irrational rotation often is referred to as quasiperiodic or multiperiodic. When returning to the context of dynamics on the 2-torus this means that in average rotations in the φ and ψ direction are not rationally related.

We now sketch some background theory.

D.3.1. Denjoy and Kolmogorov

In the 1930's Arnaud Denjoy came with his theory on circle diffeomorphisms. Two decades later, in the 1950's, Andrey Kolmogorov extended this theory greatly into what today is known as Kolmogorov-Arnold-Moser Theory. The combination of these theories forms a corner stone of the dynamical systems discipline. The heritage of Denjoy and Kolmogorov has a vast follow up that runs till the present day and that includes many applications in mathematical physics and celestial mechanics. In the present context we only lightly touch on this rich material, for general background referring to [15, 26, 35, 36, 77, 90, 111, 129, 138].

Denjoy Theory. In the Denjoy Theorem (Proposition 2, third item) regularity is essential in the following sense. There exists a C^1 -diffeomorphism of the circle with an irrational rotation number, that is *not* conjugate to a rigid rotation [53, Section 1.4]. This map is called the *Denjoy counterexample*, which largely triggered part of the follow up mentioned before.

Kolmogorov-Arnold-Moser Theory. Consider irrational numbers that are badly approximated by rational numbers in the sense that *Diophantine conditions*

$$\left| \alpha - \frac{p}{q} \right| \geq \frac{\gamma}{q^\tau} \quad (\text{D.2})$$

hold for given constants $\gamma > 0, \tau > 2$ and for all rationals p/q .

We name this set $\mathfrak{D}_{\tau,\gamma}$. As a closed set, by the Cantor-Bendixson Theorem [73], this is the union of a perfect and a discrete set. Since the rational numbers are in its complement, $\mathfrak{D}_{\tau,\gamma}$ is totally disconnected and hence the perfect set is a Cantor set. The intersection $\mathfrak{D}_{\tau,\gamma}$ with any given closed interval moreover has positive measure, that tends to full measure as $\gamma \downarrow 0$.

In the case that $\alpha \in \mathfrak{D}_{\tau,\gamma}$, the conjugacy with the rigid rotation $\mathfrak{R}_{2\pi\alpha}$ is smooth! This kind of result belongs to the *Kolmogorov-Arnold-Moser Theory* [43, Chapters 2 and 5].

Remark 30. *Kolmogorov-Arnold-Moser (KAM) Theory deals with the so-called problem of small denominators, when looking for the conjugation H of Proposition 2 in terms of Fourier series. Small denominators are very central in dynamical systems, in celestial mechanics and, more generally, in mathematical physics, see the above references.*

In the related context of linearizing quadratic polynomials on \mathbb{C} with linear part $e^{2\pi i\alpha}$, Jean-Christophe Yoccoz was awarded a 1994 Fields medal. He proved that the so-called Bruno condition on α is necessary and sufficient for linearization. The Bruno condition is an extension of the Diophantine condition (D.2) [137, 139]. The Fields medal is the analogue of the Nobel price for mathematicians and Yoccoz was the first Fields medalist in the field of dynamical systems.

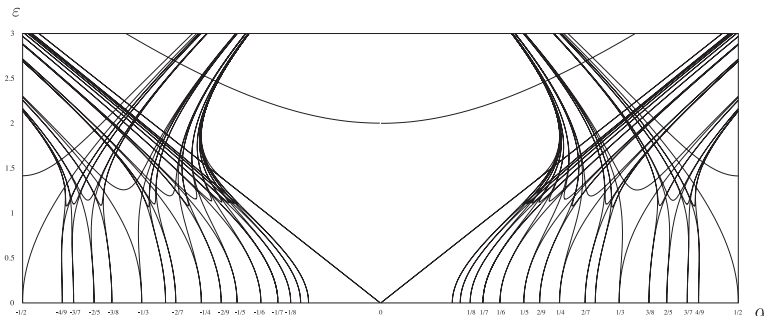


Figure D.4: *Arnold resonance tongues in the (α, ε) -plane* [27]

D.3.2. The Arnold family of circle maps

The simplest non-trivial case of a parametrized circle map is the following:

$$\begin{aligned} \mathfrak{A}_{\alpha, \varepsilon} : \mathbb{S}^1 &\rightarrow \mathbb{S}^1 \\ \varphi &\mapsto \varphi + 2\pi\alpha + \varepsilon \sin \varphi, \end{aligned} \tag{D.3}$$

the so-called *Arnold family* of circle maps [8]. This example already contains many interesting properties that can help to understand Huygens's experiment a bit better.

Without a detailed proof we present Figure D.4, that contains an array of resonance tongues, the *Arnold (resonance) tongues*, that forms a catalogue of the dynamics of the family $\mathfrak{A}_{\alpha, \varepsilon}$. In fact from each point $(\alpha, \varepsilon) = (p/q, 0)$ a resonance tongue emanates in which for the rotation number $\varrho(\mathfrak{A}_{\alpha, \varepsilon})$ we have

$$\varrho(\mathfrak{A}_{\alpha, \varepsilon}) \equiv \frac{p}{q}$$

and for parameter values inside there are periodic orbits of exactly that rotation type, in other words in $p : q$ -resonance. In particular,

within the $1 : 1$ *main tongue* emanating from $(\alpha, \varepsilon) = (0, 0)$ there are fixed points.

Such arrays of tongues occur frequently in the sciences. For an example in chronobiology we refer to [17].

On computing the tongues. To fix thoughts we compute the main tongue of the Arnold family $\mathfrak{A}_{\alpha, \varepsilon}$. So we are looking for fixed points

$$\mathfrak{A}_{\alpha, \varepsilon}(\varphi) = \varphi,$$

i.e.,

$$\varphi + 2\pi\alpha + \varepsilon \sin \varphi = \varphi,$$

which leads to

$$\sin \varphi = -\frac{2\pi\alpha}{\varepsilon}.$$

This equation has solutions in φ for all parameter values

$$2\pi\alpha \leq \varepsilon,$$

which exactly determines the main tongue. On the circle you can find two fixed points, one attracting and one repelling, that annihilate each other at the boundaries $2\pi\alpha = \varepsilon$ in a saddle-node bifurcation [53, Section 1.12]. Note that the main tongue has boundaries that at the tip $(\alpha, \varepsilon) = (0, 0)$ meet with non-zero angle.

The higher order tongues have been computed numerically, but much is known of the asymptotics at the tongue tips $(\alpha, \varepsilon) = (p/q, 0)$. In fact the tongue boundaries here are tangent of order $O(|q|)$, compare with [41] for more details.

The global picture. Another property of the rotation number is that it is a continuous function of the parameters (α, ε) . Thus, since

$\varrho(\mathcal{A}_{\alpha,0}) = \alpha$, for sufficiently small ε_0 fixed, the rotation number $\varrho(\mathcal{A}_{\alpha,\varepsilon_0})$ is continuous and non-decreasing as a function of α . Moreover it is constant for any rational value. The graph of this function, depicted in Figure D.5, is referred to as a *Devil's staircase*.

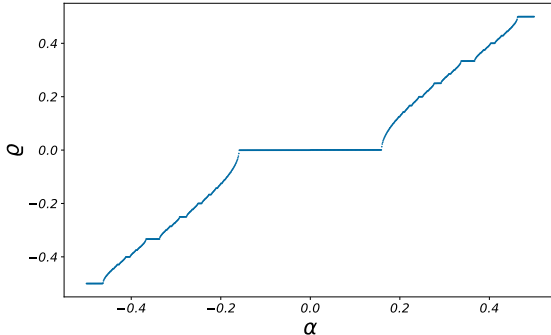


Figure D.5: *Devil's staircase: graph of $\alpha \mapsto \varrho(\mathcal{A}_{\alpha,\varepsilon_0})$ for small $\varepsilon_0 > 0$ [27]; on rational values the graph is horizontal on plateaux corresponding to the resonance tongues. The points where the function is not constant forms a fractal set in the sense of Mandelbrot [92]. This set has positive Lebesgue measure; see the main text for further explanatory remarks*

D.3.3. A second digression, on topology and on measure theory

We conclude this section on circle maps with another discussion on the topology and measure theory of the Arnold family, in particular on Figure D.4.

Again consider an horizontal line in the (α, ε) -plane at height $\varepsilon_0 > 0$, chosen sufficiently small. We observe the following.

1. The intersection of the line $\varepsilon = \varepsilon_0$ with the union of resonance tongues forms an open and dense set.

According to the Denjoy Theorem (Proposition 2, item 3), its complement is the set of parameter values with quasiperiodic dynamics. It follows that this is a totally disconnected closed set, that contains Diophantine sets $\mathfrak{D}_{\tau,\gamma}$ described above in relation to KAM Theory and, therefore, is of positive Lebesgue measure. Here we choose the constant γ as a suitable function of ε , that tends to 0 with ε . Compare with the above references. For some explanation we also refer to the first topological digression from Appendix C or [59].

2. According to Mandelbrot [92], we speak of a fractal set when its Hausdorff dimension is larger than its topological dimension [59, 73, 108]. Without going into all definitions we just mention the following: the fact that the set of parameter values with quasiperiodic dynamics has positive measure implies that the Hausdorff dimension equals 1 while the fact that it is totally disconnected implies that the topological dimension equals 0. Granted the details, this shows that the parameter points with quasiperiodic dynamics form a fractal set.

Finally we mention that the Arnold family \mathfrak{A} in many respects is already generic, in the sense that most of the above properties also hold for circle maps where the periodic term $f(\varphi) = \sin \varphi$ in (D.1) is replaced by an arbitrary trigonometric polynomial or even a general smooth periodic function. The only difference with what has been described here is the order of contact that the boundaries of a given tongue may have, again see [41].

D.3.4. Back to Huygens's clocks

We now return to the torus-circle model for Huygens's weakly coupled pendulum clocks. Generically the periodic term in the corresponding Poincaré map (D.1) has a main tongue as described above,

so where the tongue boundaries meet with a positive angle at $(\alpha, \varepsilon) = (0, 0)$; in fact all tongues open up a bit. Since the pendulum clocks are almost identical, the corresponding (α, ε) must be in this main tongue, which implies synchronization on average.

We like to note the universal nature of the above approach. To find sharper forms of synchronization, i.e, where the pendulums moving in phase or anti-phase, also the dynamics of the beam has to be taken into account. We here refer to, e.g., [19, 112].

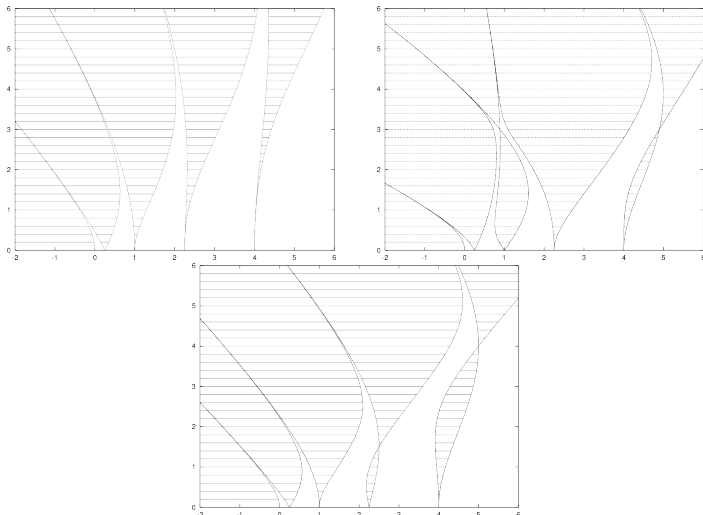


Figure D.6: Tongues in the Mathieu equation [96] (upper left), a modified Mathieu equation [40] (upper right) and Square Hill equation [38] (below)

D.4. Parametric resonance: Mathieu's equation and the like

In Section 2.4.1 we already got acquainted with parametric resonance. Instead of (2.11) we here, as in Appendix C, use the swing

form (C.3)

$$\ddot{x} + (a + \varepsilon f(t)) \sin x = 0 \quad \text{with} \quad f(t + 2\pi) \equiv f(t). \quad (\text{D.4})$$

We also use the system form (C.4) and the ensuing Poincaré map. For f we distinguish the following alternatives

$$\begin{aligned} f_\varepsilon(t) &= \cos t + \varepsilon \cos(2t) \\ f(t) &= \operatorname{sign}(\cos t). \end{aligned}$$

In the sequel we shall also use the linearized version of (D.4)

$$\ddot{x} + (a + \varepsilon f(t))x = 0, \quad (\text{D.5})$$

The case of $f = f_0$ is the classical Mathieu equation, see [96]. The case f_ε for $\varepsilon > 0$ is the modified Mathieu equation, see [40] and the other case is known as Square Hill equation [38].

The stability diagram

We consider the trivial periodic solution $x \equiv 0 \equiv \dot{x}$ and its stability. In terms of the Poincaré map this amounts to whether the corresponding fixed point $(x, y) = (0, 0)$ is an elliptic point or a saddle point, something that can be read out from the derivative $D_{(0,0)}P$. In turn, this derivative is completely determined by the linearized, Mathieu-like equation (D.5) that for $\varepsilon = 0$ turns into

$$\ddot{x} + ax = 0.$$

The system form then is

$$\begin{pmatrix} \dot{x} \\ \dot{y} \end{pmatrix} = \begin{pmatrix} 0 & 1 \\ -a & 0 \end{pmatrix} \begin{pmatrix} x \\ y \end{pmatrix}$$

The eigenvalues are $\pm i\sqrt{a}$ and therefore

$D_{(0,0)}P$ has eigenvalues $e^{\pm i\sqrt{a}}$.

For $a > 0$ these are always elliptic (i.e., imaginary) but for

$$a = \frac{1}{4}k^2, \quad k = 0, 1, 2, \dots$$

they equal ± 1 . In the (a, ε) -plane the points $(a, \varepsilon) = (\frac{1}{4}k^2, 0)$, $k = 0, 1, 2, \dots$ turn out to be tips of resonance tongues in which the eigenvalues are real, which means that the fixed point $(x, y) = (0, 0)$ is a saddle point and is therefore unstable. Bifurcations (so-called sub-harmonic bifurcations) then take place at the corresponding tongue boundaries. For instance the tongue with $k = 1$ when the eigenvalues of $D_{(0,0)}P$ are close to -1 , this bifurcation is a period doubling and we speak of a $1 : 2$ -resonance. For more details see below. In Figure D.6 we displayed three diagrams with tongues in the (a, ε) -plane for different choices of f .

Note that the $1 : 2$ -resonance near the tongue tip with $k = 1$ resembles the Botafumeiro motion as described in the introduction to this appendix.

Remark 31. *In two of the three stability diagrams tongues occur with intersections in their boundary curves. It turns out that the corresponding patterns are universally arranged by so-called \mathbb{A}_{2k-1} -singularities, see [14, Chapter 15] for details.*

The nonlinear dynamics

In this section we focus on the $1 : 2$ -resonance tongue emanating from $(a, \varepsilon) = (\frac{1}{4}, 0)$ and the corresponding dynamics. As said before the ensuing bifurcation is a period doubling.

One way to get information on the nonlinear dynamics of (D.4) is to consider its system form.

$$\begin{aligned}\dot{x} &= y \\ \dot{y} &= -(a + \varepsilon f(z)) \sin x \\ \dot{z} &= 1,\end{aligned}\tag{D.6}$$

compare (C.4), and by a repeated averaging procedure arrive at a planar vector field defined on an appropriate covering space. This procedure largely follows Takens [130]. The Poincaré map then is approximated to arbitrarily high order by the time 1 map of this Takens vector field T , composed with the reflection $-\text{Id}$. The vector field T also is invariant under $-\text{Id}$. For details see [44]. The Takens vector field sometimes also is called *interpolating*, for a phase portrait see Figure D.7.

We shall not go into the details here, but just comment on the numerically obtained stroboscopic phase portraits in Figure D.7.

We can still more or less recognise the underlying vector field T . The parameters (α, ε) are inside the tongue so the central fixed point, corresponding to the trivial periodic solution $x = 0 = y$, is a saddle point. The vector field T has a figure-8 homoclinic loop, enclosing two equilibria. However, by the flipping for the Poincaré map this is a periodic orbit of period 2 and a 4π -periodic solution of the system (D.6). In fact all equilibria of the Takens vector field T occur in pairs that form period 2 orbits. Moreover

1. There exist (pairs of) families of invariant circles, that are densely filled by quasiperiodic dynamics. This is in accordance with the KAM Theory described in Section D.3.
2. As is to be generically expected all homo- and heteroclinic connections of the Takens vector field turn into tangle, with its abundance of Smale horseshoes [43, Chapter 4]. In the sim-

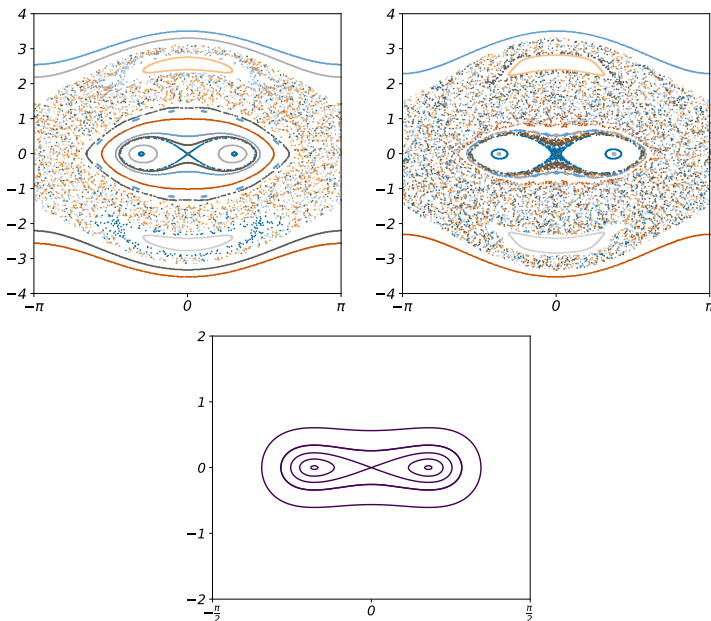


Figure D.7: Stroboscopic phase portraits near $1 : 2$ -resonance in the case of Mathieu forcing; top left $\epsilon = 0.25$, top right $\epsilon = .40$. Compare Figure C.5. Bottom: approximating Takens vector field

ulations we don't see the tangle, but just orbits that seem to densely fill up large areas. In Appendix C, particularly in Section C.3.2 we discussed this type of conservative chaos. As spelled out there, the long-standing Arnold conjecture is that the Lebesgue measure is ergodic for the Poincaré map at hand [13].

D.5. Scholium

This appendix is concluded by a number of examples where several kinds of resonance play a role. In the first example the forcing is quasiperiodic and we touch on the corresponding Mathieu equation being the spectral equation of a Schrödinger operator.

The second example deals with celestial resonances, that turn out to occur often in the solar system. Here we distinguish between sheer orbital resonances and spin-orbit resonances.

D.5.1. Quasiperiodic Hill versus Schrödinger

In this section we consider a quasiperiodic analogue of the Mathieu equation, given by

$$\ddot{x} + (a + \varepsilon f(t))x = 0 \quad (\text{D.7})$$

with $f(t) = F(\omega_1 t, \omega_2 t, \dots, \omega_n t)$ for a sufficiently smooth (or real analytic) map $F: \mathbb{T}^n \rightarrow \mathbb{R}$.

This equation can be largely treated in the same way as (D.5) [34], where we assume ω to be quasiperiodic. It turns out that the geometry per tongue is as before, but that globally we find the same fractal geometry as in the case of the Arnold family (D.3).

Schrödinger operators

The connection between dynamical systems, including KAM Theory, and spectral theory runs deep and is subject of ongoing research in mathematical physics. Here we shall not go into the details of quantum chaos and semiclassical analysis and restrict ourselves to some relevant aspects.

The equation (D.7) is of special interest since it is the spectral equation of the one-dimensional Schrödinger operator

$$(H_\varepsilon x)(t) = -\ddot{x}(t) - \varepsilon f(t)x(t)$$

for $x = x(t) \in L^2(\mathbb{R})$, with quasi-periodic potential εf . Here $L^2(\mathbb{R})$ is the space of Lebesgue measurable functions $x = x(t)$ such that $\int_{\mathbb{R}} |x(t)|^2 dt < \infty$.

This operator is widely being studied, among others by Dinaburg and Sinai [55] and by Moser, Pöschel, Eliasson and by Broer, Puig en Simó [39, 57, 98], where tools from both KAM- and singularity theory are being used. The lettering however is mostly chosen differently: the time t then is replaced by a spatial variable x , and the potential $\varepsilon f(t)$ by $V(x)$ or $U(x)$.

From gaps to tongues. Usually ε is not taken into account as a parameter and, in the above terms, one is just dealing with a fixed, (sufficiently) small $\varepsilon_0 > 0$. The intersection with the tongues then are spectral gaps. In [39] a rotation number ϱ is introduced that, as before, is a continuous function of the parameters a and ε . In Figure D.8 a graph is depicted with which shows another Devil's staircase. Here we often speak of *Cantor spectrum*.

Moser and Pöschel [98] state that generically the gaps do not close. However, the results of [39] show that the addition of the parameter

D. More on resonance

ε leads to a generic gap-closing theory where the pattern again is governed by the singularities \mathbb{A}_{2k-1} , again compare [14].

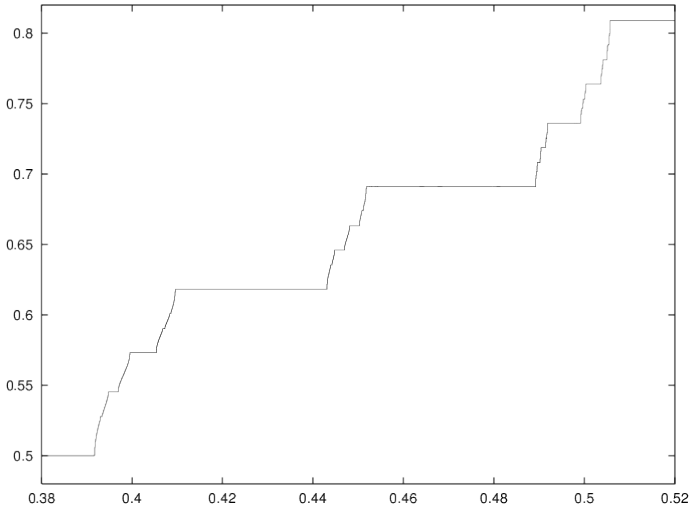


Figure D.8: *Another Devil's staircase* [39], where we take $n = 2$, $\omega_1 = 1$ and $\omega_2 = \frac{1}{2}(\sqrt{5} - 1)$, for $\varepsilon = \varepsilon_0$ sufficiently small; The description in the caption of Figure D.5 largely applies also here

From continuous to discrete. Next we consider a discrete Schrödinger operator, also known as *almost Mathieu operator*,

$$(H_{\lambda, \alpha, \theta} x)_n = x_{n+1} + x_{n-1} + 2\lambda \cos(2\pi\alpha n - \theta)x_n$$

where $\lambda, \alpha, \theta \in \mathbb{R}$ are real parameters and

$$u = (\dots, x_{-2}, x_{-1}, x_0, x_1, x_2, \dots) \in \ell^2(\mathbb{Z}),$$

where $\ell^2(\mathbb{Z})$ is the space of square-summable doubly infinite sequences, i.e., with $\sum_{n \in \mathbb{Z}} |x_n|^2 < \infty$.

The spectrum turns out to be independent of θ but varies wildly with respect to the other parameters. Here we will not go into the

effect of λ on the spectral type, but just focus on the remaining parameter α . When the value of $\alpha = p/q \in \mathbb{Q}$ is rational, the spectrum

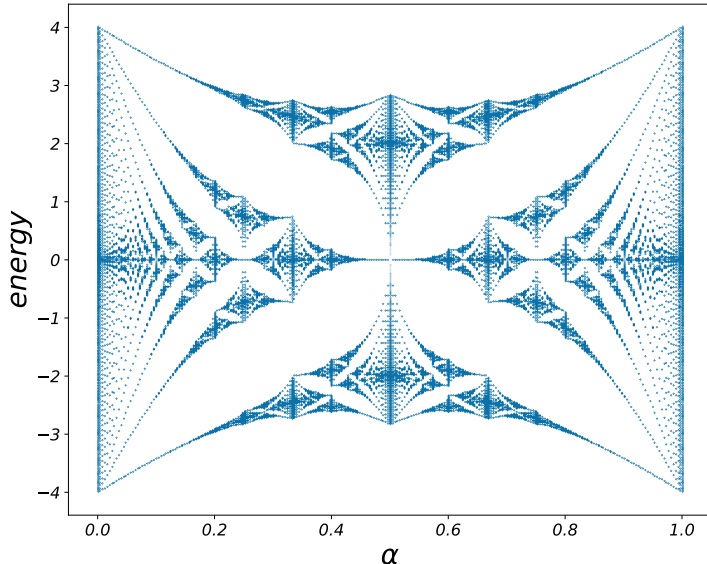


Figure D.9: Hofstadter's butterfly [80] is the fractal obtained by plotting the spectrum of the operators $H_{1,\alpha,\theta}$ for the rational values $\alpha \in \mathbb{Q} \cap [0, 1]$; It describes the spectral properties of non-interacting electrons in a two dimensional lattice under the influence of a perpendicular magnetic field

of $H_{\lambda,p/q,\theta}$ is given by the union of q intervals possibly touching at endpoints (see Figure D.9). This follows from Floquet theory, which we have met in disguise in the previous discussion of the Hill and Mathieu equation. When α is irrational, we again deal with a Cantor spectrum for all $\lambda \neq 0$ and therefore with Devil's staircases.

Remark 32. The latter statement is commonly referred to as the Ten Martini problem. It was conjectured by Barry Simon in 1981, who named it after a prize offered by Mark Kac for its solution [121, Problem 4]. The conjecture was proven by Avila and Jitomirskaya 24

years later, in 2005 [6, 7, 88].

This operator arises in the context of the Integer Quantum Hall Effect, at the center stage of the Nobel prize in physics in 1985 [106]. And it brings us to the verge of many recent mathematical advances, contributing to the award of a 2014 Fields medal to Artur Avila [63].

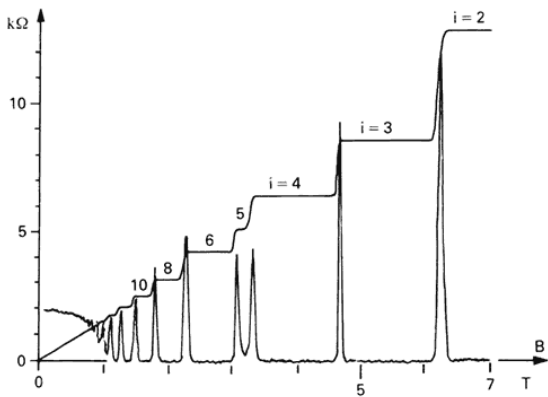


Figure D.10: The Hall resistance varies stepwise with changes in magnetic field B . The lower peaked curve represents the Ohmic resistance, which disappears at each step [66]. Note that this figure relates to the case of rational α and therefore does not correspond to a Devil's staircase. Perhaps that you can yet see the ghost of such a staircase ...

Abundance of Cantor sets and Devil's staircases. Referring to the Figures D.5 and D.8, to Smale horsehoees, tangle and the like [43], and also to the general discussion on KAM Theory in Section D.3, it should be no longer a surprise that Cantor sets and Devil's staircases appear widely in dynamical systems and in various theories within mathematical physics. Here it is noteworthy that Cantor sets sometimes have positive measure and sometimes measure 0.

Remark 33. 1. In the literature on theoretical solid state physics,

field theory and statistical mechanics, one stumbles over these gadgets [64]. For instance, it turns out [88] that models like the almost Mathieu operators presented here are also at the roots of the so-called Fractional Quantum Hall Effect [16, 65] (see also Figure D.10), a phenomenon whose discovery led to a Nobel prize in physics in 1998 [66].

2. *We also like to point out that the mathematics used in the history of Simon's conjecture and the various proofs of partial results that appeared over the years, heavily rest on application of KAM Theory (see e.g. [5, 55, 58, 76, 120]).*

D.5.2. Celestial resonance

When looking at the night sky we may see a lot of oscillation, especially when studying the heavenly bodies within our solar system. These motions form the main subject of celestial mechanics. And although the dimensions of the phase spaces are much higher than in the present book, the mechanical principles remain the same: one works mainly within the Newtonian theory, now and again applying a relativistic correction.

A taste of resonance. The solar system knows many resonances. We distinguish between two types of these: orbital and spin-orbit resonances.

An example of the former resonance is given by the inner three Galilean moons of Jupiter: Io, Europa and Ganymedes. These trace their almost circular orbits in an orbital $1 : 2 : 4$ resonance. This means that Europa has a period of revolution that is twice that of Io and similarly that Ganymedes takes twice as long as Europa to revolve.

D. More on resonance

This resonance was discovered by Laplace [87], for later references see [122, 123] and [32, 33, 45].

An example of a spin-orbit resonance is given by the motion of the moon around the earth. Since the moon always shows the same face, its revolution around the earth and the rotation (spin) around its own axis must be equal (at least on average). We speak of a 1 : 1 spin-orbit resonance. Other examples are the Galilean moon Io with respect to the planet Jupiter, and Enceladus and Rhea both with respect to Saturn. Similarly Mercury is in a 3 : 2 spin-orbit around the sun: it rotates twice about its axis against two revolutions around the sun [47].

One main physical explanation is given by the tidal effects that the celestial bodies exert on each other and that by friction slow down the rotation about their axes. Indeed, to give an idea consider the tidal waves caused moon (and sun) on the earth, that are clearly visible in the oceans. However, also the earth surface itself, at the equator, in each wave is lifted for about 40 cm. In this way the earth has *captured* the moon into this 1 : 1 spin-orbit resonance, but in the very long run the earth itself will also be captured. Then day and month have become equally long and the pair will move around in the solar system as a rigid body. By the same mechanism Pluto and his companion Charon have already been captured in this mutual embrace. For an overview see [27].

An adiabatic Ansatz. The general philosophy is that by the tidal effects the rotations decrease in an *adiabatic* way, being captured in a resonance now and again [75]. A caricature think of the Arnold tongues in Figure D.4, where the parameter α is moving adiabatically towards 0. The system then passes through many resonances, where the higher order ones are barely observed, finally ending up being captured in the lowest possible, ‘synchronizing’ 1 : 1 reso-

nance.

When considering orbital resonances with more satellites, validity of Kepler's third law may well lead to a final $1 : 2 : 4$ resonance capture [32, 33] ...

A spin-orbit model. To further explain the capture in a spin-orbit resonance, we introduce a mathematical model [71, 46] to describe the spinning motion of a satellite around a central heavy body.

The simplest form of the model assumes that a triaxial satellite is orbiting a larger, heavier body on a Keplerian ellipse. Furthermore, we also assume that its spin-axis is perpendicular to the orbital plane and that it coincides with the smallest axis of the satellite. The equation of motion that describe the rotation of such a satellite around its spin-axis ends up being a particular damped forced oscillator, ruled by two parameters: the asphericity of the satellite and the elliptic eccentricity of the orbit.

It was one of the great achievements of Newton to recognise the central role of the *linear momentum* in his *Philosophiae Naturalis Principia Mathematica* [104]. This linear momentum, for a body of mass m that moves with velocity \dot{x} , reads

$$p = m\dot{x}. \quad (\text{D.8})$$

Newton's famous second law (1.1), then gets the form

$$F = \dot{p}. \quad (\text{D.9})$$

It is to be noted that usually these notions go in vectorial form.

Similar equations exist for rotating motion. Assuming that the body moves along an angle θ with an angular velocity $\dot{\theta}$, then we can re-

D. More on resonance

place the expression (D.8) by

$$L = I\dot{\theta},$$

the *angular momentum*. Here I is the *moment of inertia* of the spinning body [69], with respect to the (instantaneous) axis of rotation. Just like the mass m of an object can be understood as the physical property that resists to its velocity \dot{x} , so can de moment of inertial I be understood as the property that resists to its rotational velocity $\dot{\theta}$. The role of the force F is now taken over by the *torque* N and equation (D.9) for this case reads

$$N = \dot{L}.$$

Since I also depends on t we here get

$$\dot{L} = I\dot{\theta} + \ddot{\theta}$$

and so the equation of motion of the spin-orbit motion reads

$$N(\theta, t) = I\dot{\theta} + \ddot{\theta}. \quad (\text{D.10})$$

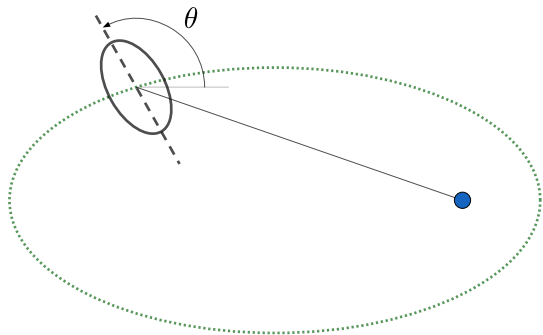


Figure D.11: Schematic representation of the spin-orbit model

It turns out that it is a realistic assumption that I has the format

$$I(t) = \tilde{I} + \lambda \cos(\Omega t),$$

so with average \tilde{I} that varies periodically with some frequency Ω . Moreover the torque $N = N(\theta, \dot{\theta}, t)$, that accounts for the revolution of the satellite around the heavy body, is also assumed to be periodic in t . Damping is included as well in the model, to express tidal friction. As in the models of Chapter 2 and Appendix C, the small damping is dealt with in a perturbative way. Thus we can rewrite the equation of motion (D.10) in the familiar form

$$\ddot{\theta} + \frac{dI}{dt} \frac{\dot{\theta}}{I} - \frac{N(\theta, \dot{\theta}, t)}{I} = 0, \quad (\text{D.11})$$

assuming that $I \neq 0$. As in Appendix C, we can plot stroboscopic phase portraits to get an idea of the dynamics of (D.11), for examples see Figures D.12 and D.13.

Resonance capture. Compared to the general philosophy of Ansatz D.5.2, the spin-orbit model gives a more realistic view and more details idea of a specific resonance capture, especially in Figure D.13. Nevertheless, the time scale in Figure D.13 also here indicates an adiabatic process. For details we refer to [67, 68, 75, 114].

Given the perturbative nature of damping in (D.11), the evolution of the damped system for a long time remains close to an orbit of the undamped system. In Figure D.13 we can witness a ‘chaotic’ orbit being captured over a long time span into a $1 : 1$ resonance: after some time the satellite effectively is in synchrony with the revolution around the planet, with only remarkably small deviations.

We note that the present model has two frequencies which makes it harder to analyse, also compare Section D.5.1. Indeed, a full understanding of this phenomenon is still subject of scientific debate [99, 100, 101]. Considering the spin-orbit resonances in our solar system, it remains quite unclear why certain ‘non-synchronizing’ resonances, like the $2 : 3$ spin-orbit resonance of Mercury, are so prevalent. Nevertheless, a careful analysis of the spin-orbit problem of

D. More on resonance

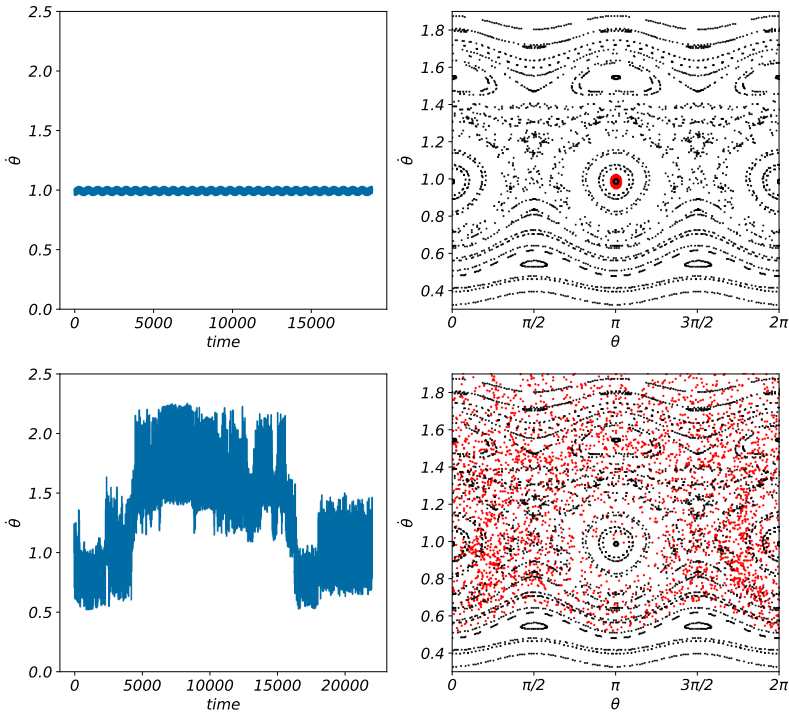


Figure D.12: The left hand panels present the time-evolution of $\dot{\theta}$ for the spin-orbit model (D.10) in the non-resonant case $\Omega = \sqrt{2}$ for $\lambda = 0.01$ (top) and $\lambda = 0.2$ (bottom). The right hand panels show the stroboscopic phase portraits of the damped model (red or gray dots) as compared to the un-damped model with $\lambda = 0$ (black dots) [25].

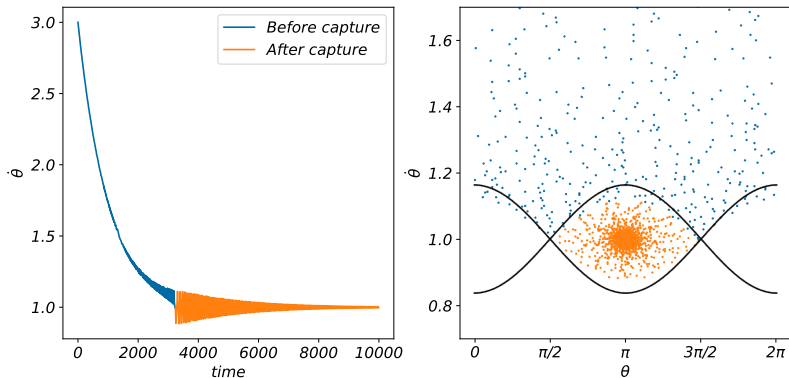


Figure D.13: The evolution of $\dot{\theta}$ for the spin-orbit model (D.11) in the case of capture in the synchronous 1 : 1 resonance (left); The stroboscopic phase portrait on the right clearly confirms this resonance capture [25]

the Earth-Moon system [46] indicates that the system may well be in the middle of a narrow tongue close to the frequency 1, which again confirms the adiabatic philosophy of Ansatz D.5.2.

Remark 34. Considering the dissipative stroboscopic phase portraits of Figure D.12, one may well ask whether there is chaos in the sense of Appendix C. For recent research in this direction see [51, 52]. On the other hand the graphics also suggests the possibility of infinitely many sinks in the sense of Newhouse [102, 103], also compare with [109].

D.5.3. A final exercise on Kepler's third law

In this exercise we determine Kepler's third law from mathematical principles under Newtonian gravitation, also using Newton's second law

$$\mathbf{F} = m \mathbf{a} \quad (\text{D.12})$$

D. More on resonance

compare with [104]. For simplicity we restrict to uniform circular motions.

In the plane consider two point masses M (the sun) and m (a planet). Let x and y be cartesian co-ordinates and set

$$\mathbf{r}(t) = \begin{pmatrix} x(t) \\ y(t) \end{pmatrix}.$$

The sun is positioned at the origin and the planet moves in a uniform circular orbit

$$\mathbf{r}(t) = R \begin{pmatrix} \cos\left(\frac{2\pi}{T} t\right) \\ \sin\left(\frac{2\pi}{T} t\right) \end{pmatrix}, \quad (\text{D.13})$$

so with radius R and period of revolution T .

- Under the assumption of a Newtonian inverse square central force

$$\mathbf{F} = -\frac{kMm}{r^2} \mathbf{e}_r, \quad (\text{D.14})$$

where \mathbf{e}_r is the unit vector in the radial direction, show that

$$T = \text{cst. } R^{3/2},$$

and determine the cst. This result is known as Kepler's third law or also as Kepler's 3/2 law.

- What changes in the above when Newton's inverse square law is replaced by

$$\mathbf{F} = -\frac{kMm}{r^\kappa} \mathbf{e}_r \quad (\text{D.15})$$

for a constant $\kappa \neq 0$?

Remark 35. 1. For completeness we also briefly discuss Kepler's first two laws for planetary motion. The first is that the planet travels along an ellipse with the sun in one of its focal points.

The second law says that in equal times the radius \mathbf{r} of the planet sweeps out equal areas. Note that the motion (D.13) surely is in agreement with these two laws.

By the way, in Arnold [8, Section 7], it is shown that Kepler's second law holds for any central force field (D.15).

2. *From the above exercise it follows that the inverse square attraction law is equivalent to Kepler's 3/2 law. Until the early 1680's Newton (and some of his contemporaries) understood that the sun attracts each planet according to the inverse square law, but there was no mention yet of universal gravitation.*

Then Newton proposes the following crucial experiment: he asks the First Astronomer Royal John Flamsteed to check Kepler's third law on the four Galilean moons of Jupiter (which happen to follow almost circular orbits). After an affirmative answer Newton concludes that Jupiter also attracts its moons with the inverse square law and only then he dares to postulate the law of universal gravitation. See Westfall [134].

Newton immediately realized that this was the end of all these beautiful Keplerian ellipses, since these were perturbed by their mutual gravitational interactions. This may well have given him severe headaches but it also marked the onset of ages of perturbation theory.

E. Solutions of selected exercises

E.1. Exercises from Chapter 1.6

E.1.1. Exercise 1.6.1

1. Since m is at rest, the sum of the gravitational force $-mg$ and the spring force $-kx$ should be equal to 0. This means that $-mg - kx = 0$, and therefore that the position is $x = -mg/k$.
2. Newton's law gives

$$m\ddot{x} = -kx - mg.$$

We can use the change of variables $s(t) = x(t) + \frac{mg}{k}$, which shifts the rest position to 0, to get to the following equation of motion

$$m\ddot{s} = -ks.$$

3. We already know the solutions of this equation of motion, namely

$$s(t) = A \cos\left(\sqrt{\frac{k}{m}}t\right) + B \sin\left(\sqrt{\frac{k}{m}}t\right).$$

E. Solutions of selected exercises

For x we therefore we find the solutions

$$x(t) = -\frac{mg}{k} + A \cos\left(\sqrt{\frac{k}{m}} t\right) + B \sin\left(\sqrt{\frac{k}{m}} t\right).$$

E.1.2. Exercise 1.6.2

Since there are no forces in the direction of the motion, the equation of motion is

$$\ell \ddot{x} = 0 \quad \text{or} \quad \ddot{x} = 0.$$

The corresponding solutions are of the form $x(t) = At + B$, where $A = \frac{dx}{dt}(0)$ and $B = x(0)$.

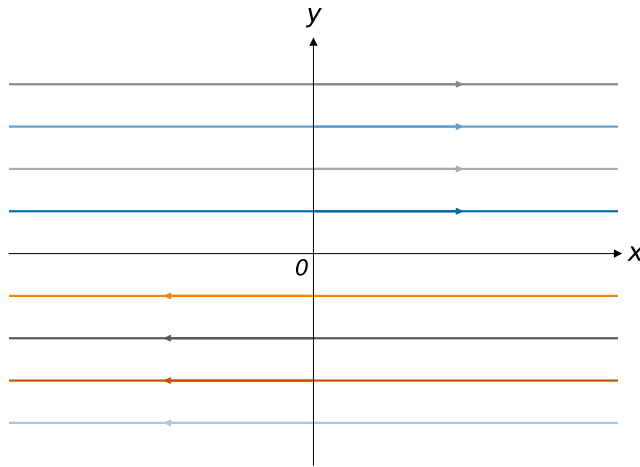


Figure E.1: Phase portrait of the horizontal pendulum

Since the potential energy in this example is identically zero, the energy here is $H(x, y) = \frac{1}{2}\ell^2 y^2$, and so the integral curves are horizontal lines, while all points on the x axis are singular. This horizontal pendulum can be considered as the limit of an ordinary vertical

pendulum when we let the gravity g go to zero. Furthermore, as $E \rightarrow \infty$ (E being the value of the energy), there is increasingly less difference between the solutions of the equation of motion of the horizontal and the vertical pendulum.

E.1.3. Exercise 1.6.3

In the direction (ξ, η) defined at (x, y) we have

$$-F(x)\xi + y\eta = 0,$$

and therefore

$$-F(x)\xi + (-y)(-\eta) = 0.$$

It follows that the line element field is symmetrical under the reflection on the x -axis.

Let now the direction in $(x, 0)$ be given by (ξ, η) . Then, by the above discussion (ξ, η) and $(\xi, -\eta)$ correspond to the same direction and therefore $\xi = 0$ or $\eta = 0$. From the formula for the line element field it follows that at a point $(x, 0)$ for which $F(x) \neq 0$, the direction is vertical (i.e., in the y direction), while at a point $(x, 0)$ for which $F(x) = 0$, we have a singularity.

When the map $x \mapsto y(x)$ defines an integral curve, by the symmetry, $x \mapsto -y(x)$ also defines an integral curve. The “motions” associated with these integral curves are each other’s “inverse” in the sense that the latter in x can be obtained by performing the former backwards in x . The integral curve and its mirror image may or may not be equal, as you can see in Figure E.2. (What does the potential $V(x)$ look like?)

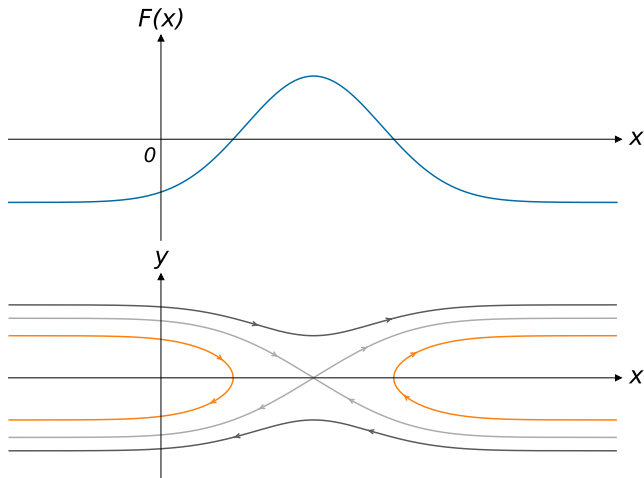
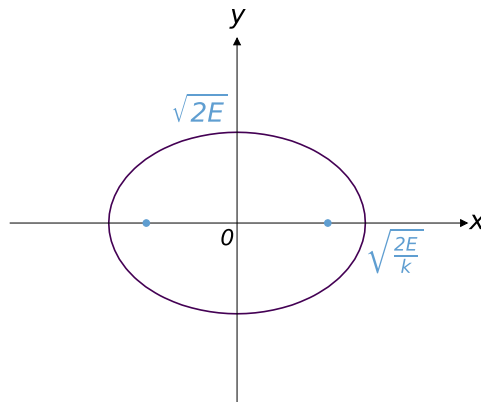


Figure E.2: Integral curves for a given force $F = F(x)$

E.1.4. Exercise 1.6.4

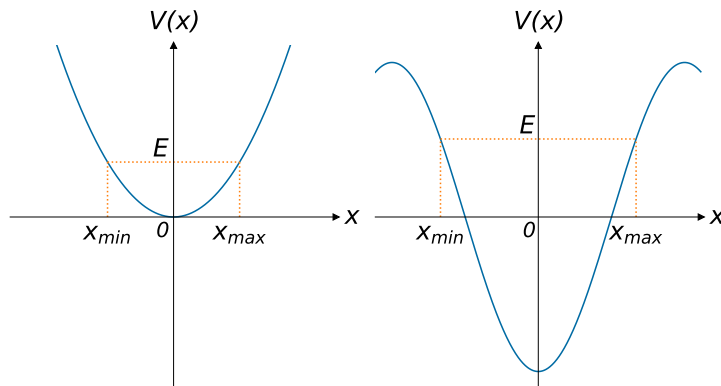
The equation of motion is $\ddot{x} = -kx$, the potential energy is $V(x) = \frac{1}{2}kx^2$ and the total energy is $H(x, y) = \frac{1}{2}y^2 + \frac{1}{2}kx^2$, where $y = \dot{x}$.

1. The energy level for some energy E is described by the equation $\frac{1}{2}y^2 + \frac{1}{2}x^2 = E$. Curves described by such an equation are called *ellipses* (see Figure E.3).
2. Substituting $y = z\sqrt{k}$ in the equation for the energy level with value E gives $\frac{1}{2}kx^2 + \frac{1}{2}kz^2 = E$: the equation of a circle.
3. For $\tau = \sqrt{k}t$ the Chain Rule gives that $\frac{dx}{d\tau} = \frac{1}{\sqrt{k}}\frac{dx}{dt}$ and thus $\frac{d^2x}{d\tau^2} = \frac{1}{k}\frac{d^2x}{dt^2} = -x$. That is, the transformation $z = \frac{1}{\sqrt{k}}y$ has the same effect as the time rescaling $z = \frac{dx}{d\tau}$.

Figure E.3: *Elliptic integral curve*

E.1.5. Exercise 1.6.5

An oscillation with energy E occurs between x_{\min} and x_{\max} ; since at maximum deviation the velocity and therefore the kinetic energy are zero, these values of x satisfy $V(x) = E$. Therefore, the amplitude is $\frac{1}{2}(x_{\max} - x_{\min})$.

Figure E.4: *Oscillation bounds for the two potentials in Exercise 1.6.5*

E. Solutions of selected exercises

In the first case, we get $x_{\max} = -x_{\min} = \sqrt{\frac{2E}{k}}$ and this is the amplitude. Similarly for the second potential we find the amplitude

$$\arccos\left(\frac{-\ell E}{g}\right),$$

where $-\frac{g}{\ell} \leq E < \frac{g}{\ell}$. For the other values of E there is no oscillation.

E.1.6. Exercise 1.6.6

The integral curves are of the form $y(x) = \pm\sqrt{2E - V(x)}$. So for solutions above the x axis local maxima and local minima of V correspond to local minima, resp. maxima, of the function $x \mapsto y(x)$ that defines the integral curve. Moreover, the local maxima and minima of V correspond to singularities of the line element field on the x -axis. The configuration of integral curves in such configurations depends on whether there is a local maximum or local minimum, see Figure E.5.

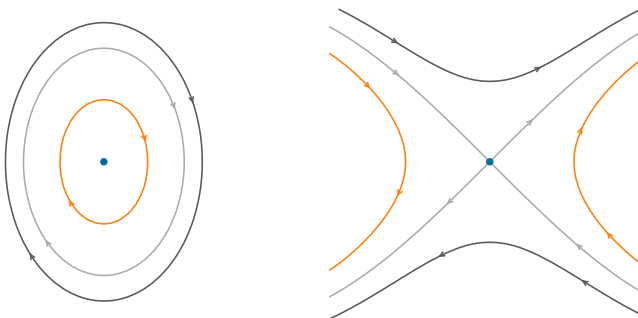


Figure E.5: Left: integral curves around a local minimum of V , this singularity is called a center; Right: integral curves around a local maximum of V , this singularity is called a saddle point

Horizontal asymptotes correspond to a separation between integral curves that go to infinity and bounded integral curves.

In Figure E.6 we drew the phase portraits associated to the potentials in Figure 1.18.

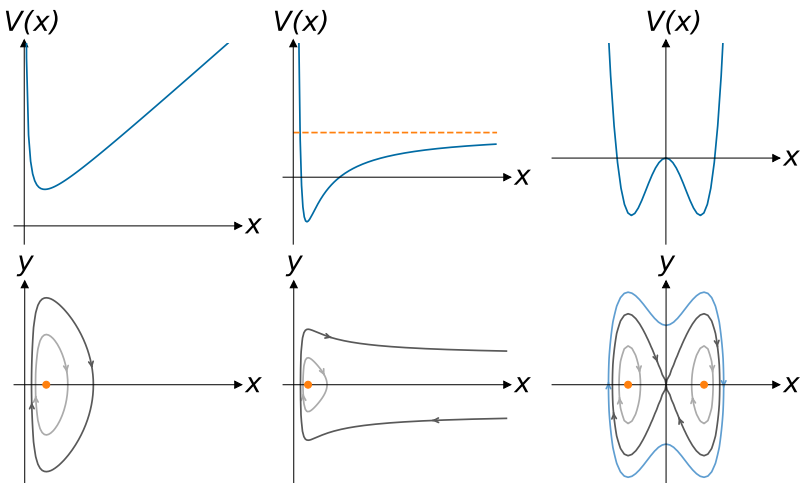


Figure E.6: Phase portraits for the potentials in Exercise 1.6.6

E.1.7. Exercise 1.6.7

- Let (x, y, φ) be the variables as indicated in Exercise 1.6.7 and the figure therein. The parametrization of the center of the wheel then is given by $x(\varphi) = -R\varphi$, $y(\varphi) = R$. The vector from the center of the wheel to the valve is $(-R \sin \varphi, -R \cos \varphi)$, which leads to the following parametrization of the valve:

$$x(\varphi) = -R(\varphi + \sin \varphi), \quad y(\varphi) = R(1 - \cos \varphi).$$

- The figure is symmetric with respect to the y -axis, see Figure E.7 (just replace φ with $-\varphi$). At a point with horizontal

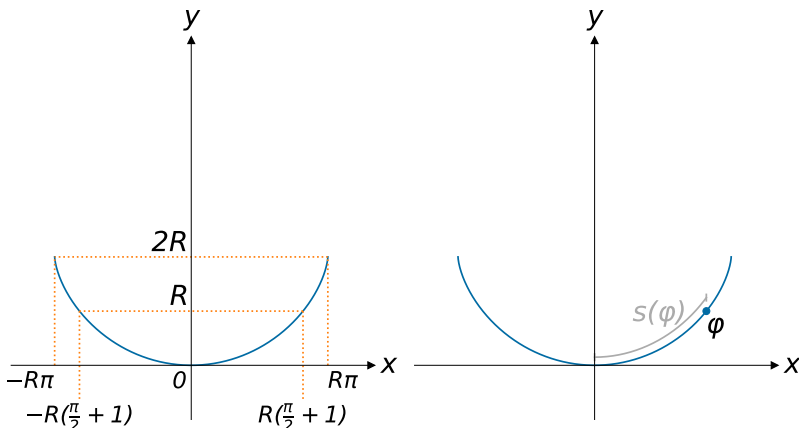


Figure E.7: Cycloid and its arclength

tangent line we get $\frac{dy}{d\varphi} = 0$ or $R \sin \varphi = 0$. Such points, therefore, occur for $\varphi = k\pi$ or $x = Rk\varphi$. Similarly we can determine points with a vertical tangent line and so obtain the points $x = (2k+1)R\pi$, $y = 2R$. Finally, at $\varphi = (k+1/2)\pi$ we have $y(\varphi) = R$.

NB: in the points $x = (2k+1)R\pi$, $y = 2R$, there is both a vertical and a horizontal tangent. The curve has a *cusp* there.

3. We indicate the position of the bead (or marble) with the distance, measured along the cycloid, from the bead to the lowest point of the curve. Since the position of the bead is $(-R(\varphi + \sin \varphi), R(1 - \cos \varphi))$, from the previous discussion we obtain $s(\varphi) = 2\sqrt{2R\sqrt{1 - \cos \varphi}} = 4R \sin(\frac{1}{2}\varphi)$, which can be interpreted as an arclength ‘with sign’; so the variable s can serve as a new coordinate.
4. The proof is part of the above item.

E.1.8. Exercise 1.6.8

The potential energy here is the height in the y coordinates, thus $V(s(\varphi)) = R(1 - \cos \varphi) = \frac{s(\varphi)^2}{8R}$. This means that the potential energy associated to this exercise reads $V(s) = \frac{1}{8R}s^2$. Therefore the motion is harmonic. This proves isochronicity of the motion. For tautochronicity we observe that dropping the bead from a certain height amounts to one quarter of an oscillation.

Note that if we are working with the potential energy, we have to use “real distances” to indicate the position, see also in Section 1.4.1, when defining

$$V(x) = - \int_0^x F(s) \, ds.$$

E.1.9. Exercise 1.6.9

We don't present a rigorous proof here, but rather an argument based on working with “infinitesimal quantitites” such as dE, dx , etc.

We aim to show that the area of the region between $H(x, y) = E$ and $H(x, y) = E + dE$ is equal to $P(E) dE$, see Figure 1.19. Indeed, if we denote the enclosed areas by $A(E)$ and $A(E + dE)$ then this would mean that

$$A(E + dE) - A(E) = P(E) dE,$$

which would prove our point.

We know that $H(x, y) = \frac{1}{2}y^2 + V(x)$. This means that the intersections of the line with equation $x = x_0$ with the energy levels E and $E + dE$ (above the x -axis) have y -coordinates

$$y_0 = \sqrt{E - V(x_0)} \quad \text{and} \quad \sqrt{2(E + dE - V(x_0))}.$$

E. Solutions of selected exercises

Since dE is supposed to be a small quantity, we can rewrite the latter expression as

$$\begin{aligned} y_0 + \frac{dy_0}{dE} dE &= y_0 + \frac{dE}{\sqrt{2(E - V(x_0))}} \\ &= y_0 + \frac{dE}{y_0}. \end{aligned}$$

The distance between these two points is therefore equal to dE divided by the velocity y_0 . This, indeed, means that the shaded area in Figure 1.19 must be equal to $dE \times dt$, where dt is the time the oscillator needs to travel from x_0 to $x_0 + dx$. We can now integrate this and find the following expression for the area between the energy levels for E and $E + dE$

$$\left(2 \int_{x_{\min}}^{x_{\max}} \frac{1}{y_0(x_0)} dx_0 \right) dE.$$

We already know that the expression in brackets denotes the period.

E.1.10. Exercise 1.6.10

Using the substitution $z = \cos x$ gives $dz = -\sin x dx$ and

$$dx = -\frac{1}{\sin x} dz = -\frac{1}{\sqrt{1-z^2}} dz.$$

Note that since $\sin x = \pm\sqrt{1-\cos^2 x}$, we here made a small omission ... We then obtain

$$\int \frac{dx}{\sqrt{2\cos x + C}} = - \int \frac{dz}{\sqrt{1-z^2}\sqrt{C+2z}} = - \int \frac{dz}{\sqrt{C+2x-cz^2-2z^3}}.$$

This final equation has the desired shape.

For the length of the ellipse, we start with $(ds)^2 = (dx)^2 + (dy)^2$ so

$$ds = \sqrt{1 + \left(\frac{dy}{dx}\right)^2}.$$

To compute $\frac{dy}{dx}$ we write y as a function of x and then differentiate. Recalling that an ellipse is the solution set of $\frac{x^2}{a^2} + \frac{y^2}{b^2} = 1$, we have $y^2 = b^2(1 - x^2/a^2)$ or $y = b\sqrt{1 - x^2/a^2}$. Therefore, we get $\frac{dy}{dx} = -\frac{bx}{a\sqrt{a^2-x^2}}$, and

$$\begin{aligned} ds &= \sqrt{1 + \frac{b^2x^2}{a^4 - a^2x^2}} dx \\ &= \sqrt{\frac{a^4 - a^2x^2 + b^2x^2}{a^4 - a^2x^2}} dx \\ &= \frac{a^4 - a^2x^2 + b^2x^2}{\sqrt{(a^4 - a^2x^2 + b^2x^2)(a^4 - a^2x^2)}} dx, \end{aligned}$$

so that now $\int ds$ indeed takes the desired form.

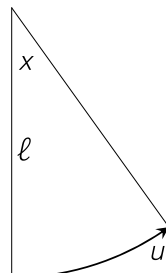
E.1.11. Exercise 1.6.11

Let us indicate our new variable, the *arclength*, by u . Then we have $u = \ell x$. The equation of motion then is given by

$$\frac{d^2}{dt^2}(\ell x) = -g \sin x,$$

which can be rewritten as

$$\ddot{u} = -g \sin \frac{u}{\ell} = F(u).$$



E. Solutions of selected exercises

If we use this to compute the potential energy, we find

$$\begin{aligned} V(u) &= - \int_0^u F(s) \, ds \\ &= \int_0^u g \sin \frac{s}{\ell} \, ds \\ &= -\ell g \cos \frac{s}{\ell} \Big|_{s=0}^{s=u} \\ &= g\ell(1 - \cos \frac{u}{\ell}). \end{aligned}$$

If you instead calculate the potential energy using the formula

$$\frac{d^2x}{dt^2} = -g \sin x = F(x),$$

you get $V(x) = \frac{g}{\ell}(1 - \cos x)$ which is wrong. Nevertheless, you can find the correct equation of motion in this way ...

E.2. Exercises from Chapter 2.6

E.2.1. Exercise 2.6.1

With the help of the chain rule we get

$$\begin{aligned} \frac{dx}{d\tau} &= \frac{dx}{dt} \frac{dt}{d\tau} = -\frac{dx}{dt}, \\ \frac{d^2x}{d\tau^2} &= \frac{d}{dt} \left(\frac{dx}{dt} \right) \frac{dt}{d\tau} = \frac{d^2x}{dt^2}. \end{aligned}$$

So, the equation

$$\frac{d^2x}{dt^2} = -\frac{dV}{dx} - c \frac{dx}{dt} \quad (\text{E.2})$$

transforms to

$$\frac{d^2x}{d\tau^2} = -\frac{dV}{dx} + c \frac{dx}{d\tau}.$$

Indeed we see that the transformation $\tau = -t$ reverses the sign of the friction term. If we know the phase portrait of an oscillator, or even for the solutions of a general equation of the form (E.2), then, after applying the change of variable $\tau = -t$, we can get the phase portrait after transformation as follows:

- We flip the image around the x -axis (after all $\frac{dx}{d\tau} = -\frac{dx}{dt}$);
- We reverse the directions of the arrows (after all, the arrows indicate the direction of the time).

It may be clear now, that with negative damping the energy will increase. Here you can also see that when there is no friction, the transformation $\tau = -t$ does not change the equation (compare this with Exercise 1.6.1).

E.2.2. Exercise 2.6.2

We first give the phase portrait of the frictionless equation that we find by determining the level curves of $H(x, y) = \frac{1}{2}y^2 + V(x)$. There are three types of oscillations.

1. Oscillations where the x -variable is always positive (for small energy these oscillations are very close to the point $x = 1$);
2. Oscillations where the x -variable is always negative;
3. Oscillations where x changes sign twice in each period. For this kind of oscillation, the amplitude is greater than $\sqrt{2}$. These regions of oscillation are separated from each other by a “figure 8” consisting of one saddle point $(x, y) = (0, 0)$ and two solutions which converge to $(x, y) = (0, 0)$ both as $t \rightarrow +\infty$ and

E. Solutions of selected exercises

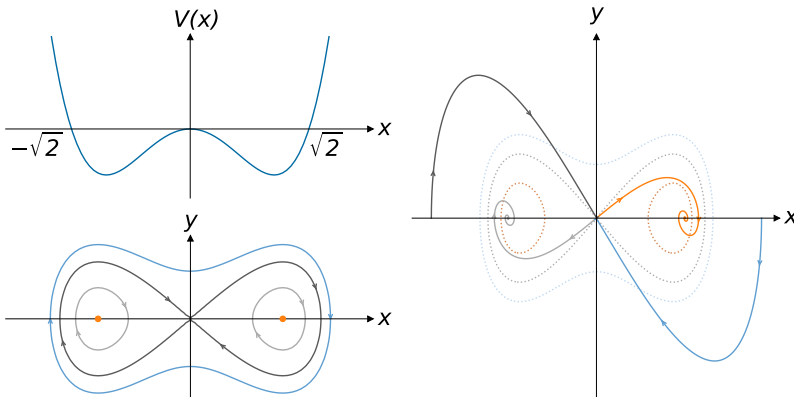


Figure E.8: Left: phase portrait of frictionless system from Exercise 2.6.2;
Right: phase portrait after introducing friction.

as $t \rightarrow -\infty$.

As the result of adding friction, the motion continuously loses energy. If we assume that the friction is low, we will get approximately the phase portrait on the right hand side of Figure E.8. In this case we have only shown the solutions that reach the saddle point as $t \rightarrow +\infty$ or $t \rightarrow -\infty$. All other solutions will converge to $x = 1$ or $x = -1$ as $t \rightarrow \infty$.

If we denote by L the part of the phase plane where the solutions converge to $x = -1$ and by R the part where the solutions go to $x = 1$, then we can see that L and R have “the same shape”: by reflection in the x -axis, L is mapped to R en vice versa. If we choose a “random point” in the phase plane, then the probability that the corresponding solution goes to $x = -1$ (heads) is just as large as the one that it goes to $x = 1$ (tails); the probability of the solution going to the saddle point is zero. (Why?)

E.2.3. Exercise 2.6.3

The integral curves are composed of semicircles. In the positive half-plane ($y > 0$) these are semicircles with center $(x, y) = (-a, 0)$, and in the negative half-plane semicircles with center $(x, y) = (a, 0)$. For $y = \dot{x} = 0$ our equation is actually not defined. Outside the interval from $x = -a$ to $x = a$ on the x -axis, we can continue the solutions continuously, but not in this interval. The displacement of the

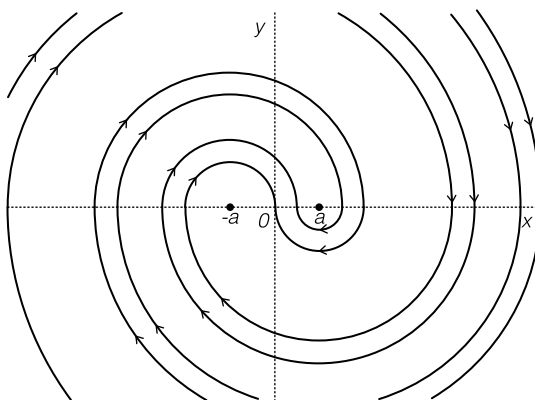


Figure E.9: A controlled oscillator

center of a harmonic oscillator can be described in terms of application of a constant external force. We can therefore also interpret our equations of motion as a harmonic oscillator (with center zero) on which an extra force of size a acts in a direction that is always opposite to the motion. This means that the extra force behaves like dry friction.

E.2.4. Exercise 2.6.4

- We compute the energy as the integral of the product of force and speed. The desired amount of energy then is

$$\begin{aligned} \int_0^{\frac{2\pi}{\Omega}} F \frac{dx}{dt} dt &= \int_0^{\frac{2\pi}{\Omega}} AB\Omega \sin(\Omega t) \cos(\Omega t + \phi) dt \\ &= AB\Omega \int_0^{\frac{2\pi}{\Omega}} \sin(\Omega t) (\cos(\Omega t) \cos(\phi) - \sin(\Omega t) \sin(\phi)) dt \\ &= -AB\pi \sin \phi. \end{aligned}$$

- By the same reasoning we now find

$$\begin{aligned} \int_0^{\frac{2\pi}{\Omega}} c \left(\frac{dx}{dt} \right)^2 dt &= cB^2\Omega^2 \int_0^{\frac{2\pi}{\Omega}} \cos^2(\Omega t + \phi) dt \\ &= cB^2\Omega\pi. \end{aligned}$$

- Since the motion is periodic, the energy absorbed and the energy delivered must be equal per period. Using the above results we find

$$-A\sin \phi = cB\Omega. \quad (\text{E.3})$$

Since A, B, c, Ω are all positive, necessarily $\sin \phi < 0$.

- Since here the mass equals 1, the force must be equal to the acceleration, which is $= B\Omega^2$. This, in turn, must be equal to the sum of the oscillating force $-B$ and the external force $A \sin(\frac{1}{2}\pi - \phi)$. Therefore

$$-B\Omega^2 = -B + A \sin\left(\frac{1}{2}\pi - \phi\right) = -B + A \cos \phi,$$

which implies

$$A \cos \phi = B(a - \Omega^2). \quad (\text{E.4})$$

5. The ratio of (E.3) and (E.4) gives

$$\tan \phi = \frac{c\Omega}{1 - \Omega^2}.$$

Using the identity

$$\sin \phi = -\sqrt{\frac{\tan^2(\phi)}{1 + \tan^2(\phi)}},$$

where the minus sign follows from the third item above, we obtain

$$\sin \phi = -c\Omega \sqrt{\frac{1}{c\Omega^2 + (1 - \Omega^2)^2}}.$$

The latter, replaced in (E.3) gives

$$B = \frac{A}{\sqrt{c\Omega^2 + (1 - \Omega^2)^2}}.$$

E.2.5. Exercise 2.6.5

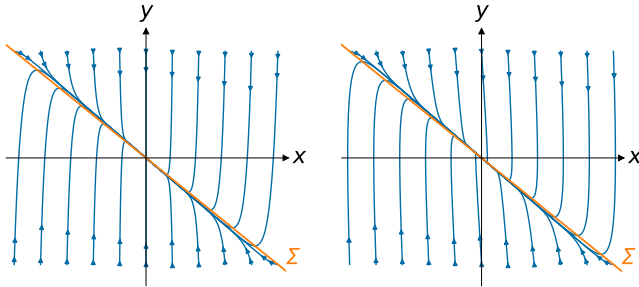


Figure E.10: Exercise 2.6.5

Left: phase portrait of the second and third case; Right: phase portrait of the fourth case

a) See Figure 2.19;

E. Solutions of selected exercises

- b) See the left hand side related to Figure E.10;
- c) See the left hand side related to Figure E.10 (this is no mistake, they are effectively the same);
- d) See the right hand side related to Figure E.10;
- e) See Figure E.11. In this case, if the solution approaches P or Q , there will be another (short) time interval in which the rapid motion of the second equation dominates. This is due to the fact that the solution can no longer follow Σ : for example near P the solution must move to the right ($y > 0$) and thus will have to move away from Σ .

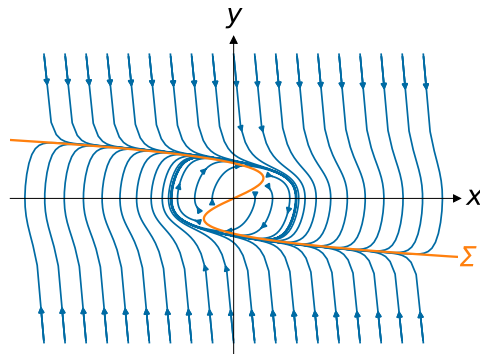


Figure E.11: Exercise 2.6.5, last case

For $\mu \geq 0$, the phase portrait of

$$\dot{x} = y, \quad \epsilon \dot{y} = -(x + \mu y + y^3)$$

is not essentially different from the right hand side of Figure E.10: all the solutions eventually will go to the origin. For $\mu < 0$, on the other hand, we get a phase portrait similar to Figure E.11.

It can be shown that for $\mu < 0$ our equation has a periodic solution, i.e., a solution $(x(t), y(t))$ such that there is certain period $T > 0$ for which $x(t + T) = x(t)$ and $y(t + T) = y(t)$ for all $t \in \mathbb{R}$. Moreover, all solutions will approach this periodic solution, with the only exception of $x(t) = 0 = y(t)$. As μ approaches 0, the periodic solution, as a figure in the phase plane, becomes smaller and approaches the origin. See also Section 3.4.

E.3. Exercise from Chapter 3

Solution of Part 1. The solution consists of two steps.

The Steiner ellipse. Let Z be the center of mass of $A_1 A_2 A_3$. Then the Steiner ellipse S of $A_1 A_2 A_3$ exactly is the ellipse passing through the vertices A_1, A_2 and A_3 , that has Z as its centre. Moreover the areas of the sectors $A_1 Z A_2$, $A_2 Z A_3$ and $A_3 Z A_1$ of S are equal.

Proof. The assertion is obviously true for an equilateral triangle, in which case the Steiner ellipse is the circumscribed circle. Now there exists an affine transformation F from the equilateral triangle to $A_1 A_2 A_3$ and this transformation has the following properties:

1. F preserves the center of mass;
2. F preserves parallelity of straight lines and hence maps the circumscribed circle to S ;
3. F maps equal areas to equal areas.

E. Solutions of selected exercises

The latter follows since F multiplies all areas by a fixed constant (a Jacobian determinant). From this the assertion follows. \square

Equation of motion. Let \mathbf{r} denote the position of P with respect to Z . Then its equation of motion is

$$\ddot{\mathbf{r}} = -3k\mathbf{r}.$$

Proof. Let \mathbf{a}_i denote the position vector of A_i with respect to Z ($i = 1, 2, 3$). Then $\mathbf{F}_i = k(\mathbf{a}_i - \mathbf{r})$ and therefore for the total force F we have

$$\mathbf{F} = \mathbf{F}_1 + \mathbf{F}_2 + \mathbf{F}_3 = -3k\mathbf{r} + k(\mathbf{a}_1 + \mathbf{a}_2 + \mathbf{a}_3) = -3k\mathbf{r}.$$

From this the assertion follows by Newton's second law. \square

From the latter assertion it directly follows that the possible motions of P are all Lissajous ellipses with centre Z . One of these is the Steiner ellipse S . It also follows that the motion of P takes place in a central force field where Kepler's second law holds true: equal areas are swept out in equal times. In view of the former assertion this solves the problem.

Solution of Part 2.

Let particle A_i have the three-dimensional position \mathbf{x}_i . Then the equations of motion read

$$m_i \ddot{\mathbf{x}}_i = \sum_{j=1}^n k^2 m_i m_j (\mathbf{x}_j - \mathbf{x}_i), \quad (i = 1, 2, \dots, n).$$

Let

$$\mathbf{z} = \frac{1}{M} \sum_{j=1}^n m_j \mathbf{x}_j$$

be the center of mass, where $M = \sum_{j=1}^n m_j$. It then follows that

$$\ddot{\mathbf{x}}_i = k^2 M \mathbf{z} - k^2 M \dot{\mathbf{x}}_i.$$

Summation yields that $M\ddot{\mathbf{z}} = 0$, i.e., the center of mass moves uniformly. The relative motion of the particle A_i ($i = 1, 2, \dots, n$) with respect to \mathbf{z} moreover is given by

$$\ddot{\mathbf{x}}_i + k^2 M \mathbf{x}_i = 0 \quad (i = 1, 2, \dots, n),$$

which describes a system of three decoupled harmonic motions. This leads to 3-dimensional Lissajous figures. We shall now argue why this still is a planar Lissajous ellipse.

Indeed, the projection in all three co-ordinate directions form 2-dimensional Lissajous figures. Since all frequencies are equal, the latter are just planar Lissajous ellipses. But then the 3-dimensional Lissajous figure also is an ellipse moving in a plane that is generic with respect to the co-ordinate directions. Thus each particle A_i moves in a plane along a Lissajous ellipse with center \mathbf{z} and period $T = 2\pi/k\sqrt{M}$.

E.4. Exercise from Appendix B

For $i = 1, 2, 3$ let x_i denote the position of P_i on ℓ_i , measured from O , and with all x_i of the same sign in the same ‘half’ of the cone. We write $\mathbf{x} = (x_1, x_2, x_3)^T$ as a vector. This is a linear problem with kinetic energy T and potential energy U , which read

$$T = \frac{1}{2}(\dot{x}_1^2 + \dot{x}_2^2 + \dot{x}_3^2)$$

and

$$\begin{aligned} U &= \frac{1}{2}k^2 \left(\overline{P_1 P_2}^2 + \overline{P_2 P_3}^2 + \overline{P_3 P_1}^2 \right) \\ &= \frac{1}{2}k^2(x_1^2 + x_2^2 + x_3^2 - x_1 x_2 \cos \alpha - x_2 x_3 \cos \alpha - x_3 x_1 \cos \alpha). \end{aligned}$$

E. Solutions of selected exercises

So in the format $T = \frac{1}{2}\langle A\dot{\mathbf{x}}, \dot{\mathbf{x}} \rangle$ and $U = \frac{1}{2}\langle B\mathbf{x}, \mathbf{x} \rangle$ we have $A = \text{Id}$, while

$$B = k^2 \begin{pmatrix} 2 & -\cos \alpha & -\cos \alpha \\ -\cos \alpha & 2 & -\cos \alpha \\ -\cos \alpha & -\cos \alpha & 2 \end{pmatrix}$$

Direct computation yields that B has a single eigenvalue $\omega_1^2 = 2k^2(1 - \cos \alpha)$ and a double eigenvalue $\omega_2^2 = 2k^2(1 + \cos \alpha)$. The corresponding eigenspaces are the diagonal

$$\left[\begin{pmatrix} 1 \\ 1 \\ 1 \end{pmatrix} \right]_{\mathbb{R}},$$

where $[-]$ takes the linear span, and its orthogonal complement, which is the plane given by the equation $x_1 + x_2 + x_3 = 0$. The corresponding characteristic oscillations are as follows.

1. The three particles oscillate in an equilateral triangle perpendicular to the diagonal with characteristic frequency

$$\omega_1 = k\sqrt{2}\sqrt{1 - \cos \alpha};$$

2. The vector \mathbf{x} oscillates in the plane $x_1 + x_2 + x_3 = 0$ in Lissajous ellipses, with characteristic frequency

$$\omega_2 = k\sqrt{2}\sqrt{1 + \cos \alpha}.$$

E.5. Exercise from Appendix D

Given the uniform circular motion with period T and radius R , the velocity is

$$\mathbf{v}(t) = \begin{pmatrix} \dot{x}(t) \\ \dot{y}(t) \end{pmatrix} = R \begin{pmatrix} -\frac{2\pi}{T} \sin\left(\frac{2\pi}{T} t\right) \\ \frac{2\pi}{T} \cos\left(\frac{2\pi}{T} t\right) \end{pmatrix}$$

and the (centripetal) acceleration

$$\mathbf{a}(t) = \begin{pmatrix} \ddot{x}(t) \\ \ddot{y}(t) \end{pmatrix} = R \begin{pmatrix} -\left(\frac{2\pi}{T}\right)^2 \cos\left(\frac{2\pi}{T}t\right) \\ -\left(\frac{2\pi}{T}\right)^2 \sin\left(\frac{2\pi}{T}t\right) \end{pmatrix} = -R \left(\frac{2\pi}{T}\right)^2 \mathbf{e}_r.$$

Combining (D.12) and (D.14) now gives

$$m\mathbf{a} = -mR \left(\frac{2\pi}{T}\right)^2 \mathbf{e}_r = -\frac{kMm}{R^2} \mathbf{e}_r$$

and so

$$T^2 = \frac{4\pi^2}{kM} R^3,$$

which amounts to Kepler's third law for this case of circular motion. The answer in the case when the central force has size $-kMm/R^\kappa$ reads

$$T^2 = \frac{4\pi^2}{kM} R^{\kappa+1}.$$

By the way, the case where $\kappa = -1$ corresponds exactly to Hooke's universe in Section 3.5, when the motion is isochronous. For a neat connection between the Hookian and the Newtonian ellipse see Arnold [11, Appendix 1].

Bibliography

- [1] J.M. Aarts, *Christiaan Huygens: Het Slingeruurwerk. Een studie.* Epsilon Uitgaven **80** 2015
- [2] H. Aldersey-Williams. *Dutch Light. Christiaan Huygens and the Making of Science in Europe.* Pan Macmillan 2021
- [3] C. Andriesse, *Titan kan niet slapen, biografie van Christiaan Huygens.* Olympus Pockets 2007
- [4] T.M. Apostol, *Calculus, Vol. 1: One-Variable Calculus, with an Introduction to Linear Algebra.* Second edition. John Wiley 1967
- [5] A. Avila, B. Fayad and R. Krikorian, A KAM scheme for $SL(2\mathbb{R})$ cocycles with Liouvillean frequencies. *Geom. Funct. Anal.* Vol. 21 (2011) 1001-1019
- [6] A. Avila and S. Jitomirskaya. *Solving the Ten Martini Problem.* In: J. Asch, A. Joye (eds.), Mathematical Physics of Quantum Mechanics. Lecture Notes in Physics, vol 690. Springer 2006
- [7] A. Avila and S. Jitomirskaya. *The Ten Martini problem.* *Ann. Math.* (2) **170**(1) 303-342 (2009)
- [8] V.I. Arnold, *Mathematical Methods of Classical Mechanics.* GTM **60** Springer 1978; second edition, Springer 1989

Bibliography

- [9] V.I. Arnold, *Geometrical Methods in the Theory of Ordinary Differential Equations*. Springer 1983
- [10] V.I. Arnold, *Catastrophe theory* (Third edition). Springer-Verlag 1992
- [11] V.I. Arnold, *Huygens & Barrow, Newton & Hooke*. Birkhäuser 1990
- [12] V.I. Arnold, *Mathematical Understanding of Nature: Essays on Amazing Physical Phenomena and Their Understanding by Mathematicians*. AMS 2014
- [13] V.I. Arnold and A. Avez, *Problèmes Ergodiques de la Mécanique Classique*. Gauthier-Villars 1967; *Ergodic Problems of Classical Mechanics*. Addison-Wesley 1989
- [14] V.I. Arnold, S.M. Gusein-Zade and A.N. Varchenko, *Singularities of Differentiable Maps Volume 1: Classification of Critical Points, Caustics and Wave Fronts*. Modern Birkhäuser Classics, Birkhäuser 1985
- [15] V.I. Arnold, V.V. Kozlov and A.I. Neishtadt, Mathematical Aspects of Classical and Celestial Mechanics. In: V.I. Arnol'd (ed.) *Dynamical Systems III*. Encyclopædia of Mathematical Sciences 3 Springer 1988
- [16] P. Bak and R. Bruinsma, *One-Dimensional Ising Model and the Complete Devil's Staircase*. Phys. Rev. Lett. **49** (1982) 249
- [17] D.G.M. Beersma, H.W. Broer, K. Efstathiou, K.A. Gargar and I. Hoveijn, Pacer cell response to periodic Zeitgebers. *Physica D: Nonlinear Phenomena* **240**(19) (2011) 1516-1527

- [18] M. Benedicks and L. Carleson, The dynamics of the Hénon map. *Ann. Math.* **133** (1991) 73-169
- [19] M. Bennett, M.F. Schatz, H. Rockwood and K. Wiesenfeld, Huygens's clocks. *Proc. R. Soc. Lond. A* **458** (2002) 563-579
- [20] J. Bernoulli, *Opera Johannis Bernoullii* (G. Cramer ed.; 4 vols), Genève 1742
- [21] H.M. Bos, Huygens, Christiaan (Also Huyghens, Christian). *Complete Dictionary of Scientific Biography* Encyclopedia.com 2012
- [22] O. Bottema, Problem 673, *Nieuw Archief voor Wiskunde* **2** **1** (1983)
- [23] O. Bottema, Problem 683, *Nieuw Archief voor Wiskunde* **3** **1** (1983)
- [24] O. Bottema, Problem 701, *Nieuw Archief voor Wiskunde* **2** **2** (1984)
- [25] A. Bravetti, M. Seri, M. Vermeeren, F. Zadra, Numerical integration in Celestial Mechanics: a case for contact geometry *Celestial Mechanics and Dynamical Astronomy* **132** (2020)
- [26] H.W. Broer, KAM theory: The legacy of Kolmogorov's 1954 paper. *Bulletin of the American Mathematical Society* **41**(4) (2004) 507-521
- [27] H.W. Broer, Resonance and fractal geometry. *Acta Applicandae Mathematicæ* **120** DOI 10.1007/s10440-012-9670-x (2012) 61-86

Bibliography

- [28] H.W. Broer, *Hemelverschijnselen Nabij de Horizon*. Epsilon Uitgaven **77** 2013
- [29] H.W. Broer, Bernoulli's light ray solution of the brachistochrone problem through Hamilton's eyes. *Int. J. Bifurcations Chaos* **24**:1440009, 2014
- [30] H.W. Broer, *Near the Horizon: an Invitation to Geometric Optics*. The Carus Mathematical Monographs **33** MAA 2016
- [31] H.W. Broer, J. Epema and M. Kuipers, *Oscillaties: trillingen en slingerbewegingen vanuit wiskundig oogpunt*. Internal Publication Rijksuniversiteit Groningen 1987
- [32] H.W. Broer and H. Hanßmann, On Jupiter and his Galilean satellites: librations of De Sitter's periodic motions. *Indag Math NS* **27**(5) (2016) 1305-1337
- [33] H.W. Broer and H. Hanßmann, A Galilean dance: 1:2:4 resonant periodic motions and their librations of Jupiter and his Galilean moons. *DCDS-S* **13**(4) (2020) 1043-1059
- [34] H.W. Broer, H. Hanßmann, Á. Jorba, J. Villanueva and F.O.O. Wagener, Normal-internal resonances in quasi-periodically forced oscillators: a conservative approach. *Nonlinearity* **16** (2003) 1751-1791
- [35] H.W. Broer, H. Hanßmann and F.O.O. Wagener, *Quasi-periodic bifurcation theory. The geometry of KAM*. Springer Verlag, in preparation
- [36] H.W. Broer, G.B. Huitema and M.B. Sevryuk, *Quasi-periodic tori in families of dynamical systems: order amidst chaos*. Springer LNM **1645** (1996) (195 p)

- [37] H.W. Broer and B. Krauskopf, Chaos in periodically driven systems. In: B. Krauskopf and D. Lenstra (eds.), *Fundamental Issues of Nonlinear Laser Dynamics*. Amer. Inst. Phys. (2000) 31-53
- [38] H.W. Broer and M. Levi, Geometrical aspects of stability theory for Hill's equations. *Archive Rat. Mech. An.* **131** (1995) 225-240
- [39] H.W. Broer, J. Puig and C. Simó, Resonance tongues and instability pockets in the quasi-periodic Hill-Schrödinger equation. *Commun. Math. Phys.* **241** (2003) 467-503
- [40] H.W. Broer and C. Simó, Resonance tongues in Hill's equations: a geometric approach. *Journ. Diff. Eqns.* **166** (2000) 290-327
- [41] H.W. Broer, C. Simó and J.C. Tatjer, Towards global models near homoclinic tangencies of dissipative diffeomorphisms. *Nonlinearity* **11** (1998) 667-770
- [42] H.W. Broer and H.S.V. de Snoo, Mathematische Fysica in Groningen I: Van Mees tot Zernike. *Nederlands Tijdschrift voor Natuurkunde* to appear
- [43] H.W. Broer and F. Takens, *Dynamical Systems and Chaos*. Epsilon Uitgaven **64** 2009; Appl. Math Sc. **172** Springer 2011
- [44] H.W. Broer and G. Vegter, Bifurcational aspects of parametric resonance. *Dynamics Reported, New Series* **1** (1992) 1-51
- [45] H.W. Broer and Lei ZHAO, De Sitter's theory of Galilean satellites and the related quasi-periodic orbits. *Celest. Mech. Dyn. Astr.* **127** (2017) 95-119
- [46] A. Celletti, Analysis of resonances in the spin-orbit problem

Bibliography

- in celestial mechanics: The synchronous resonance, Part I *J. Appl. Math. Phys. (ZAMP)* **41**, 174; Part II: *ZAMP* **41**, 453 (1990)
- [47] A. Correia and J. Laskar, Mercury's capture into 3/2 spin-orbit resonance as a result of its chaotic dynamics. *Nature* **429** (2004) 848-850
- [48] N. Chernov, R. Markarian, *Chaotic billiards*. Mathematical Surveys and Monographs, vol. **127**. AMS 2006
- [49] I. De Blasi, S. Terracini, Refraction periodic trajectories in central mass galaxies, *Nonlinear analysis*, **218** 112766 (2021)
- [50] I. De Blasi, S. Terracini, On some Refraction Billiards, *arXiv preprint*, arXiv:2108.11159 (2021)
- [51] A. Celletti and L. Chierchia Measures of basins of attraction in spin-orbit dynamics. *Celest Mech Dyn Astr* (2008) 101:159170 DOI 10.1007/s10569-008-9142-9
- [52] A. Celletti and L. Chierchia Quasi-Periodic Attractors in Celestial Mechanics *Arch. Rational Mech. Anal.* **191** (2009) 311345 (DOI) 10.1007/s00205-008-0141-5
- [53] R.L. Devaney, *An Introduction to Chaotic Dynamical Systems* Second Edition. Addison Wesley 1989
- [54] F.J. Dijksterhuis, *Lenses and waves: Christiaan Huygens and the Mathematical Science of Optics in the Seventeenth Century*. Springer 2004
- [55] E.I. Dinaburg and Ya.G. Sinai, The one-dimensional Schrödinger equation with quasiperiodic potential. *Funktional. Anal. i Prilozhen.* **9**(4) (1975) 8-21

- [56] M. Einsiedler, T. Ward, *Ergodic Theory with a view towards Number Theory*. GTM **259** Springer 2011
- [57] L.H. Eliasson, Floquet solutions for the one-dimensional quasi-periodic Schrödinger equation. *Commun. Math. Phys.* **146** (1992) 447-482
- [58] L.H. Eliasson, Discrete one-dimensional quasi-periodic Schrödinger operators with pure point spectrum, *Acta Math.* **179** (1997) 153-196
- [59] R. Engelking, *General Topology*. - Revised and Completed Ed. Helderman 1989
- [60] Euclid, *The thirteen books of the Elements*. Three volumes translations and commentary by T.L. Heath. Dover 1956
- [61] L. Euler, *Leonhardi Euleri Opera Omnia*. 72 vols. Bern 1911-1975
- [62] R.P. Feynman, R.B. Leighton and M. Sands, *The Feynman Lectures on Physics* Vols. **1**, **2** and **3**. Addison-Wesley 1963, 1964 and 1965
- [63] Press release: Fields Medal 2014, Arthur Avila.
https://www.mathunion.org/fileadmin/IMU/Prizes/Fields/2014/news_release_avila2.pdf Accessed on Fri. 10 Jun 2022.
- [64] G. Gallavotti, G. Gentile and V. Mastropietro, Field theory and KAM theory. *MPEJ* **1** 1995
- [65] A. Di Gioacchino, M. Gherardi, L.G. Molinari, P. Rotondo. *Jack on a Devil's Staircase*. In: P. Bortignon, G. Lodato, E. Meroni,

Bibliography

M. Paris, L. Perini, A. Vicini (eds.) Toward a Science Campus in Milan. CDIP 2017. Springer 2018

- [66] Press release: Nobel Prize in Physics 1998.
<https://www.nobelprize.org/prizes/physics/1998/press-release/> Accessed on Fri. 10 Jun 2022.
- [67] I. Gkolias, C. Efthymiopoulos, A. Celletti, G. Pucacco, Hamiltonian formulation of the spin-orbit model with time-varying non-conservative forces *Commun Nonlinear Sci Numer Simulat* **51** (2017) 23-38
- [68] I. Gkolias, C. Efthymiopoulos, A. Celletti, G. Pucacco, Accurate modelling of the low-order secondary resonances in the spin-orbit problem *Commun Nonlinear Sci Numer Simulat* **77** (2019) 181-202
- [69] H. Goldstein, *Classical Mechanics*. Addison-Wesley 1950 (second edition 1980)
- [70] H.H. Goldstine, *A History of the Calculus of Variations from the 17th through the 19th Century*. Studies in the History of Mathematics and Physical Sciences **5** Springer 1980
- [71] P. Goldreich, S. Peale, Spin-orbit coupling in the solar system. *The Astronomical Journal* **71** (1966)
- [72] K.P. Hart, De Cycloïde. *Pythagoras* **39**(4) 2000
- [73] F. Hausdorff, *Set Theory*. Second Edition. Chelsea 1962
- [74] M. Hendriks, *Introduction to Physical Hydrology*. Oxford University Press 2010

- [75] J. Henrard, Capture into resonance: An extension of the use of adiabatic invariants. *Celestial Mechanics* **27** (1982) 3-22
- [76] M. Herman, Une méthode pour minorer les exposants de Lyapounov et quelques exemples montrant le caractère local d'un théorème d'Arnold et de Moser sur le tore de dimension 2, *Comment. Math. Helv.* **58**:3 (1983) 453-502
- [77] M. Herman, Sur la conjugaison différentiable des difféomorphismes du cercle à des rotations. *Publ. Math. IHES* **49** (1979) 5-234
- [78] A. L. Hodgkin and A. F. Huxley, A quantitative description of membrane current and its application to conduction and excitation in nerve. *J. Physiol.* **117** (1952) 500-544
- [79] R.A. Horn, C.R. Johnson, *Matrix analysis*. Second edition. Cambridge University Press 2013
- [80] D.R. Hofstadter. Energy levels and wavefunctions of Bloch electrons in rational and irrational magnetic fields. *Physical Review B*. **14** 6 (1976)
- [81] M.W. Hirsch, S. Smale and R.L. Devaney, *Differential Equations, Dynamical Systems, and an Introduction to Chaos*. Academic Press 2004; 2013
- [82] Chr. Huygens, *Œuvres Complètes de Christiaan Huygens publiées par la Société Hollandaise des Sciences* **16**, Martinus Nijhoff, The Hague 1929 Vol. **5** 241-262; Vol. **17** 156-189
- [83] J. Israel, *The Dutch Republic: Its Rise, Greatness, and Fall, 1477-1806*. Oxford University Press 1995

Bibliography

- [84] H. Kamerlingh Onnes, *Nieuwe Bewijzen voor de Aswenteling der Aarde*. Proefschrift Universiteit Groningen 1879
- [85] D.E. Kirk, *Optimal Control Theory: an Introduction*. Dover 2004
- [86] A. Knauf, *Mathematical Physics: Classical Mechanics*. Unitext **109** Springer 2018
- [87] P.S. de Laplace, *Traité de Mécanique Céleste, Œuvres Complètes*. Tome **4** (1799), 1-501
- [88] Y. Last, Spectral Theory of Sturm-Liouville Operators on Infinite Intervals: A Review of Recent Developments. In: W.O. Amrein,A.M. Hinz, D.P. Pearson (eds) *Sturm-Liouville Theory*. Birkhäuser 2005
- [89] G.W. Leibniz, *Nova methodus pro maximis et minimis. Acta Eruditorum* 1684; In: D.J. Struik, *A Source Book in Mathematics 1200-1800*. Harvard University Press 1969 271-281
- [90] R. de la Llave, A tutorial on KAM Theory. In A. Katok et al. (Eds.), *Proceedings of Symposia in Pure Mathematics* **69** Amer. Math. Soc. (2001) 175-292
- [91] J.A. van Maanen, *Een Complexe Grootheid, leven en werk van Johann Bernoulli*, 1667–1748. Epsilon Uitgaven **34** 1995
- [92] B.B. Mandelbrot, *The Fractal Geometry of Nature*. Freeman 1977
- [93] R. Mañé, *Ergodic Theory and Differentiable Dynamics*. Ergebnisse der Mathematik und ihrer Grenzgebiete 3. Folge Band **8** Springer 1987

- [94] J. Martin, The Helen of Geometry. *The College Mathematical Journal* **41** (2010) 17-28
- [95] R.M. May, Simple mathematical models with very complicated dynamics. *Nature* **261** (1976) 459-466
- [96] J. Meixner and F.W. Schäfke, *Mathieusche Funktionen und Sphäroidfunktionen*. Die Grundlehren der Mathematischen Wissenschaften in Einzeldarstellungen, Band **LXXI**, Springer 1954
- [97] M.G.J. Minnaert, *De Natuurkunde van 't Vrije Veld* delen **1**, **2** en **3**, Vijfde Editie, ThiemeMeulenhoff 1996; *The Nature of Light and Colour in the Open Air*, Dover 1954 (first edition 1937-40)
- [98] J. Moser and J. Pöschel, An extension of a result by Dinaburg and Sinai on quasi-periodic potentials. *Comment. Math. Helvetici* **59** (1984) 39-85
- [99] M. Misquero and R. Ortega, Some Rigorous Results on the $1 : 1$ Resonance of the Spin-Orbit Problem. *SIAM J. Appl. Dyn. Syst.* **19**(4) (2020) 2233-2267
- [100] A. Neishtadt, Averaging, passage through resonances, and capture into resonance in two-frequency systems. *Russ. Math. Surv.* **69**(5) (2014) 771
- [101] A. Neishtadt and A. Okunev, Averaging and passage through resonances in two-frequency systems near separatrices. ArXiv preprint arXiv:2108.08540v2
- [102] S.E. Newhouse, Diffeomorphisms with infinitely many sinks. *Topology* **13** (1974) 9-18

Bibliography

- [103] S.E. Newhouse, The abundance of wild hyperbolic sets and nonsmooth stable sets for diffeomorphisms. *Publ. Math. I.H.E.S.* **50** (1979) 101-151
- [104] I. Newton, *Philosophiae Naturalis Principia Mathematica*. Translated by I. Bernard Cohen and Anne Whitman as *Isaac Newton, The Principia – Mathematical Principles of Natural Philosophy*. University of California Press 1999 (first edition 1687)
- [105] E. Noether, Invariante Variationsprobleme. *Nachrichten der Königlichen Gesellschaft der Wissenschaften zu Göttingen, Math-phys. Klasse* (1918) 235-257
- [106] Press release: Nobel Prize in Physics 1985.
<https://www.nobelprize.org/prizes/physics/1985/press-release/> Accessed on Fri. 10 Jun 2022.
- [107] P.J. Olver, *Introduction to Partial Differential Equations*. Springer 2014
- [108] J. Oxtoby, *Measure and Category*. Springer 1971
- [109] J. Palis and F. Takens, *Hyperbolicity & sensitive chaotic dynamics and homoclinic bifurcations*. Cambridge studies in advanced mathematics **35** 1993
- [110] J.P. Philips, Brachistochrone, Tautochrone, Cycloid – Apple of Discord. *The Mathematics Teacher* **60**(5) (1967) 506-508
- [111] J. Pöschel, KAM à la R. *Regular Chaotic Dynamics* **16** (2011) 17-23
- [112] A. Pogromsky, D. Rijlaarsdam and H. Nijmeijer, Experimental Huygens synchronization of oscillators. In: M. Thiel, J. Kurths,

M.C. Romano, A. Moura and G. Károlyi, *Nonlinear Dynamics and Chaos: Advances and Perspectives*. Springer Complexity (2010) 195-210

- [113] T. Poston and I. Stewart, *Catastrophe Theory and its Applications*. Pitman 1978
- [114] Alice C. Quillen, Reducing the probability of capture into resonance, *Monthly Notices of the Royal Astronomical Society* **365**, 4 (2006) 1367-1382
- [115] D. Ruelle and F. Takens, On the nature of turbulence. *Commun. Math. Phys.* **20** (1971) 167-192; **23** (1971) 343-344
- [116] L. Russo and S. Levy. *The Forgotten Revolution: How Science Was Born in 300 BC and Why it Had to Be Reborn*. Springer-Verlag, Berlin, Heidelberg 2004
- [117] E.O. Schulz-DuBois, Foucault Pendulum Experiment by Kamerlingh Onnes and Degenerate Perturbation Theory. *American Journal of Physics* **38**, 173 (1970)
- [118] H. Seifert and W. Threlfal, *Variationsrechnung im Grossen*. Chelsea Publishing Company 1938
- [119] G.F. Simmons, *Differential Equations with Applications and Historical Notes* Third Edition. CRC Press 2017
- [120] B. Simon, Almost Periodic Schrödinger operators: a review. *Adv. in Applied Mathematics* **3** (1982) 463-490
- [121] B. Simon, Schrödinger operators in the twenty-first century. In: *Mathematical Physics 2000* (A. Fokas, A. Grigoryan, T. Kibble, and B. Zegarlinski, eds.), Imp. Coll. Press, London, 2000, 283-288

Bibliography

- [122] W. de Sitter, Outlines of a new mathematical theory of Jupiter's satellites *Ann. Sterrewacht Leiden* **12** (1925) 1-55
- [123] W. de Sitter. Jupiter's Galilean satellites (George Darwin lecture). *Monthly Notices of the Royal Astronomical Society* **91** (1931) 706-738
- [124] D.G. Shafer, The brachistochrone: historical gateway to the calculus of variations. *MATerials MATemàtiques* **5**(14) 2007
- [125] D. Sobel, *Longitude*. Walker 1995; 2005
- [126] I.H. Stadhuis, Christiaan Huygens correspondeert met zijn broer over levensduur. Hoe wetenschappelijke begrippen kunnen ontstaan. In: *De Zeventiende Eeuw*. **12** (1996) 161-170
- [127] Steven H. Strogatz, *Nonlinear Dynamics and Chaos: With Applications to Physics, Biology, Chemistry, and Engineering*, 2n ed. Westview Press, 2015
- [128] H.J. Sussmann and J.C. Willems, 300 years of optimal control from the brachystochrone to the maximum principle. *IEEE Control Systems* (1997) 32-44
- [129] F. Takens, A C^1 counterexample to Moser's twist theorem. *Indag Math* **74** (1971) 379-386
- [130] F. Takens, Forced oscillations and bifurcations. In: Applications of Global Analysis I, *Comm. of the Math. Inst. Rijksuniversiteit Utrecht* 1974; In H.W. Broer, B. Krauskopf and G. Vegter (eds.), *Global Analysis of Dynamical Systems*. IOP (2001) 1-62
- [131] Toonder Studio's, *Kappie en de Meester en De Kraak* 1951

- [132] R. Vermeij, *Christiaan Huygens. De mathematisering van de werkelijkheid.* Veen 2007
- [133] B.L. van der Waerden, *Erwachende Wissenschaft. Ägyptische, Babylonische und Griechische Mathematik.* Zweite Auflage. Birkhäuser 1966
- [134] R. Westfall, *Never at rest: a biography of Isaac Newton.* Cambridge University Press 1983
- [135] S.M. Wieczorek, B. Krauskopf, T.B. Simpson and D. Lenstra, The dynamical complexity of optically injected semiconductor lasers. *Physics Reports* **416**(1-2) (2005) 1-128
- [136] E.A. Whitman, Some historical notes on the cycloid. *The American Mathematical Monthly* **50**(5) (1943) 309-315
- [137] J.C. Yoccoz, Conjugaison différentiable des difféomorphismes du cercle dont le nombre de rotation vérifie une condition diophantienne. *Ann. Sci. École Norm. Sup.* (4) **17** (1984) 333-359
- [138] J.C. Yoccoz, Travaux de Herman sur les tores invariants. *Séminaire Bourbaki* **34** (1991-1992) 311-344
- [139] J.C. Yoccoz, Théorème de Siegel, nombres de Bruno et polynômes quadratiques. Petits diviseurs en dimension 1. *Astérisque* **231** (1995) 3-88
- [140] J.G. Yoder, *Unrolling Time. Christiaan Huygens and the Mathematization of Nature.* Cambridge University Press 1988
- [141] E.C. Zeeman, *Catastrophe Theory: Selected Papers 1972-1977.* Addison-Wesley 1977